MARTIN MARIETTA ENERGY SYSTEMS LIBRARIES

3 4456 0278664 3

LACE TR-022
(ORNL/M-365)

ornl

OAK RIDGE
NATIONAL
LABORATORY

MARTIN MARIETTA

Summary of Posttest Aerosol Code Comparisons for LWR Aerosol Containment Experiment (LACE) LA1

A. L. Wright
P. C. Arwood
J. H. Wilson

OAK RIDGE NATIONAL LABORATORY
CENTRAL RESEARCH LIBRARY
CIRCULATION SECTION
4500N ROOM 175
LIBRARY LOAN COPY
DO NOT TRANSFER TO ANOTHER PERSON
If you wish someone else to see this report, send in name with report and the library will arrange a loan.

OPERATED BY
MARTIN MARIETTA ENERGY SYSTEMS, INC.
FOR THE UNITED STATES
DEPARTMENT OF ENERGY

This report was prepared as an account of work sponsored by an agency of the United States Government. Neither the United States Government nor any agency thereof, nor any of their employees, makes any warranty, express or implied, or assumes any legal liability or responsibility for the accuracy, completeness, or usefulness of any information, apparatus, product, or process disclosed, or represents that its use would not infringe privately owned rights. Reference herein to any specific commercial product, process, or service by trade name, trademark, manufacturer, or otherwise, does not necessarily constitute or imply its endorsement, recommendation, or favoring by the United States Government or any agency thereof. The views and opinions of authors expressed herein do not necessarily state or reflect those of the United States Government or any agency thereof.

LACE TR-022
ORNL/M-365

Chemical Technology Division

SUMMARY OF POSTTEST AEROSOL CODE COMPARISONS FOR LWR AEROSOL CONTAINMENT EXPERIMENT (LACE) LA1

Principal Investigators

A. L. Wright
P. C. Arwood
J. H. Wilson

Prepared for
ELECTRIC POWER RESEARCH INSTITUTE
3412 Hillview Avenue
Palo Alto, California 94303

EPRI Project No. 2135-18

Date Issued — October 1987

Prepared by the
OAK RIDGE NATIONAL LABORATORY
Oak Ridge, Tennessee 37831
operated by
MARTIN MARIETTA ENERGY SYSTEMS, INC.
for the
U.S. DEPARTMENT OF ENERGY
under contract DE-AC05-84OR21400

MARTIN MARIETTA ENERGY SYSTEMS LIBRARIES

3 4456 0278664 3

NOTICE

This report was prepared by the organization(s) named below as an account of work sponsored by the Electric Power Research Institute, Inc. (EPRI). Neither EPRI, members of EPRI, the organization(s) named below, nor any person acting on behalf of any of them: (a) makes any warranty, express or implied, with respect to the use of any information, apparatus, method, or process disclosed in this report or that such use may not infringe privately owned rights; or (b) assumes any liabilities with respect to the use of, or for damages resulting from the use of, any information, apparatus, method or process disclosed in this report.

Prepared by

OAK RIDGE NATIONAL LABORATORY
Oak Ridge, Tennessee 37831

[redacted]

[illegible]

CONTENTS

Page

ABSTRACT..... iii

1. INTRODUCTION..... 1

2. SUMMARY OF CODE INPUTS AND REQUESTED CODE OUTPUTS FOR LA1 POSTTEST CALCULATIONS..... 2

3. SUMMARY OF LA1 PIPE CODE-EXPERIMENT COMPARISON RESULTS..... 18

4. SUMMARY OF "FIRST SET" OF LA1 VESSEL CODE-EXPERIMENT COMPARISON RESULTS..... 33

5. SUMMARY OF "SECOND SET" OF LA1 VESSEL CODE-EXPERIMENT COMPARISON RESULTS..... 86

6. SUMMARY AND CONCLUSIONS..... 116

7. ACKNOWLEDGEMENTS..... 121

8. REFERENCES..... 121

ABSTRACT

This report describes work performed as part of the LACE Code-Experiment Comparison Project, and was sponsored by the Electric Power Research Institute (EPRI Project No. 2135-18). The report presents and summarizes comparisons of test results and aerosol computer-code calculations for LACE LA1. The LACE tests are being performed at the Westinghouse Hanford Engineering Development Laboratory (HEDL) operated by the Westinghouse Hanford Company for the U.S. Department of Energy (US/DOE). LACE LA1 was done to simulate "containment bypass" accident sequence conditions. In the test, measurements were made to characterize (1) the aerosol transport through a 0.063-m diameter, 28.9-m length steel pipe, and (2) the aerosol behavior in a 852-m^3 test vessel. Results from one set of pipe calculations and two sets of vessel calculations are given and discussed in the report.

SUMMARY OF POSTTEST AEROSOL CODE COMPARISONS FOR LWR AEROSOL CONTAINMENT EXPERIMENT (LACE) LA1

A. L. Wright
P. C. Arwood

1. INTRODUCTION

The Light-Water Reactor (LWR) Aerosol Containment Experiments (LACE) are being performed to investigate, at large scale, the aerosol retention behavior in reactor coolant system piping and in containment under simulated, severe, LWR accident conditions. An additional, and equally important, objective of these tests is to provide a data base for validating aerosol containment computer codes and related thermal-hydraulic computer codes. The LACE tests are internationally funded and are being performed at the Hanford Engineering Development Laboratory (HEDL) — operated by the Westinghouse Hanford Company — under the leadership of an overall project board and the Electric Power Research Institute (EPRI).

The overall LACE project has two components: (1) the experiments being performed at HEDL and (2) aerosol-transport and thermal-hydraulic code-comparison activities. The aerosol-transport code-comparison activities are being coordinated at the Oak Ridge National Laboratory, while the thermal-hydraulic code-comparison activities are being coordinated at Intermountain Technologies, Inc. (ITI) in Idaho Falls, Idaho. For each of the six planned LACE tests, pretest and posttest aerosol-transport code calculations are being performed. The ORNL code-comparison activities include (1) providing guidance to participating aerosol code analysts to help them in performing calculations, (2) compiling the results from the calculations, and (3) critically evaluating the code results and comparisons to the test data.

This report summarizes the results from the posttest calculations performed for test LA1. These calculations were "blind" in that the code analysts did not have access to the LA1 results when they performed their

calculations. As defined in the LA1 test plan,[1] this test was designed to simulate a "containment bypass" accident sequence. Because of this plan, aerosol behavior through a pipe and aerosol behavior in the Containment Systems Test Facility (CSTF) vessel were investigated.

The next section of this report relates an overall description of LACE LA1. It then summarizes the defined code inputs and requested code outputs for the LA1 posttest calculations. Three separate types of calculations were performed for LA1: (1) calculations for aerosol behavior in the test pipe, (2) the so-called "first set" of vessel calculations, to model aerosol behavior in the CSTF vessel during and after the aerosol generation period, and (3) the "second set" of vessel calculations, to model vessel aerosol behavior after the aerosol generation period. Two sets of vessel calculations were necessary because the aerosol source rate to the vessel (the aerosol released from the test pipe) could not be well-specified. The next three sections (Sects. 3, 4 and 5) of the report discuss the code results and comparisons to the test data. Included in these sections are discussions and evaluations of each set of code results. Finally, in Sect. 6 a summary of the results and insights gained from the LA1 posttest code-experiment comparisons is presented.

2. SUMMARY OF CODE INPUTS AND REQUESTED CODE OUTPUTS FOR LA1 POSTTEST CALCULATIONS

Test LA1 was designed to simulate LWR "containment bypass" accident sequence conditions. Figure 1 illustrates the experimental set-up for test LA1; additional details are presented in the LA1 test plan.[1] CsOH and MnO aerosols were injected into a 0.063-m-diam, approximately 30-m-long test pipe; the pipe had six 90° bends. The pipe inlet flow velocity was roughly 100 m/s, and the outlet flow velocity was roughly 200 m/s (due to the pressure drop through the pipe). Aerosols that transported out of the pipe were then allowed to become airborne in the 852-m^3 CSTF vessel, where their subsequent aerosol behavior was then studied. During part of the experiment (the aerosol generation period), steam, non-condensable gas, and aerosols were vented or "leaked" to a scrubber.

ORNL DWG 86-676R

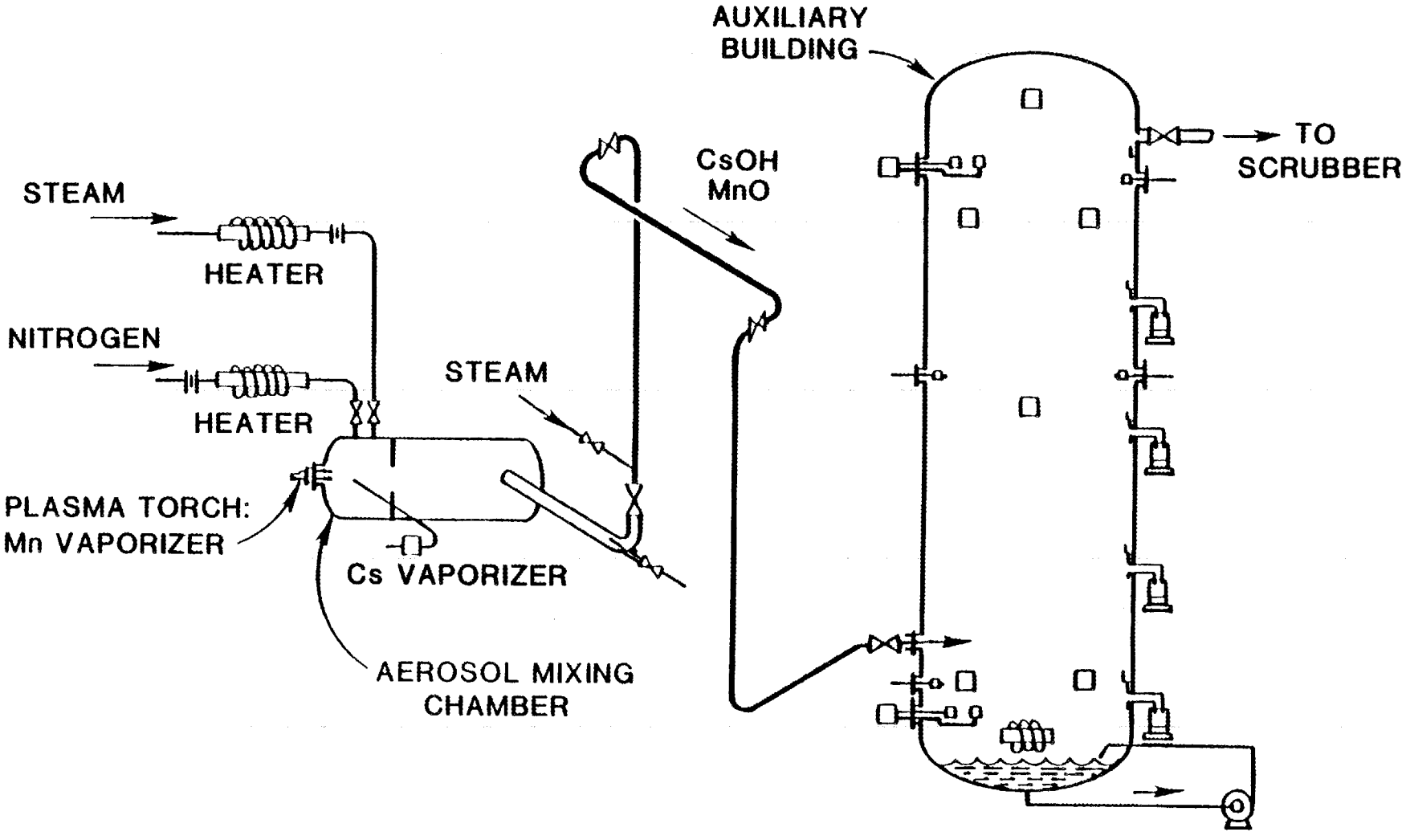

Fig. 1. LA1 experimental arrangement.

Two letters describing aerosol code inputs for the LA1 posttest calculations were sent to LACE program participants. The first letter[2] provided instructions for the test pipe calculations and for the "first set" of vessel calculations. The second letter[3] provided instructions for the "second set" of vessel calculations. The contents of these letters are summarized in this section.

The majority of the data required for performing the posttest calculations was contained on IBM-PC floppy disks - in the form of text files - that were transmitted from HEDL to LACE program participants.[4] The text files containing aerosol input information are named LA1AB10.TXT, LA1AB11.DAT, LA1AB12.DAT, LA1AB23.DAT, LA1AB24.DAT, LA1AB25.DAT, and LA1AB26.DAT. These text files will be referred to in this section.

Table 1 summarizes the data used for performing the LA1 pipe calculations. The test pipe geometry was defined in text file LA1AB10.TXT, and is reproduced in Table 2. Note that calculations were to be performed only for pipe sections 4-19, which had an overall length of 28.94 m. The aerosol source defined in Table 1 was based on the mass-balance data for sections 4-19. Although aerosol concentration and size measurements were made as a function of time upstream of pipe section 4, it was decided that constant values of aerosol source rate and aerosol size parameters would be specified. Also note that no aerosol shape factor values were specified, because they could not be measured.

Table 3 summarizes the requested code output parameters for the pipe calculations. Note that we requested that code analysts provide aerosol deposition and airborne aerosol size data for each of the pipe "control volumes" that they used to characterize the pipe; code analysts were free to choose how they wanted to nodalize the pipe. As shown in Table 3, we requested code output data for six times. However, since the actual deposition data could only be obtained by a posttest mass balance, we only used the data for t=3,600 seconds.

Table 1. Summary of information used for LA1 posttest pipe calculations

Code input data	Where information found[a]		
1. Test pipe geometry, layout:	Tables 1,2 in LA1AB10.TXT. Only pipe sections 4-19 are to be used for calculations.		
2. Average aerosol source rate to pipe inlet:	Table 5 in LA1AB10.TXT. CsOH: 0.48 g/s, MnO: 0.65 g/s		
3. Aerosol source time:	0 to 3,600 s		
4. Aerosol source size distribution:	Table 6 in LA1AB10.TXT.		
	CsOH	MnO	Mixed
Aerodynamic mass-median diameter (AMMD), μm	2.11	1.47	1.64
Geometric standard deviation (GSD)	1.80	2.00	1.91
5. Aerosol agglomerate density and shape factors.	To be specified by code user. HEDL measured deposit density = 3.9 g/cm.^{3} Theoretical solid density, based on source mass ratios = 4.52 g/cm^3		
6. Test pipe temperatures:	Tables B.15,B.16 in LA1AB23.DAT. Measurement locations noted in Table 12(F) in LA1AB10.TXT.		
7. Test pipe pressures:	Table C.2: LA1AB24.DAT. Measurement locations noted in Sect. I.4 in LA1AB10.TXT.		
8. Test pipe flow rates:	The sum of inlet steam and inlet nitrogen flow rates in Table C.1 in LA1AB24.DAT.		

[a]Refers to tables on IBM-format floppy disks (supplied by HEDL staff[4]) containing input conditions.

Table 2. LA1 test pipe geometry

Sect. No.	Pipe description	Orientation	Diameter (m)	Length (m)
4	Straight	Vertical	0.063	2.26
5	90° Bend	Vertical	0.063	0.36
6V	Ball Valve	Horizontal	0.063	0.19
6	Straight	Horizontal	0.063	4.2
7	90° Bend	Horizontal	0.063	0.36
8	Straight	Horizontal	0.063	3.74
9	Straight	Horizontal	0.063	4.32
10	90° Bend	Horizontal	0.063	0.36
11	Straight	Horizontal	0.063	0.62
11V	Ball Valve	Horizontal	0.063	0.19
12	90° Bend	Vertical	0.063	0.36
13	Straight	Vertical	0.063	4.32
14	Straight	Vertical	0.063	4.34
15	90° Bend	Vertical	0.063	0.35
16	Straight	Horizontal	0.063	1.74
17	90° Bend	Horizontal	0.063	0.33
18	Ball Valve	Horizontal	0.063	0.19
19	Straight	Horizontal	0.063	0.71

Overall length of sections 4-19 = 28.94 m.

Table 3. Summary of requested code output data for LA1 posttest pipe calculations

Output times (s): 300, 600, 900, 1,800, 2,700, 3,600

Output parameters and units:

A. For each pipe control volume[a] at each output time:

1. Cumulative aerosol mass - for MIXED aerosol and for EACH species (if possible) - deposited in each control volume - in grams.

2. Airborne aerosol size in each control volume - for MIXED aerosol and for EACH species (if possible): provide the aerodynamic mass-median diameter - in μm - and the geometric standard deviation - dimensionless.

B. At pipe outlet for each output time:

1. Cumulative aerosol mass - for MIXED aerosol and for EACH species (if possible) - transported out of test pipe - in grams.

2. Airborne aerosol size transported out of test pipe - for MIXED aerosol and for EACH species (if possible): provide the aerodynamic mass-median diameter - in μm - and the geometric standard deviation - dimensionless.

[a]Code analysts were to determine, based on their own judgement, the number of control volumes needed to model the test pipe.

At the LACE Technical Advisory Committee (TAC) meeting held on December 10-12, 1985, it was decided that two sets of LA1 posttest calculations for aerosol behavior in the CSTF vessel should be performed. The "first set" of calculations was performed to calculate aerosol behavior during and after the aerosol source period. The "second set" was performed to model aerosol behavior only after the source period was over. It was decided to perform two calculations because measurements of the aerosol source rate into the vessel (from the pipe outlet) could not be made. The first set of calculations, then, used as input an average aerosol source, based on the posttest CSTF vessel material balance. The

second set of calculations, however, used measured values of the airborne aerosol concentration and size distribution at the end of the source period as input.

The data used for performing the first set of vessel calculations is summarized in Tables 4 and 5. The floppy-disk data included nitrogen vent flow (to the scrubber) data, but it did not include calculated steam and overall vent flow data; the latter were calculated and provided in Table 5. The following formula was used to calculate the steam vent flows to the scrubber:

$$Q_s = (M_s/M_n)\cdot(F_s/F_n)\cdot Q_n \qquad (1)$$

where

Q_s = steam vent flow rate to scrubber
Q_n = measured nitrogen vent flow rate to scrubber
M_s = molecular weight of steam
M_n = molecular weight of nitrogen
F_s = measured steam volume fraction in vessel
F_n = nitrogen volume fraction in vessel

Note that estimates of aerosol shape factors and aerosol densities, gas-wall temperature gradients, and steam condensation rates (onto the walls and/or the airborne aerosols) for times greater than 550 min were to be provided by the code users.

The aerosol source data for the first set of LA1 calculations was determined from the vessel mass-balance data — i.e., the total airborne aerosol recovered in the vessel plus that amount of material vented from the vessel.[5] However, as illustrated in Table 6, this data differed slightly from the aerosol source rate estimated from the sum of (1) aerosol settling (determined from the amounts of aerosol deposited in small "settling cans" located throughout the vessel), (2) plateout (determined from the aerosol deposited onto small sections of the vessel wall), and

Table 4. Summary of information used for first set of LA1 posttest vessel calculations

Code input data	Where information found[a]
1. CSTF vessel geometry, properties:	Tables 3,4 in LA1AB10.TXT.
2. Average source rate for aerosol suspended in vessel:	Table 7 in LA1AB10.TXT. CsOH, 0.0038 g/s; MnO, 0.017 g/s
3. Aerosol source time:	0 to 3,600 s
4. Aerosol source size:	Table 8 in LA1AB10.TXT.

	CsOH	MnO	Mixed
AMMD (μm)	0.97	0.83	0.89
Geometric standard deviation	2.70	2.78	2.72

5. Aerosol agglomerate density and shape factors:	To be specified by code user. THEORETICAL SOLID DENSITY, based on source mass ratios = 5.0 g/cm^3.
6. Test vessel temperatures:	Spacial-average values are in Table A in LA1AB11.DAT. Spacial variations are in Tables B.1-B.7 in LA1AB12.DAT. Thermocouple locations are in Table 12(A,B) in LA1AB10.TXT.
7. Test vessel pressures:	Table A in LA1AB11.DAT.
8. Vent flow rates from vessel:	Noncondensable gas flow rates in Table C.1 in LA1AB24.DAT. Upper vessel steam fractions in Table F in LA1AB26.DAT. Calculated total flows, for selected times, in Table 5.
9. Gas-wall temperature gradients:	To be specified by code user. Some options include: Use of temperature vs distance-from-wall data in Table B.8 in LA1AB12.DAT. Use of heat flux data in Table D in LA1AB25.DAT.
10. Steam conditions in vessel:	Table F in LA1AB26.DAT. Saturated steam for t>550 min.

[a]Refers to tables on IBM-format floppy disks - supplied by HEDL staff[4] - containing input conditions.

Table 5. Calculated steam vent flows and total vent flows (to the scrubber) for test LA1

Time (s)	Noncondensable vent flow (kg/s)	Steam volume fraction	Steam vent flow (kg/s)	Total vent flow (kg/s)
0.0	0.068	0.544	0.052	0.120
144	0.195	0.543	0.149	0.344
294	0.205	0.543	0.156	0.361
444	0.224	0.542	0.171	0.395
594	0.224	0.542	0.170	0.394
744	0.211	0.541	0.160	0.371
900	0.235	0.541	0.178	0.413
1,050	0.237	0.540	0.179	0.416
1,200	0.220	0.541	0.167	0.387
1,350	0.222	0.543	0.170	0.392
1,500	0.242	0.545	0.186	0.428
1,650	0.233	0.547	0.181	0.414
1,800	0.228	0.548	0.178	0.406
1,950	0.214	0.550	0.168	0.382
2,100	0.236	0.552	0.187	0.423
2,250	0.243	0.553	0.194	0.437
2,400	0.242	0.555	0.194	0.436
2,550	0.224	0.557	0.181	0.405
2,700	0.215	0.559	0.175	0.390
2,850	0.217	0.560	0.177	0.394
3,000	0.215	0.558	0.175	0.390
3,150	0.215	0.557	0.174	0.389
3,300	0.235	0.556	0.189	0.424
3,450	0.240	0.554	0.192	0.432
3,600	0.365	0.553	0.290	0.655

for times > 3600 s, assume vent flow = 0 kg/s

Table 6. Comparisons of LA1 vessel aerosol source rates determined from mass balance and from sum of aerosol settling, plateout, and leakage

Material	Aerosol source from mass balance data		Aerosol source from sum of settling, plateout, and leakage	
	Mass (g)	Source rate (g/s)[a]	Mass (g)	Source rate (g/s)[a]
CsOH	13.68	0.0038	12.1	0.0034
MnO	61.2	0.017	46.62	0.013
CsOH+MnO	74.88	0.0208	58.72	0.0163

[a]Average source rate determined by dividing total mass by aerosol source time = 3,600 s.

(3) leakage (aerosol vented to the scrubber) in the test. The following details give more information on how the vessel aerosol source was determined:

1. The total amount of material recovered from the test vessel and aerosol scrubber was 95.4 g (this is presented later in Sect. 3, Table 15).

2. The HEDL investigators determined that a portion of the 95.4 g recovered from the vessel was actually impinged on the wall directly opposite from where the aerosol was injected into the vessel from the test-pipe outlet. It was assumed that the impinged mass was never airborne in the test vessel. The value of 74.88 g for the total true aerosol input to the vessel (Table 6) was obtained in this way. This value was used to define the aerosol source for the "first-set" calculations.

3. Individual measurements of total settling, total plateout, and total aerosol transport to the scrubber were made. From these measurements, an estimate of the total aerosol input to the vessel of 58.72 g (Table 6) was made. We believe that this is the value that should have been used in the calculations.

As illustrated in Table 6, the CsOH source rates differ by roughly 10%, while the MnO source rates differ by roughly 25%. Considering the fact that less than 100 g of aerosol was input to the vessel, these

differences are not surprising. However, the evaluation of the code comparisons for the first set of calculations should acknowledge this uncertainty in the aerosol source.

Table 7 summarizes the requested code outputs for the first set of vessel calculations. Code outputs were requested for 16 different times — 5 for the aerosol source period and 11 after the end of the source. Note that we requested values of the "aerodynamic mean settling diameter" (6b in Table 7) and also requested "discrete" code users to provide us with tables of aerosol masses in different size bins for selected times (6c in Table 7). However, these data are not included in this report because the requested times do not correspond to the times where measurements were made. For future posttest code comparisons, we will request the bin-data information at the times when aerosol size measurements are made.

The data used for performing the second set of vessel calculations are summarized in Table 8. The major aerosol input data for this set were the estimated airborne aerosol concentration and size at t=3,600 s, the end of the source period; these values were obtained (from the HEDL staff[5]) by extrapolation of the data for t>3,600 s back to t=3,600 s. Note also that for t>3,600 s there was no vent flow from the vessel.

Finally, the requested code outputs for the second set of vessel calculations are summarized in Table 9. Code outputs were requested for 11 times after t=3,600 seconds. Note that, although we requested that code users calculate settling and plateout for t>3,600 seconds, only total values of settling and plateout were measured (for times including the aerosol source period and for times after the source period). However, plots of settling and plateout are included in Sect. 5 for comparison purposes. As for the first set of vessel calculations, calculated mean settling diameters and bin aerosol-size data are not included in this report.

Table 7. Summary of requested code output parameters for first set of posttest vessel calculations

OUTPUT TIMES (s): 300, 600, 1,200, 2,400, 3,600, 3,900, 4,200, 4,800, 5,400, 6,000, 8,000, 10,000, 33,000, 60,000, 100,000, 150,000.

OUTPUT PARAMETERS AND UNITS (FOR EACH OUTPUT TIME):

1. Suspended aerosol mass concentration - for MIXED aerosol and for EACH species (if possible) - in g/m^3.

2. Concentration of water condensed on airborne CsOH and MnO aerosols - in g/m^3.

3. Cumulative aerosol settled in vessel - for MIXED aerosol and for EACH species (if possible) - in g.

4. Cumulative aerosol plated on vessel walls and ceilings - for MIXED aerosol and for EACH species (if possible) - in g.

5. Cumulative aerosol vented from vessel - for MIXED aerosol and for EACH species (if possible) - in g.

6. Airborne aerosol size parameters - for MIXED aerosol and for EACH species (if possible):

   a. The aerodynamic mass-median diameter - in μm - and the geometric standard deviation - dimensionless

   b. The aerodynamic mean settling diameter - in μm

   c. "DISCRETE" code users should provide tables of aerosol mass or mass concentration in each size group for the times 1,200, 3,600, 4,800, 10,000, and 60,000 s

Table 8. Summary of information used for second set of LA1 posttest vessel calculations

CODE INPUT DATA	WHERE INFORMATION FOUND[a]
1. CSTF vessel geometry, properties:	Tables 3,4 in LA1AB10.TXT.
2. Airborne aerosol concentration at end of aerosol source (t=3,600 s):	CsOH: $7(10^{-3})g/m^3$, MnO: $1.7(10^{-2})g/m^3$, Mixed: $2.4(10^{-2})g/m^3$.
3. Airborne aerosol size at end of aerosol source: (t=3,600 s):	

	CsOH	MnO	Mixed
AMMD (μm)	1.18	0.80	0.88
Geometric standard deviation	2.6	2.8	2.6

4. Aerosol agglomerate density and shape factors:	To be specified by code user. THEORETICAL SOLID DENSITY, based on MnO/CsOH source mass ratio of 4.47, is 5.0 g/cm^3.
5. Test vessel temperatures:	Spacial-average values are in Table A in LA1AB11.DAT. Spacial variations are in Tables B.1-B.7 in LA1AB12.DAT. Thermocouple locations are in Table 12(A,B) in LA1AB10.TXT.
6. Test vessel pressures:	Table A in LA1AB11.DAT.
7. Vent flow rates from vessel:	0 kg/s for t>3,600 s.
8. Gas-wall temperature gradients:	To be specified by code user. Some options include: Use of temperature vs distance-from-wall data in Table B.8 in LA1AB12.DAT. Use of heat-flux data in Table D in LA1AB25.DAT.
10. Steam conditions in vessel:	Table F in LA1AB26.DAT. Saturated steam for t>33,000 s .

[a]Refers to tables on IBM-format floppy disks - supplied by HEDL staff[4] - containing input conditions.

Table 9. Summary of requested code output parameters for second set of LA1 posttest vessel calculations

OUTPUT TIMES (s):[a] 3,900, 4,200, 4,800, 5,400, 6,000, 8,000, 10,000, 33,000, 60,000, 100,000, 150,000.

OUTPUT PARAMETERS AND UNITS (FOR EACH OUTPUT TIME):

1. Suspended aerosol mass concentration - for MIXED aerosol and for EACH species (if possible) - in g/m^3.

2. Concentration of water condensed on airborne CsOH and MnO aerosols - in g/m^3.

3. Cumulative (for times after 3,600 s) aerosol settled in vessel - for MIXED aerosol and for EACH species (if possible) - in grams.

4. Cumulative (for times after 3,600 s) aerosol plated on vessel walls and ceilings -for MIXED aerosol and for EACH species (if possible) - in g. Provide deposition data for EACH important plateout mechanism (diffusion, thermophoresis, diffusiophoresis, etc.)

5. Airborne aerosol size parameters - for MIXED aerosol and for EACH species (if possible):

   a. The aerodynamic mass-median diameter - in μm - and the geometric standard deviation - dimensionless

   b. The aerodynamic mean settling diameter - in μm

   c. "DISCRETE" code users should provide tables of aerosol mass or mass concentration in each size group for the times 4,800, 10,000, and 60,000 s.

[a]Note that t = 0 s corresponds to the start of the aerosol source period and t = 3,600 s corresponds to the end of the source period. Calculations should ONLY be done for times > 3,600 s. "Cumulative" values for aerosol settling and plateout should be done by assuming values of 0 for these parameters at t = 3,600 s.

Tables 10 and 11 provide additional information relevant to the first and second sets of LA1 vessel calculations. We provided, in Table 5, values of steam and nitrogen vent mass flow rates for 0-3,600 s. However, some of the codes require fractional volumetric flow rates; these were not provided in the instruction letters. Table 10 presents time-dependent calculated values of these flow parameters.

Table 10. LA1 calculated fractional volume flow rates (vent to scrubber) for 0 to 3,600 seconds

Time (s)	Vent to scrubber, fractional volume flow rate (1/s)	Vent to scrubber, fractional volume flow rate (vol%/day)
0.0	1.800E-4	1555
144	5.025E-4	4342
294	5.231E-4	4520
444	5.692E-4	4918
594	5.679E-4	4907
744	5.335E-4	4609
900	5.924E-4	5119
1,050	5.967E-4	5156
1,200	5.554E-4	4798
1,350	5.614E-4	4851
1,500	6.138E-4	5303
1,650	5.929E-4	5123
1,800	5.823E-4	5031
1,950	5.480E-4	4735
2,100	6.066E-4	5241
2,250	6.270E-4	5417
2,400	6.262E-4	5410
2,550	5.817E-4	5026
2,700	5.603E-4	4841
2,850	5.673E-4	4902
3,000	5.595E-4	4834
3,150	5.584E-4	4824
3,300	6.073E-4	5247
3,450	6.190E-4	5348
3,600	9.424E-4	8143
Average values	5.759E-4	4976

Table 11. Calculated airborne water mass and airborne steam removal rates, for t>33,000 s

Time (10^3s)	Airborne steam fraction	Airborne water mass (kg)	Steam removal rate[a] (g/s)
33.0	0.502	229.3	
35.2	0.495	227.1	0.991
43.7	0.395	183.6	5.141
51.7	0.310	145.8	4.707
61.4	0.270	128.7	1.768
71.0	0.220	106.1	2.356
79.9	0.210	102.4	0.428
97.3	0.160	79.4	1.306
150.0	0.113	58.4	0.399

[a]Steam removal rates are average values between two times. For example, 0.991 g/s is the average values between 33,000 and 35,200 s.

In the input specifications for the LA1 calculations[4] it was stated that steam saturation conditions existed in the vessel for times greater than 550 min (33,000 s). Reliable measurements of steam condensation rates could only be made prior to the start of aerosol generation. However, estimates of steam removal from the atmosphere for t>33,000 s can be obtained from the vessel steam-fraction measurements. Table 11 presents calculated values for airborne steam mass and average airborne steam removal rates. The airborne steam mass was calculated using the equation:

$$M_{air} = SFR\ P \cdot M_w\ V/(R_g \cdot T), \qquad (2)$$

where M_{air} = airborne steam mass

SFR = measured steam volume fraction

P = vessel gas pressure

M_w = steam molecular weight = 18 g/mol

V = vessel volume

R_g = universal gas constant

T = vessel gas temperature

Note that the steam fraction measurements were made by collecting all of the water airborne within a measurement volume; therefore, it includes the water airborne on the aerosols. We believe, however, that the water on the aerosols was a minor fraction of the airborne water.

3. SUMMARY OF LA1 PIPE CODE-EXPERIMENT COMPARISON RESULTS

LA1 pipe calculations were performed by six investigators; the codes used and the names and affiliations of the code analysts are listed in Table 12. The TRAP-MELT2 and AEROSIM-M codes are discrete size distribution codes, while the RETAIN-2C code is a log-normal code. The AUX2.9 code assumes that the aerosol approaches an asymptotic size distribution. AEROSIM-M is actually a containment aerosol transport code, but it was used in a "Lagrangian" mode (following an aerosol/gas packet moving down the pipe) for this calculation.

Table 12. Summary of codes used for LA1 pipe calculations

Code[a]	Code analyst	Affiliation
AEROSIM-M (UK)	S. Ramsdale	United Kingdom, Atomic Energy Authority, Safety and Reliability Directorate
AUX2.9 (SW)	H. Haggblom	Sweden, Studsvik Energitenik AB
RETAIN-2C (FN)	J. Makynen	Finland, Technical Research Centre
TRAP-MELT2 (IT)	F. Parozzi	Italy, ENEL-Thermal and Nuclear Research Centre
TRAP-MELT2 (UK)	D. Williams	United Kingdom, Atomic Energy Authority, AEE Winfrith
TRAP-MELT2 (BCL)	V. Kogan	United States, Battelle Columbus Laboratories

[a]Initials in parentheses indicate country or organization.

The HEDL staff measured the masses of CsOH and MnO deposited in the various sections of the pipe; they also determined the aerosol transported out of the pipe into the CSTF vessel. The LA1 pipe deposition and transport data are summarized in Table 13. The table also lists calculated deposit mass ratios for the various pipe sections. Note that approximately 98% of the aerosol input to the test pipe was deposited. Also note that there were variations in the deposit mass ratios in the pipe; the mean deposit mass ratio was 1.32, with a standard deviation of 0.30. The aerosol source mass ratio was 1.35, very close to the mean deposition value.

Table 13. Summary of measured pipe-wall deposition data and aerosol transport data for LACE LA1[a]

Pipe sections	Section length (m)	CsOH deposited (g)	MnO deposited (g)	CsOH+MnO deposited (g)	MnO/CsOH deposit ratio
4	2.26	97.2	121.5	218.7	1.25
5	0.36	19.9	28.2	48.0	1.42
6V-6	4.39	301.8	426.6	728.4	1.41
7	0.36	28.3	35.7	64.0	1.26
8-9	8.06	647.9	830.5	1478.4	1.28
10	0.36	26.5	28.6	55.1	1.08
11-11V	0.81	87.9	153.4	241.3	1.74
12	0.36	34.3	43.8	78.0	1.28
13-14	8.66	371.2	463.1	834.2	1.25
15	0.35	28.8	30.9	59.7	1.07
16	1.74	19.9	26.0	45.9	1.30
17	0.33	9.3	11.5	20.7	1.24
18	0.19	3.3	2.8	6.0	0.85
19	0.71	1.1	2.4	3.5	2.11
Totals:		1677.4	2204.7	3822.1	

Total CsOH aerosol transported out of pipe = 21.0 g.
Total MnO aerosol transported out of pipe = 74.4 g.

[a]Aerosols deposited in flanges between pipe sections included.

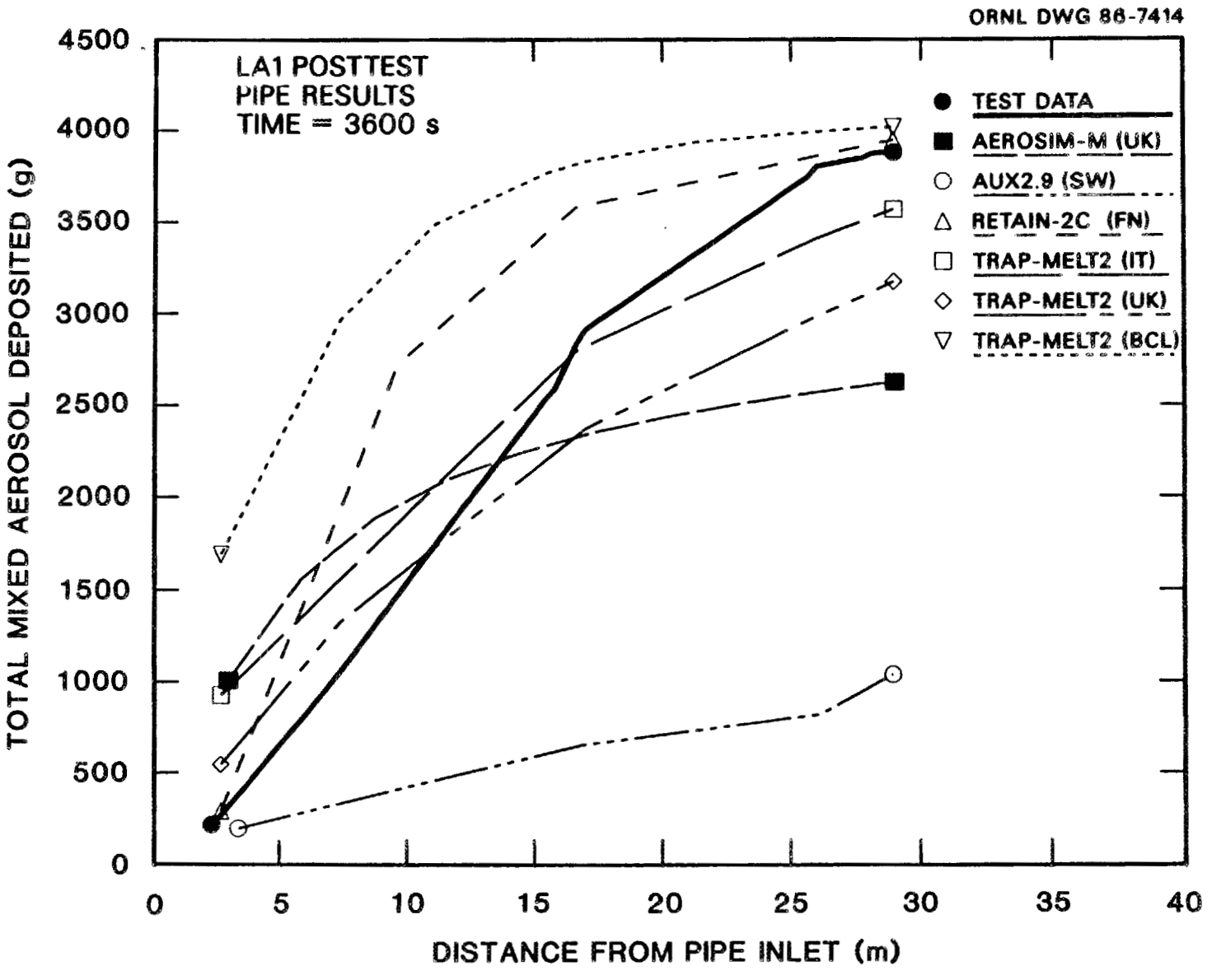

Fig. 2. LA1 posttest pipe results: total mixed aerosol mass deposited vs distance from pipe inlet.

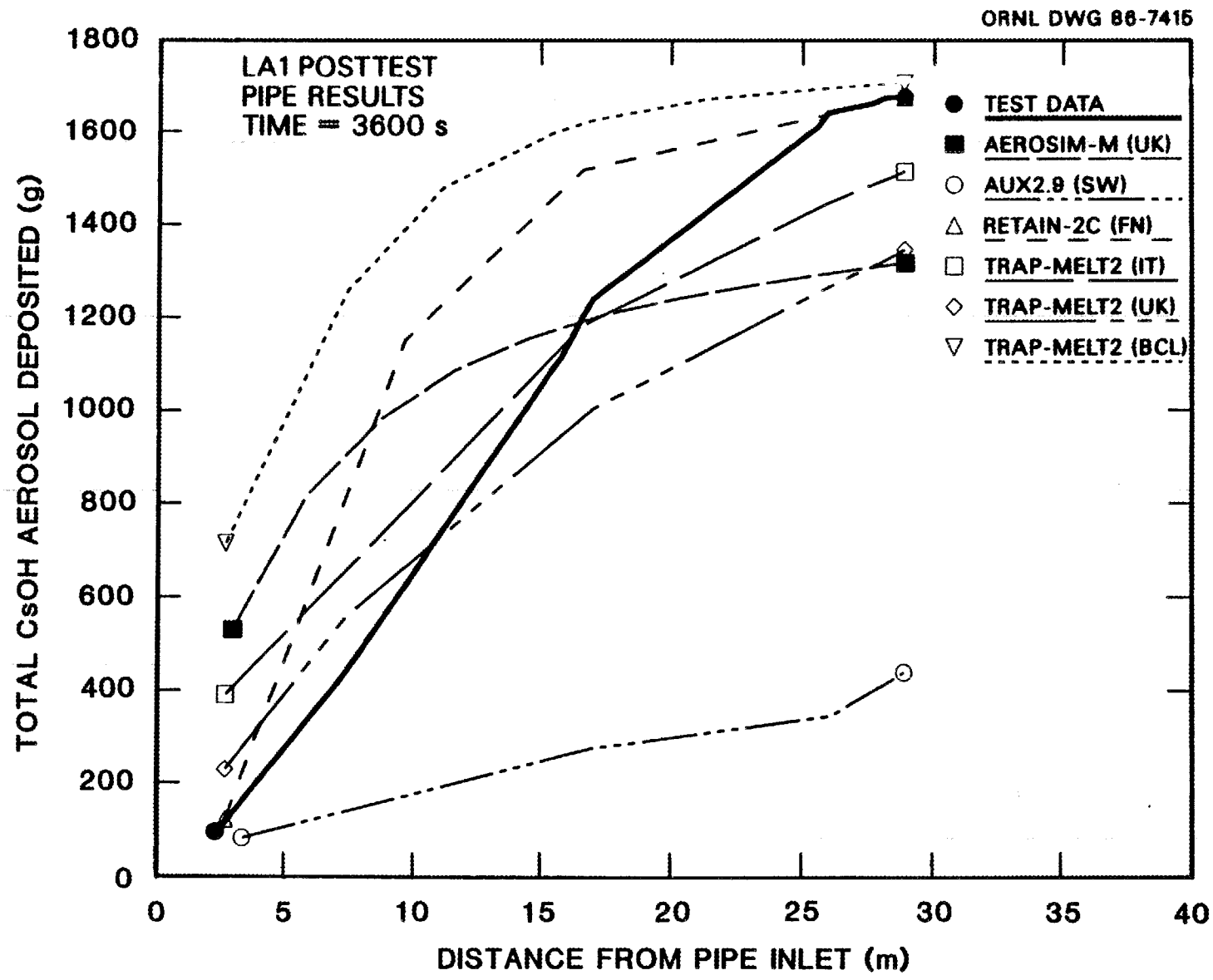

Fig. 3. LA1 posttest pipe results: total CsOH aerosol mass deposited vs distance from pipe inlet.

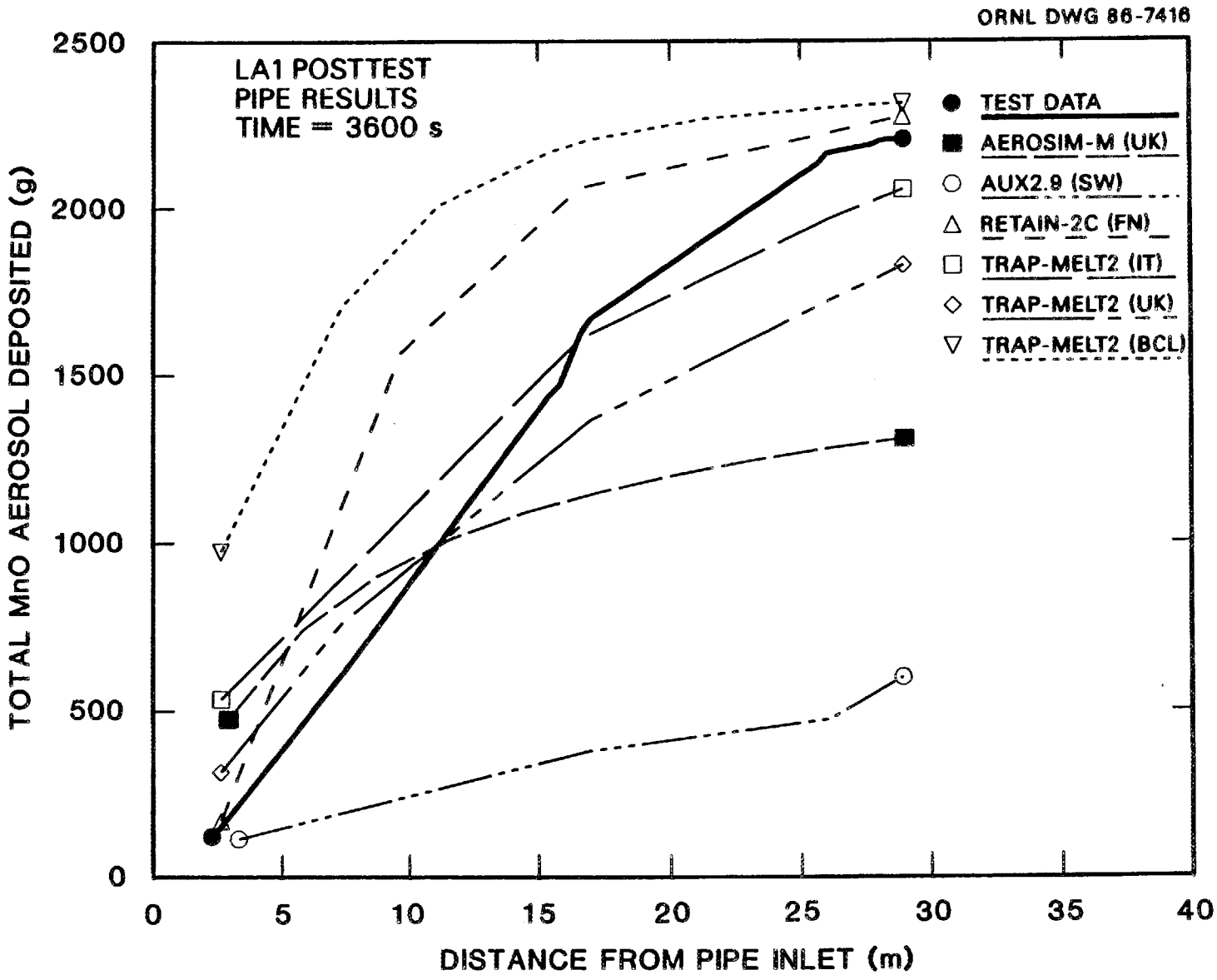

Fig. 4. LA1 posttest pipe results: total MnO aerosol mass deposited vs distance from pipe inlet.

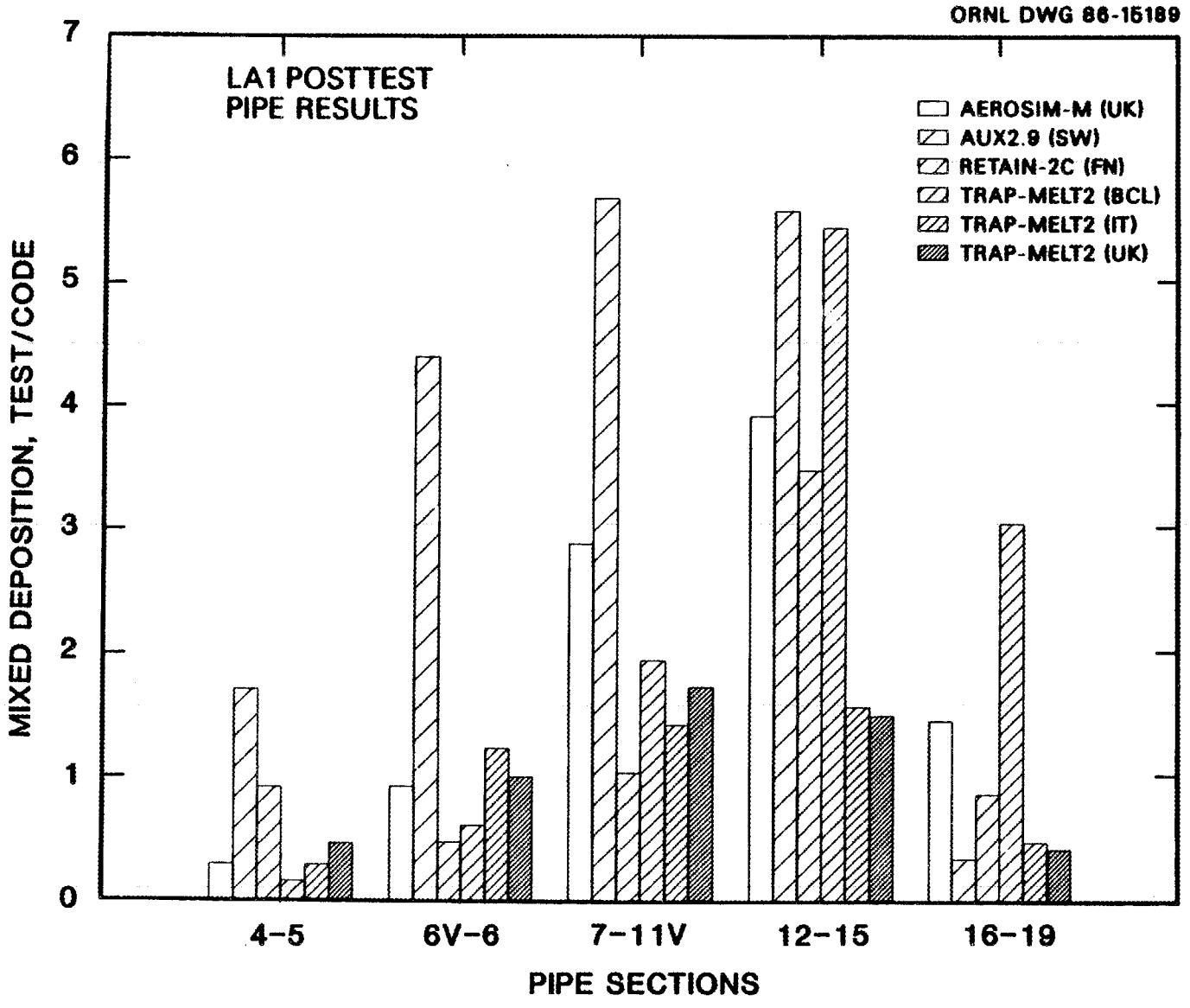

Fig. 5. LA1 posttest pipe results: ratios of measured-to-calculated mixed aerosol deposited for five different groups of pipe sections.

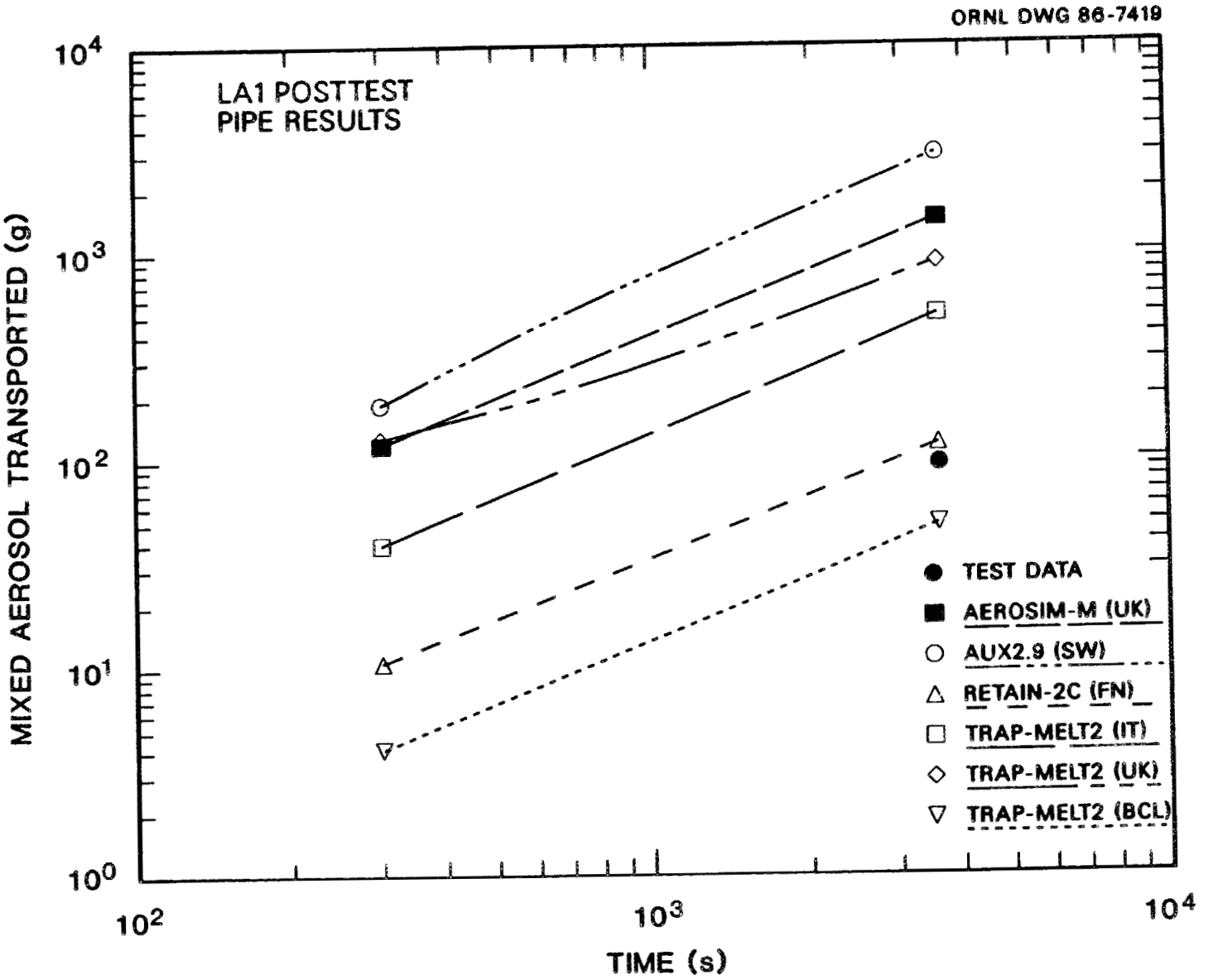

Fig. 6. LA1 posttest pipe results: mixed aerosol transported out of pipe vs time.

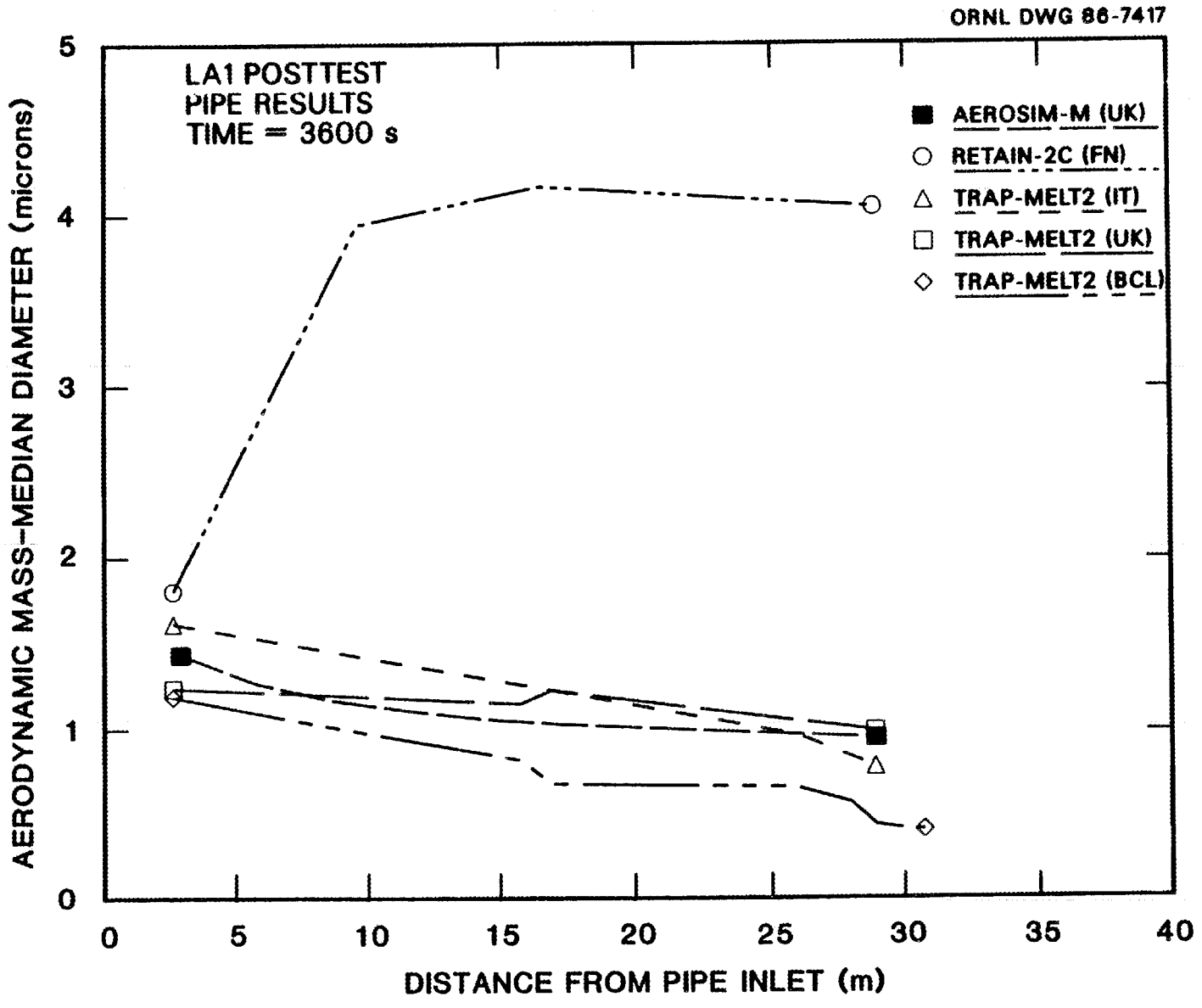

Fig. 7. LA1 posttest pipe results: calculated values of aerodynamic mass-median diameter (AMMD) vs distance from pipe inlet, at end of test (3,600 s).

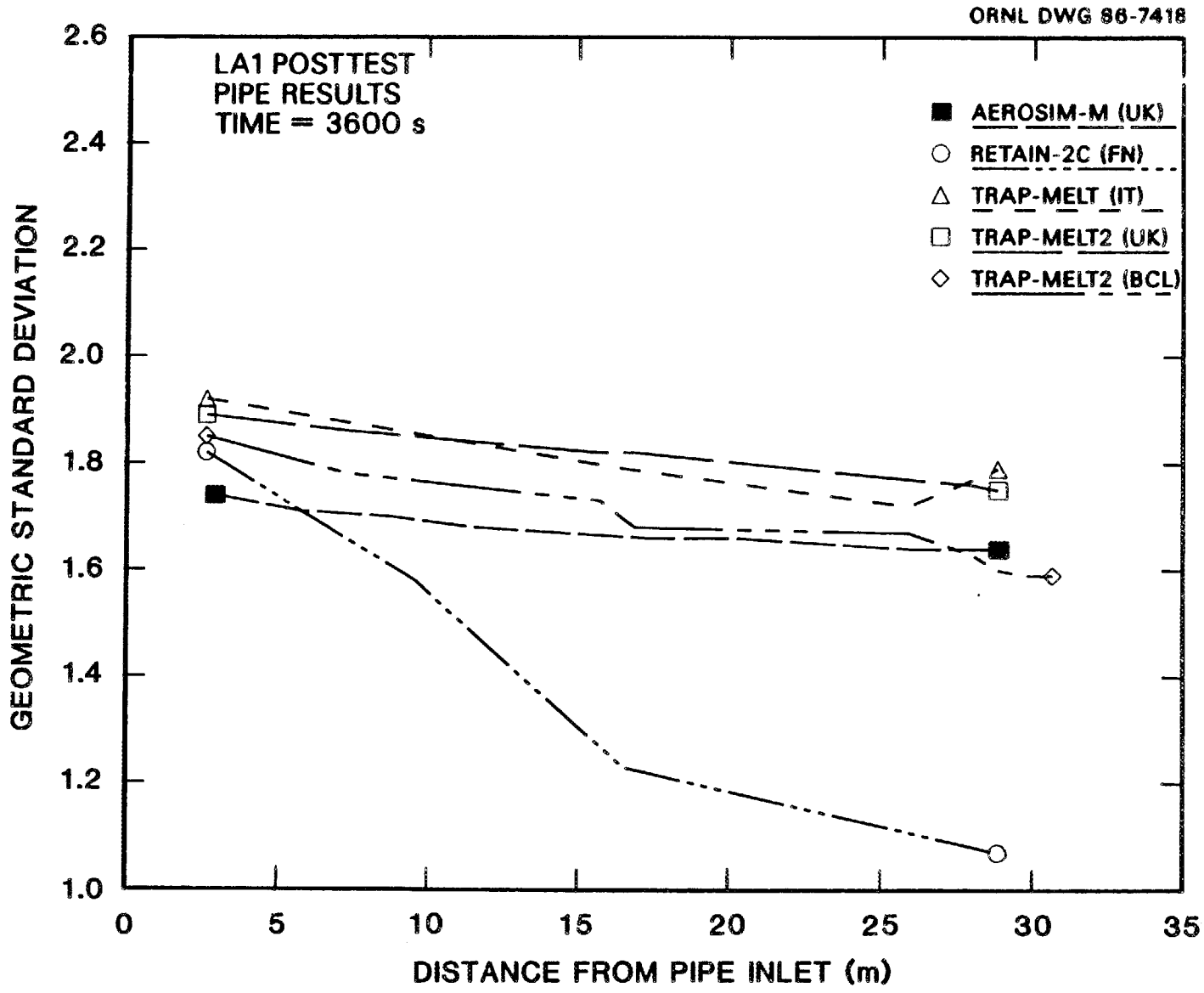

Fig. 8. LA1 posttest pipe results: calculated values of geometric standard deviation vs distance from pipe inlet at end of test (3,600 s).

function of distance from the pipe inlet. We chose another way to compare the test and code deposition results in Figure 5. Here, values of the ratio of the measured-to-calculated total aerosol deposition for five "groups" of pipe sections were determined for each of the code calculations. The data from Fig. 5 are also summarized in Table 14. Figure 6 shows calculated values of total aerosol transport out of the pipe as a function of time; the overall test value at the end of the aerosol generation period is also shown. Table 15 displays values of the ratios of measured-to-calculated total aerosol transport out of the pipe. Finally, Figs. 7 and 8 give plots of calculated values of the aerosol AMMD and geometric standard deviation as a function of distance from the pipe inlet; these are graphed for t=3,600 s, the end of the generation period.

Table 14. Values of measured-to-calculated total aerosol deposition in test LA1, for five pipe-section groups

Pipe sections	Test-to-code ratio for each pipe-section grouping: AEROSIM-M (UK)	AUX2.9 (SW)	RETAIN-2C (FN)	TRAP-MELT2 (BCL)	TRAP-MELT2 (IT)	TRAP-MELT2 (UK)
4-5	0.24	1.77	0.95	0.16	0.30	0.48
6V-6	0.74	4.29	0.47	0.60	1.21	0.98
7-11V	2.59	5.75	1.06	1.98	1.45	1.76
12-15	4.23	5.87	3.67	5.73	1.66	1.59
16-19	1.51	0.36	0.90	3.17	0.50	0.44

Table 15. Values of measured-to-calculated total aerosol transport out of test pipe for test LA1

Code	Total aerosol leaked from pipe (g)	Test/code[a]
RETAIN-2C(FN)	119.0	0.802
TRAP-MELT2(BCL)	49.0	1.95
TRAP-MELT2(IT)	496.7	0.192
TRAP-MELT2(UK)	890.0	0.107
AEROSIM-M(UK)	1436.4	0.066
AUX2.9(SW)	2950.0	0.032

[a]Measured value of aerosol leakage from pipe = 95.4 g.

The major differences in the modeling approaches used in the different calculations are illustrated in Table 16. Five different models (including the use of no model in the AUX2.9 calculation) for turbulent aerosol deposition were used. The Friedlander and Johnstone[6] model as modified by Battelle-Columbus,[7] is the standard one used in TRAP-MELT2. The model of Wood[8] includes the influence of surface roughness on deposition. This latter model has recently been included in the version of TRAP-MELT2 used at Battelle Columbus Laboratories[9] (BCL). The BCL version of TRAP-MELT2 also now includes a model to calculate aerosol deposition in pipe bends. Note finally that none of the codes included a model for resuspension of aerosols from the pipe walls.

The results illustrated in Figures 2 and 5 and in Table 14 illustrate that the Italian and United Kingdom versions of TRAP-MELT did the best job of calculating the change in aerosol deposition along the pipe length. In both of these calculations, however, the deposition in the upstream pipe sections - sections 4 and 5 - was overestimated by a factor of 2 to 3. This error reduced the aerosol available for deposition in the downstream sections and may be part of the reason that these two calculations tended to underestimate deposition in the upstream pipe sections.

Although the TRAP-MELT2 (UK) results looked reasonable, two errors were made in these calculations: (1) an argon gas flow into the pipe was assumed which caused calculated gas velocities to be too high, (2) an incorrect pipe cross-sectional area was used, causing calculated velocities to be low. Although we did not request it, the UK investigator reran the LA1 pipe calculation with the correct gas flows and pipe cross-sectional area. The results from the calculation with input errors gave a total aerosol deposition in the pipe of 3178 g; the revised calculation gave a total deposition of 3590 g. The revised results resemble those calculated by the Italian investigator who used TRAP-MELT2.

The BCL TRAP-MELT2 results significantly overestimated (by a factor of 6) the aerosol deposition in sections 4 and 5; almost half of the calculated aerosol deposition was predicted to occur in these sections. This result is a possible indication that the Wood model does not calculate turbulent deposition as well as the Friedlander and Johnstone model.

Table 16. Comparisons of modeling assumptions used in LA1 posttest pipe calculations

Code	Number of control volumes	Turbulent deposition model used	Gas property modeling assumptions	Others
AEROSIM-M (UK)	Lagrangian approach	Liu and Agarwal[10]	Mixture properties, constant flow velocity	
AUX2.9(SW)	4	Not modeled	Mixture properties	
RETAIN-2C (FN)	4	Sehmel[11]	Air-steam mixture properties	Control volumes do not match pipe layout.
TRAP-MELT2 (BCL)	9	Wood[8,9]	Steam properties, "adjusted" steam flow	Calculation performed for 24 s, then extrapolated to 3600 s. "Sand roughness" of 30 μm assumed. Deposition in bends modeled.
TRAP-MELT2 (IT)	4	Friedlander and Johnstone with Battelle modification[6,7]	Properties of steam, nitrogen, argon, hydrogen mixture calculated within code	Adjusted aerosol source used. Time step of 2 s used.
TRAP-MELT2 (UK)	7	Friedlander and Johnstone with Battelle modification[6,7]	Properties of steam, nitrogen, argon mixture input to code	Argon gas flow rates used were too high. Incorrect pipe cross-sectional area used. Time step of 2 s used.

It is also possible, however, that the 30-μm value chosen for the surface roughness parameter is not the correct value to use.

Deposition velocities calculated in the upstream pipe sections using the Wood model were about 40 cm/s, roughly twice those calculated by the Italian and United Kingdom TRAP-MELT users. As illustrated in Fig. 5 and Table 14, because turbulent deposition was over-estimated in sections 4 and 5, the airborne aerosol concentration was reduced; and the deposition in sections 7 through 19 was underestimated by factors of 2 to 5.5.

For the AEROSIM-M calculation, the flow velocity through the pipe was assumed to be a constant value of 93 m/s. This velocity is characteristic of that at the pipe inlet, but it is roughly half that expected at the pipe outlet. The Liu and Agarwal turbulent-deposition correlation[10] is proportional, for values of "dimensionless relaxation time" below a critical cut-off value, to the 5th power of the flow velocity. Therefore, it is not surprising that the AEROSIM-M results significantly underpredict deposition for pipe sections 7 through 19. We believe that had the calculation been done with two or three constant-velocity nodes - corresponding to the increased velocity in downstream pipe sections - that the comparisons to test deposition data would have been significantly improved.

The AEROSIM-M calculation was the only one that predicted different behavior, as illustrated in Figs. 3 and 4, for the CsOH and MnO aerosols. The overall MnO/CsOH deposition ratio predicted by AEROSIM-M was 0.99, as compared to the aerosol source mass ratio of 1.35. The code calculated enhanced CsOH deposition because the input CsOH aerosol was larger than the MnO aerosol.

The aerosol deposition pattern calculated by RETAIN-2C matched the experimental results reasonably well, except for the deposition calculated in volumes 12 to 15. However, as will be discussed later, the code does not calculate aerosol size correctly; therefore, the validity of the deposition results is questionable. The AUX2.9 results are clearly incorrect because turbulent deposition was not modeled by the code.

We do not know if aerosol resuspension or aerosol wall-film flow was significant in LA1. However, if these did occur, they could have had a major influence on the test results. All of the TRAP-MELT calculations and the AEROSIM-M calculation over-predicted aerosol deposition in the upstream pipe sections. Resuspension or film flow would have decreased the net deposition in the upstream sections. Therefore, it is possible that the TRAP-MELT and AEROSIM-M results do a reasonable job of estimating the turbulent flux of particles to the upstream sections, but resuspension modifies the overall amount of deposition in these sections.

Figure 6 and Table 15 have comparisons of measured and calculated aerosol transport out of the pipe in LA1. Note that RETAIN2C(FN) and TRAP-MELT2(BCL) do a reasonable job of calculating the total leaked aerosol. However, because these codes did not calculate the test deposition pattern well, the validity of the final calculated leaked-mass values is questionable. Although the Italian and United Kingdom TRAP-MELT2 deposition calculations were good, these codes over-estimated the aerosol leakage by factors of 5 and 10, respectively. However, it should be realized that these factors are large because the measured total mass transported out of the test pipe is small.

Calculated AMMD and geometric standard deviation results are shown in Figs. 7 and 8. Although size measurements were not made in the pipe, those made in the CSTF vessel[2] indicated that the mixed aerosol AMMD input to the vessel was 1.64 μm with a geometric standard deviation of 1.91. Comparing these results with the calculated ones illustrated in Figs. 7 and 8, we see that the TRAP-MELT2 and AEROSIM-M results predict reasonable values of AMMD and standard deviation at the pipe outlet. Note that TRAP-MELT2 and AEROSIM predict that the AMMD decreases with distance from the pipe inlet. This behavior is the expected dependence, since turbulent deposition is more effective for larger particles.

The RETAIN-2C AMMD and standard deviation results differ significantly from those calculated by the other codes. This difference occurs because RETAIN-2C is a "log-normal" code and cannot handle situations where an aerosol of one size is mixed with an aerosol of a

different size in a control volume. The increase in AMMD with distance from the pipe inlet is physically unrealistic and makes the validity of the calculated deposition results suspect.

A source of error in all of the LA1 pipe calculations is that average aerosol source-rate and aerosol source-size data were used, rather than the actual time-dependent data from the experiment. Tables 17 and 18 give the measured time-dependent data from test LA1. Two comments can be made about these data: (1) as illustrated in Table 17, there were significant variations in the aerosol source rate to the pipe inlet, and (2) the variations in the aerosol source size (Table 18) were not as large as the source rate variations; however, since turbulent deposition is extremely sensitive to particle size, these variations could be important. At this time, we cannot quantify the uncertainties due to using constant source parameters in the LA1 pipe calculations. We plan to provide time-dependent data for use in the future LA3 calculations.

Table 17. Measured test-pipe aerosol source rate data for test LA1[a]

Time (s)	CsOH source rate (g/s)	MnO source rate (g/s)	Total source rate (g/s)
0[b]	0.563	0.874	1.437
132	0.563	0.874	1.437
324	0.475	0.682	1.157
678	0.437	0.629	1.065
852	0.534	0.448	0.981
1,032	0.553	1.002	1.555
1,218	0.495	0.789	1.283
1,572	0.495	0.565	1.060
1,752	0.281	0.245	0.526
1,932	0.281	0.938	1.219
2,112	0.475	1.716	2.191
2,472	0.524	0.469	0.993
2,952	0.466	0.735	1.201
3,372	0.553	0.661	1.214
3,558	0.495	0.565	1.060
3,600[b]	0.495	0.565	1.060

[a]Aerosol source rate vs time values were obtained by normalizing measured source rate data so that the integrated average source rate equals the average source rate determined from the mass balance data.

[b]Source rate values at 0 and 3,600 s assumed the same as the values at the nearest measurement time.

Table 18. Measured test-pipe aerosol source size-distribution data for test LA1

Time (s)	CsOH AMMD (μm)	CsOH GSD[a]	MnO AMMD (μm)	MnO GSD[a]	CsOH+MnO AMMD (μm)	CsOH+MnO GSD[a]
498	2.09	1.67	1.75	1.73	1.89	1.69
1,398	1.95	1.77	1.50	1.93	1.70	1.85
2,292	2.20	1.84	1.44	1.98	1.67	2.04
3,132	2.01	1.90	1.34	2.13	1.65	2.01
mean values[b]:	2.06	1.80	1.51	1.94	1.73	1.90

[a]Geometric standard deviation.

[b]Note that the mean values quoted here differ slightly from the mean aerosol source values used for the LA1 pipe calculations (Table 1). The aerosol size values in Table 18 are corrected values.

4. SUMMARY OF "FIRST SET" OF LA1 VESSEL CODE-EXPERIMENT COMPARISON RESULTS

As illustrated in Table 19, twelve "first set" calculations were performed to model the vessel aerosol behavior for test LA1. The AUX2.9 code assumes that the aerosol approaches an asymptotic size distribution; all other codes used were discrete size-distribution codes. Two CONTAIN and five NAUA calculations were performed. In terms of the NAUA results, some investigators chose to perform two calculations: one ("NC") with no modeling of water condensation effects after 33,000 s, and the other ("C") where water condensation onto the walls was modeled. The designation of the NAUA-5 (IT) calculations, however, is slightly different: the NAUA-5, NC (IT) calculation considered only water condensation onto wall surfaces while the NAUA-5,C (IT) calculation considered water condensation onto walls and aerosols. In the data plots that follow, NAUA results are always presented together.

Table 20 presents the CsOH, MnO, and total (CsOH+MnO) aerosol concentration data vs time measured in test LA1. These measurements were made, at each time, at a number of locations in the test vessel using "cluster" and "through-the-wall" samplers. The mean and standard error

Table 19. Summary of codes used for first set of LA1 vessel calculations

Code[a]	Code analyst	Affiliation
AEROSIM-M (UK)	S. Ramsdale	United Kingdom, Atomic Energy Authority, Safety and Reliability Directorate
AUX2.9 (SW)	H. Häggblom	Sweden, Studsvik Energiteknik AB
CONTAIN (ORNL)	M. Tobias	United States, Oak Ridge National Laboratory
CONTAIN (UK)	P. Smith	United Kingdom, Atomic Energy Authority, AEE Winfrith
MCT-2 (NYPA)	P. Bieniarz	United States, New York Power Authority
NAUA-4 (NC,EPRI) NAUA-4 (C,EPRI)	R. Sher	United States, Electric Power Research Institute
NAUA-5 (FN)	J. Mäkynen	Finland, Technical Research Centre
NAUA-5 (NC,IT) NAUA-5 (C,IT)	M. Valisi	Italy, ENEL-Thermal and Nuclear Research Centre
QUICK-M (BCL)	V. Kogan	United States, Battelle Columbus Laboratories
REMOVAL (JN)	N. Yamano	Japan, Atomic Energy Research Institute

[a]Initials in parentheses indicate country or organization.

Table 20. Summary of measured vessel aerosol concentration results for LACE LA1

Time (s)	CsOH concentration Mean (g/m^3)	CsOH concentration Standard error of mean (%)	MnO concentration Mean (g/m)	MnO concentration Standard error of mean (%)	CsOH + MnO concentration Mean (g/m)	CsOH + MnO concentration Standard error of mean (%)	Airborne MnO/CsOH ratio
480	1.66E-3	6.9	4.55E-3	12.3	6.21E-3	11.4	2.74
636	2.68E-3	11.7	7.31E-3	5.4	9.99E-3	6.9	2.73
792	2.24E-3	11.5	9.34E-3	7.2	1.16E-2	41.4	4.17
1,080	4.44E-3	7.1	1.86E-2	10.0	2.30E-2	32.3	4.19
1,380	6.90E-3	10.4	1.69E-2	3.4	2.38E-2	2.5	2.45
1,820	6.54E-3	11.8	2.21E-2	13.1	2.86E-2	32.3	3.38
2,520	5.21E-3	10.5	1.46E-2	4.8	1.98E-2	30.8	2.80
3,120	7.24E-3	5.9	1.55E-2	7.4	2.27E-2	23.0	2.14
3,530	6.48E-3	9.3	1.61E-2	6.3	2.26E-2	29.2	2.48
3,840	6.94E-3	11.4	1.63E-2	6.0	2.32E-2	29.2	2.35
4,660	5.16E-3	5.5	1.76E-2	4.7	2.28E-2	29.0	3.41
5,520	4.73E-3	9.7	1.42E-2	8.2	1.89E-2	33.4	3.00
6,720	4.39E-3	6.2	1.65E-2	8.2	2.09E-2	29.3	3.76
9,120	4.08E-3	6.8	1.36E-2	11.3	1.77E-2	9.2	3.33
1.200	3.56E-3	11.1	1.35E-2	9.6	1.71E-2	19.1	3.79
17,000	2.39E-3	20.4	9.85E-3	21.4	1.22E-2	30.2	4.12
18,000	3.23E-3	3.0	1.37E-2	3.2	1.69E-2	18.5	4.24
19,600	2.45E-3	16.4	1.06E-2	20.7	1.31E-2	28.7	4.33
24,000	2.42E-3	13.2	8.39E-3	8.4	1.08E-2	3.6	3.47
32,100	1.75E-3	9.9	9.55E-3	7.0	1.13E-2	5.8	5.46
39,700	1.42E-3	17.5	8.97E-3	36.5	1.04E-2	33.9	6.32
56,900	9.13E-4	23.8	5.03E-3	27.4	5.94E-3	26.8	5.56
67,000	7.59E-4	6.5	3.94E-3	8.0	4.70E-3	7.6	5.19
76,000	5.66E-4	10.2	2.95E-3	13.4	3.52E-3	12.9	5.21
85,300	4.38E-4	7.0	2.26E-3	8.9	2.70E-3	8.5	5.16
95,200	3.04E-4	13.0	1.51E-3	16.7	1.81E-3	16.1	4.97

of the mean (a measure of the random error due to taking multiple measurements at each sampling time) were determined using the following formulations:

$$C_m = \sum_i (C_i)/N, \quad (3)$$

$$E_{se} = [\sum_i (C_m - C_i)^2/(N(N-1))]^{0.5} \quad (4)$$

where C_m = mean aerosol concentration,

E_{se} = standard error of the mean,

C_i = measured aerosol concentration,

N = number of concentration measurements at each sampling time.

At this time, we do not have estimates of the "systematic" sampling errors - those due to errors associated with each aerosol concentration measurement (due to uncertainties in measuring mass deposited on filters, in measuring sampling flow rates, etc). Estimates of these errors will be provided in a future HEDL report. Note that Table 20 also presents, based on the mean concentration values, the airborne MnO/CsOH mass ratio as a function of time.

Table 21 summarizes the measured aerosol removal by settling, wall plateout, and transport (by leakage from the vessel to the scrubber) in LA1. Note that settling and plateout were comparable in LA1, and that the sum of settling and plateout were comparable to the total aerosol leakage. Table 22 lists results from cascade impactor measurements of AMMD and geometric standard deviation for test LA1.

Table 21. Summary of measured aerosol deposition and leakage results for LACE LA1

	CsOH	MnO	CsOH+MnO
Total aerosol settled, g	3.16	10.7	13.86
Total aerosol plated, g	1.65	10.22	11.87
Total aerosol leaked from vessel, g	7.29	25.7	32.99

Table 22. Summary of measured aerosol size-distribution results for LACE LA1

Sample time (s)	Mixed aerosol aerodynamic mass-median diameter (μm)	Geometric standard deviation
1,470	0.95	2.65
3,210	0.95	2.63
5,076	0.81	2.65
7,320	1.00	2.35
7,680	1.15	2.35
10,680	1.20	2.18
13,500	1.22	2.21
14,100	1.15	2.11
24,700	1.26	1.83
43,800	1.60	1.67
95,400	1.30	1.61

Figures 9 through 15 graph the aerosol concentration comparison results for the first set of vessel calculations. Comparisons with calculated total, CsOH, and MnO concentrations are shown in Figs. 9 through 14 while Fig. 15 shows comparisons of calculated and measured airborne MnO/CsOH mass ratio. These data are only shown for AEROSIM-M, CONTAIN, and QUICK-M; for all other codes the mass ratio was fixed throughout the calculation at a value of 4.47.

Error estimates for the aerosol concentration calculations were made for two time periods: the aerosol source period (0 to 3,600 s) and the aerosol source plus depletion periods (0 to 100,000 s). The aerosol concentration error-estimate results are presented in Tables 23 and 24. These were based on calculations of "relative mean-square errors" at given concentration sampling times, defined as follows:

$$E_{rms,i} = [(C_m - C_c)^2/C_m^2] \qquad (5)$$

where $E_{rms,i}$ = relative mean-square error at given sampling time,

C_m = measured aerosol concentration,

C_c = calculated aerosol concentration.

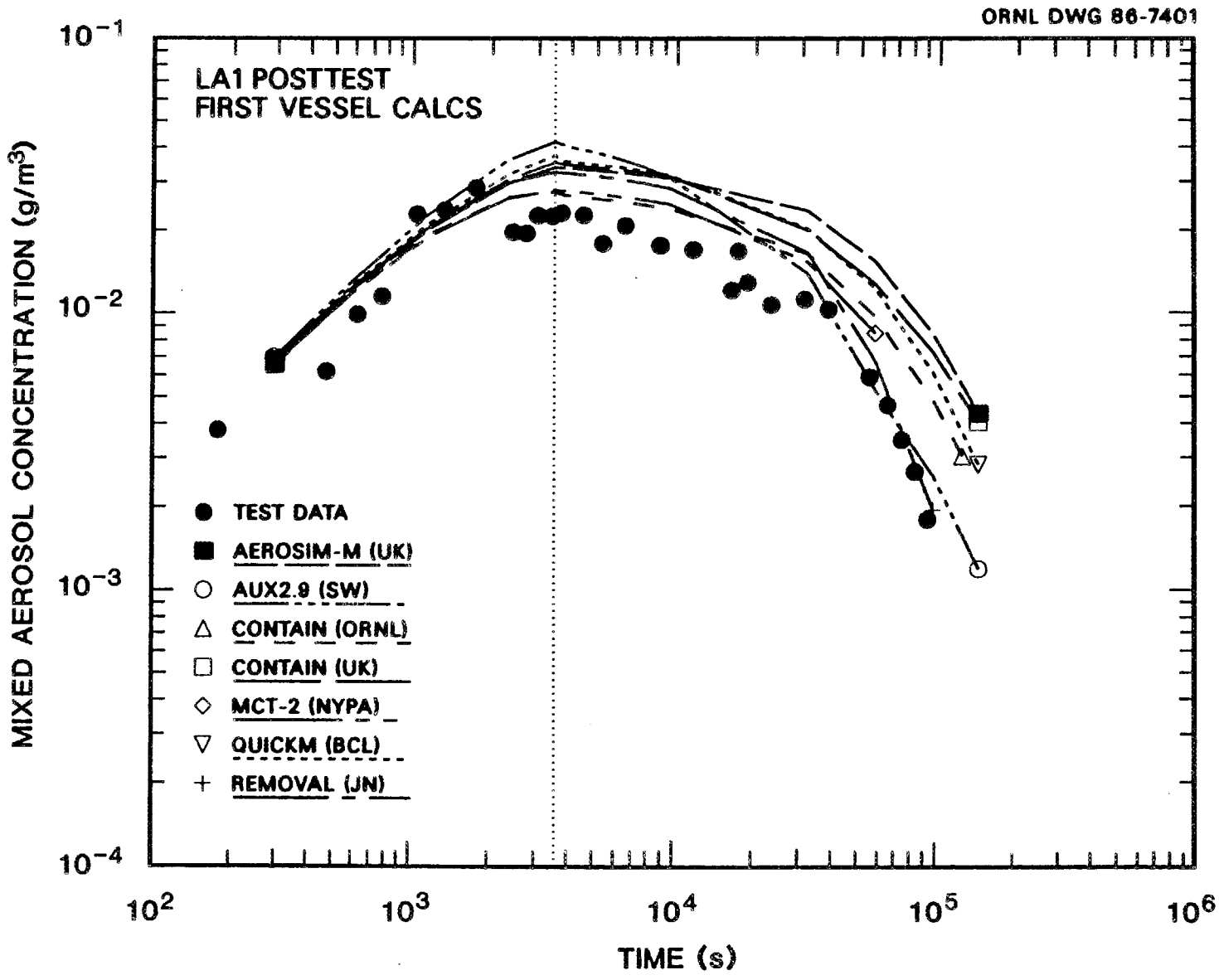

Fig. 9. LA1 "first set" vessel results: airborne mixed aerosol concentration vs time, for codes other than NAUA.

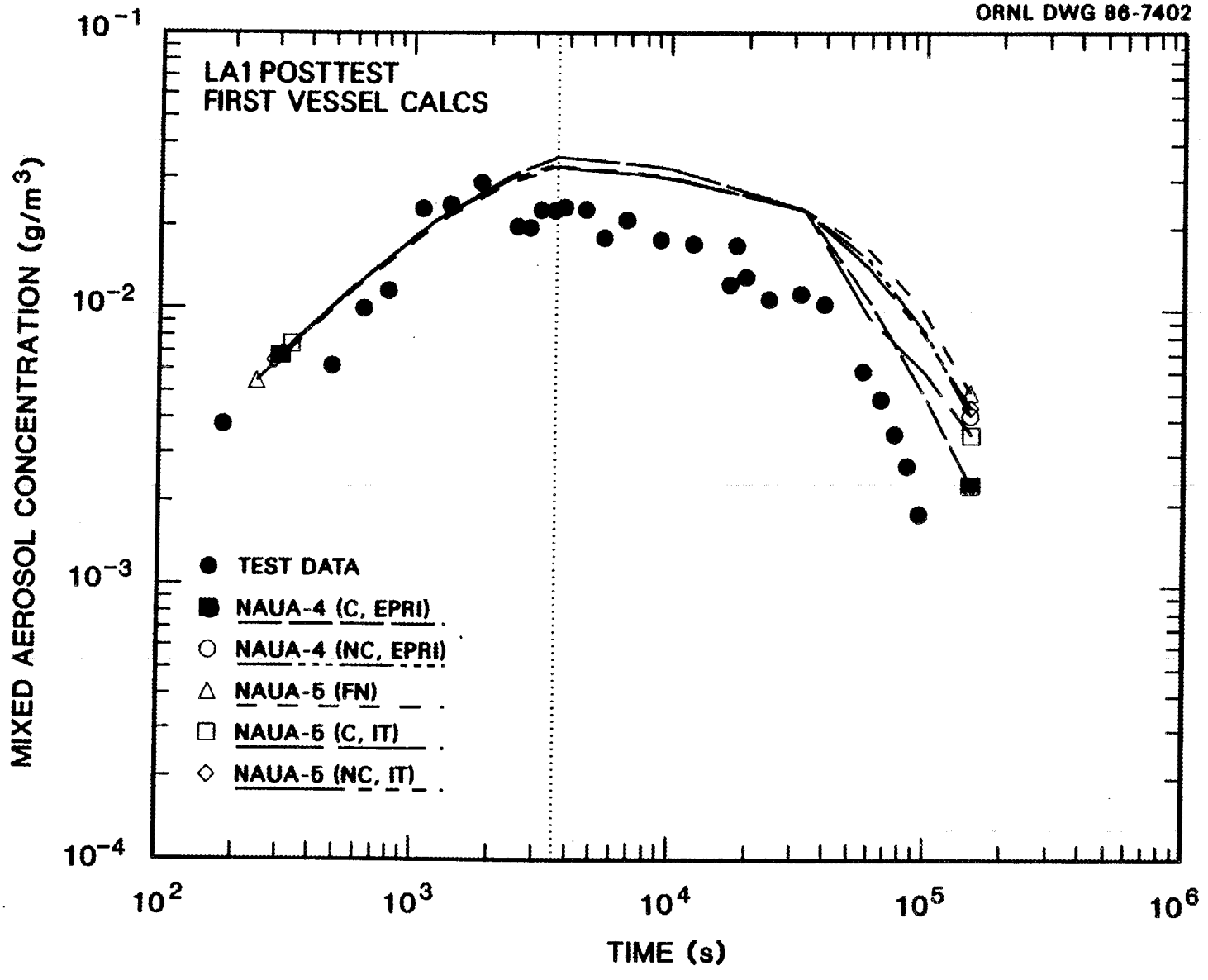

Fig. 10. LA1 "first set" vessel results: airborne mixed aerosol concentration vs time, for NAUA calculations.

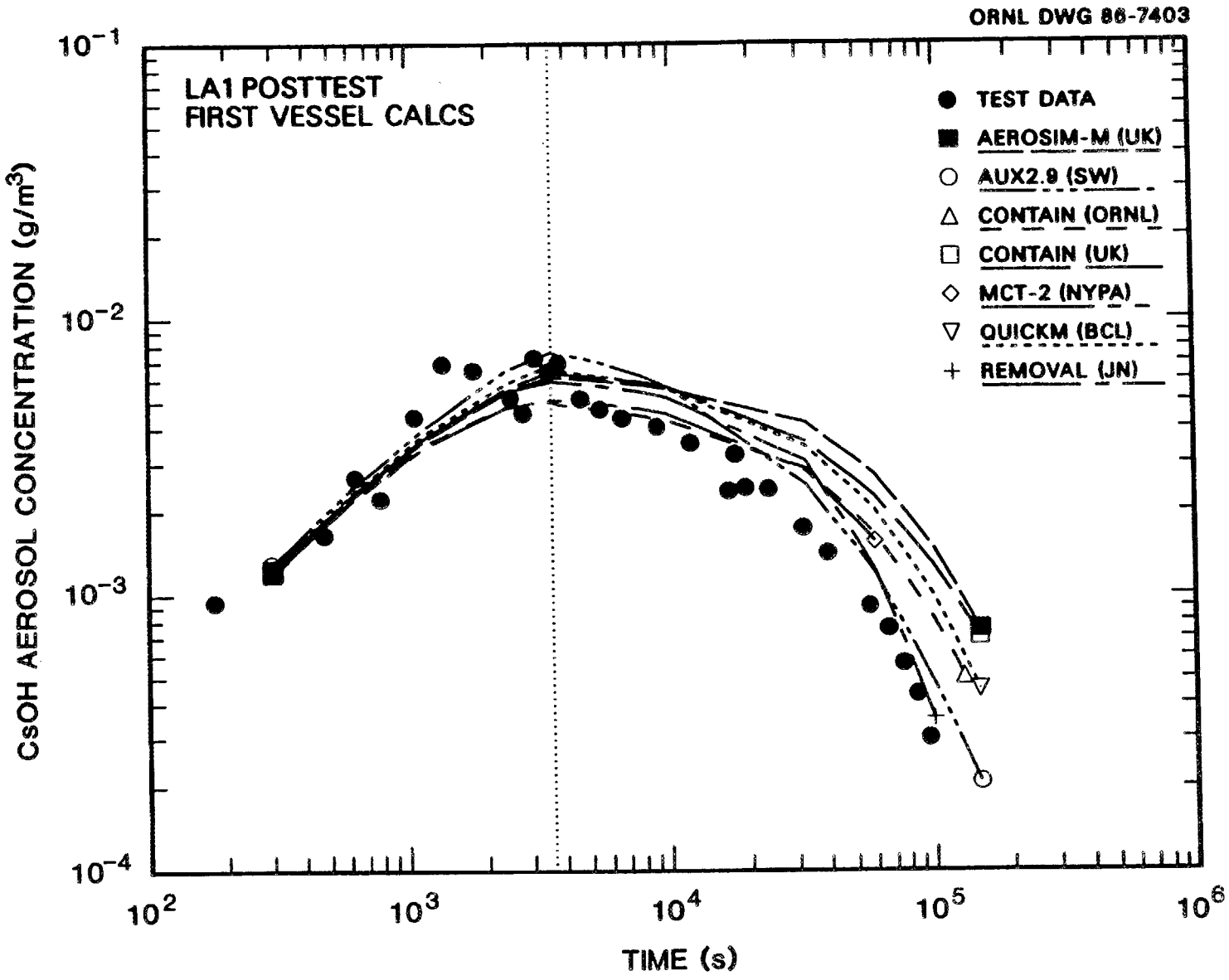

Fig. 11. LA1 "first set" vessel results: airborne CsOH aerosol concentration vs time, for codes other than NAUA.

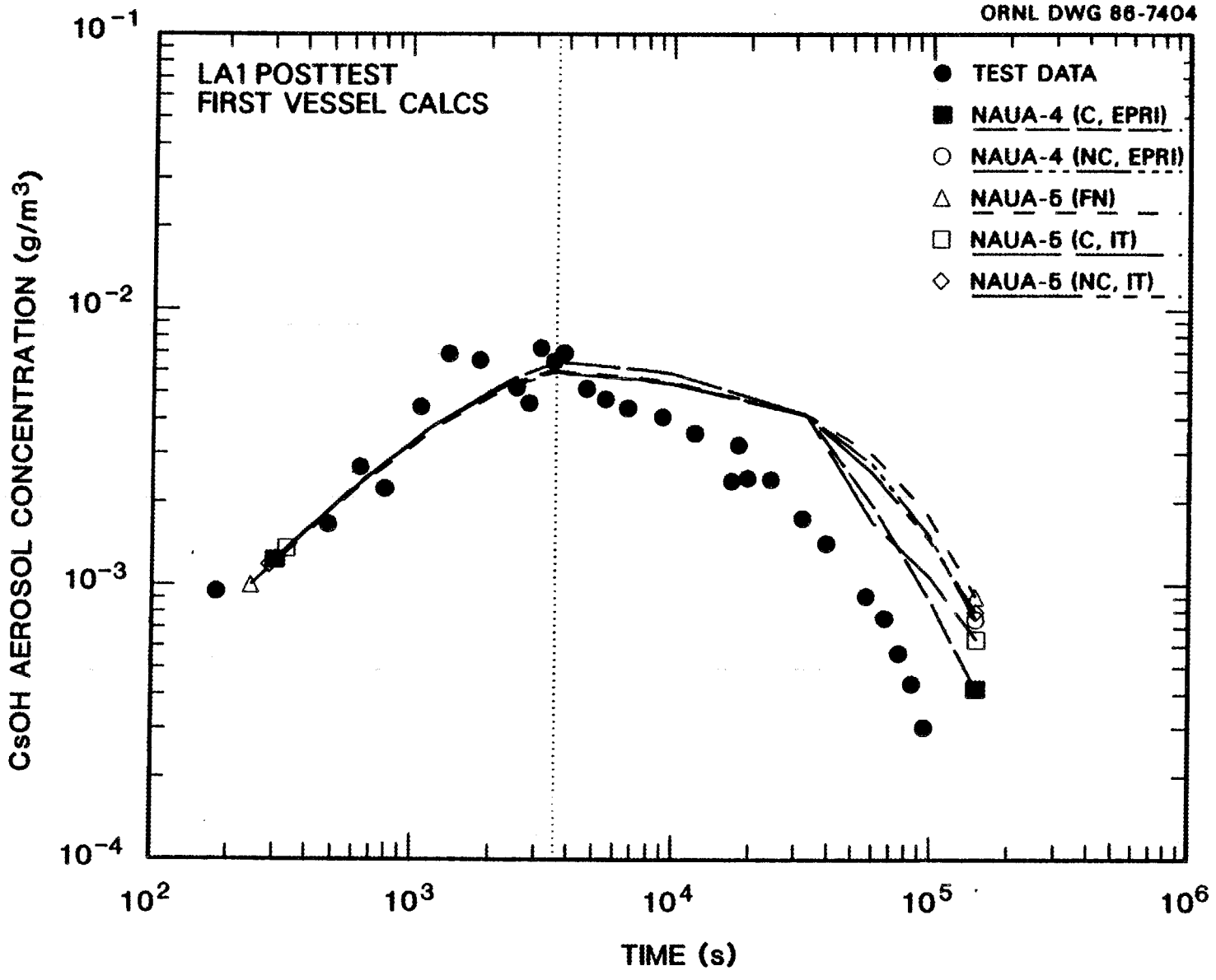

Fig. 12. LA1 "first set" vessel results: airborne CsOH aerosol concentration vs time, for NAUA calculations.

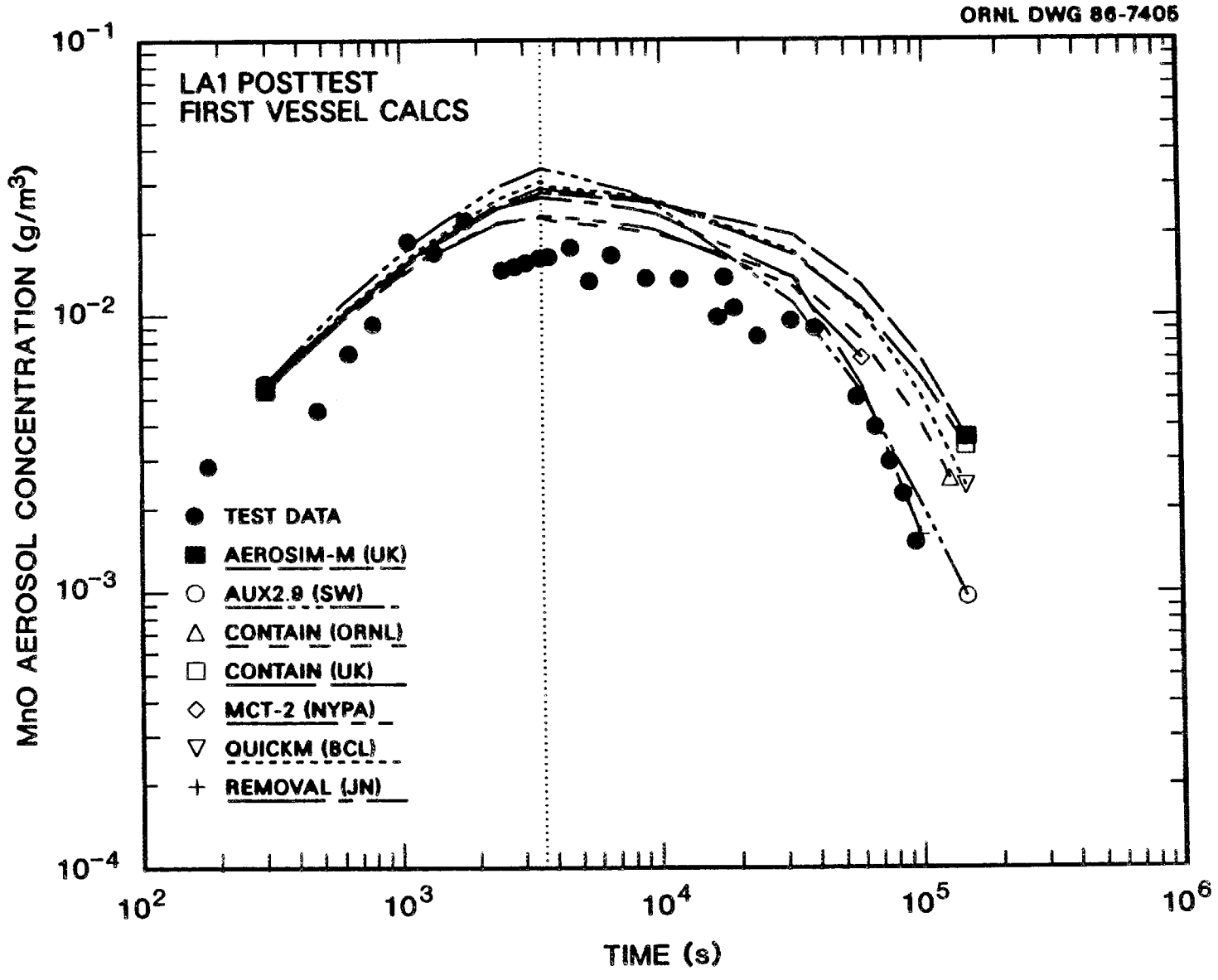

Fig. 13. LA1 "first set" vessel results: airborne MnO aerosol concentration vs time, for codes other than NAUA.

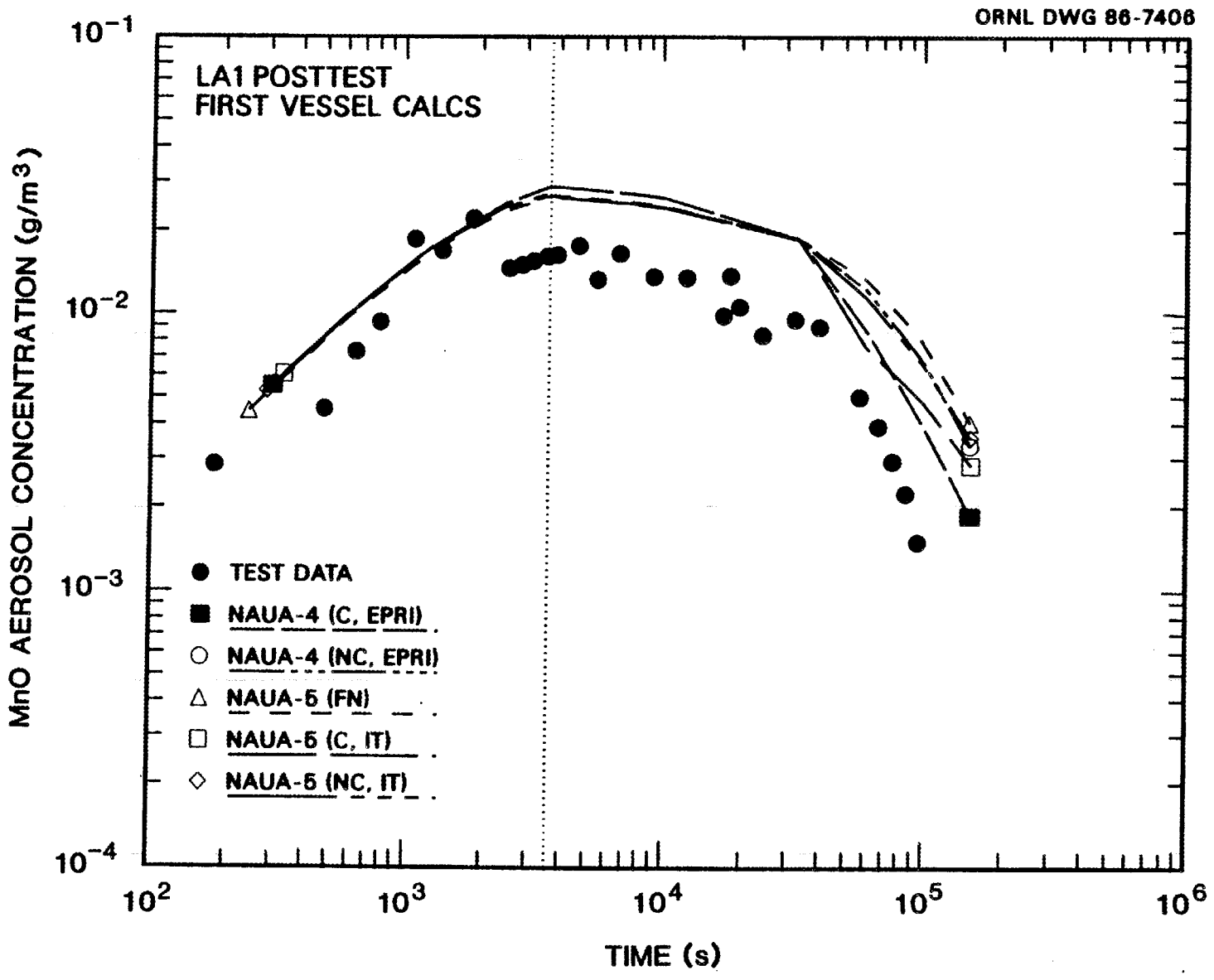

Fig. 14. LA1 "first set" vessel results: airborne MnO aerosol concentration vs time, for NAUA calculations.

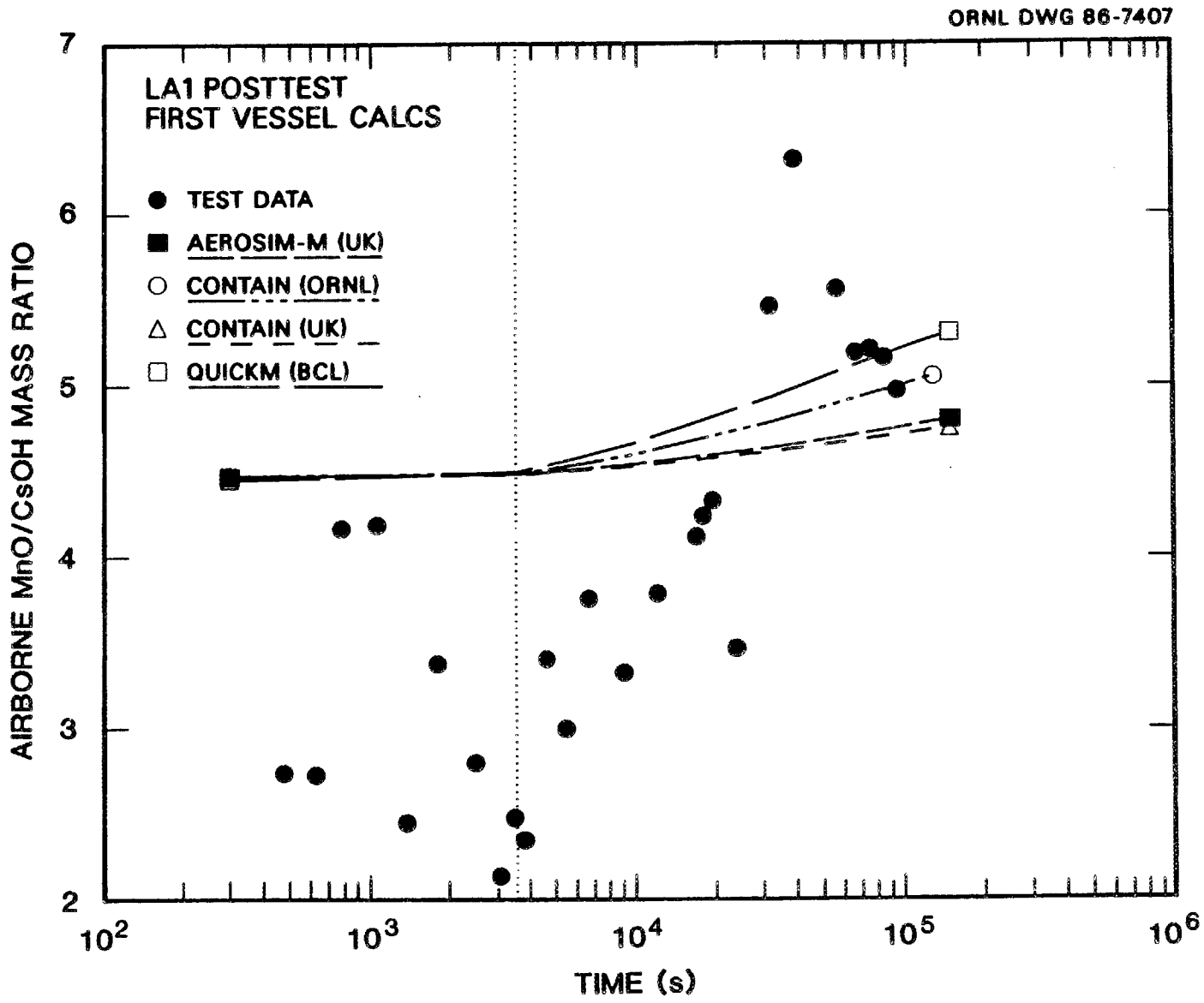

Fig. 15. LA1 "first set" vessel results: airborne MnO/CsOH mass ratio vs time calculated by "multi-component" codes.

Table 23. Calculated errors in predicted aerosol concentrations during aerosol source period (0 to 3,600 s); first set calculations

CsOH+MnO		CsOH		MnO	
Code	Average mean square error (%)	Code	Average mean square error (%)	Code	Average mean square error (%)
AEROSIM-M (UK)	37.1	AEROSIM-M (UK)	22.0	AEROSIM-M (UK)	71.1
AUX2.9 (SW)	55.6	AUX2.9 (SW)	21.5	AUX2.9 (SW)	73.5
CONTAIN (ORNL)	28.6	CONTAIN (ORNL)	26.3	CONTAIN (ORNL)	57.8
CONTAIN (UK)	40.3	CONTAIN (UK)	21.3	CONTAIN (UK)	55.1
MCT-2 (NYPA)	28.9	MCT-2 (NYPA)	26.5	MCT-2 (NYPA)	39.8
NAUA-4,C(EPRI)	39.6	NAUA-4,C(EPRI)	21.3	NAUA-4,C(EPRI)	54.3
NAUA-4,NC(EPRI)	39.6	NAUA-4,NC(EPRI)	21.3	NAUA-4,NC(EPRI)	54.3
NAUA-5 (FN)	34.1	NAUA-5 (FN)	22.7	NAUA-5 (FN)	47.4
NAUA-5,C (IT)	36.6	NAUA-5,C (IT)	22.3	NAUA-5,C (IT)	50.3
NAUA-5,NC (IT)	37.2	NAUA-5,NC (IT)	21.9	NAUA-5,NC (IT)	51.2
QUICK-M (BCL)	44.3	QUICK-M (BCL)	20.6	QUICK-M (BCL)	60.0
REMOVAL (JN)	36.7	REMOVAL (JN)	22.0	REMOVAL (JN)	50.6

Table 24. Calculated errors in predicted aerosol concentrations (0 to 100,000 s); first set calculations

CsOH+MnO		CsOH		MnO	
Code	Average mean square error (%)	Code	Average mean square error (%)	Code	Average mean square error (%)
AEROSIM-M (UK)	107.5	AEROSIM-M (UK)	114.4	AEROSIM-M (UK)	110.5
AUX2.9 (SW)	59.0	AUX2.9 (SW)	39.7	AUX2.9 (SW)	71.1
CONTAIN (ORNL)	53.1	CONTAIN (ORNL)	54.5	CONTAIN (ORNL)	57.8
CONTAIN (UK)	89.3	CONTAIN (UK)	91.6	CONTAIN (UK)	94.2
MCT-2 (NYPA)	39.8	MCT-2 (NYPA)	43.7	MCT-2 (NYPA)	45.7
NAUA-4,C(EPRI)	79.9	NAUA-4,C(EPRI)	83.3	NAUA-4,C(EPRI)	85.3
NAUA-4,NC(EPRI)	104.6	NAUA-4,NC(EPRI)	115.6	NAUA-4,NC(EPRI)	107.4
NAUA-5 (FN)	111.1	NAUA-5 (FN)	126.4	NAUA-5 (FN)	112.1
NAUA-5,C (IT)	74.2	NAUA-5,C (IT)	78.9	NAUA-5,C (IT)	78.8
NAUA-5,NC (IT)	96.9	NAUA-5,NC (IT)	107.8	NAUA-5,NC (IT)	99.2
QUICK-M (BCL)	85.7	QUICK-M (BCL)	77.0	QUICK-M (BCL)	93.0
REMOVAL (JN)	48.2	REMOVAL (JN)	42.0	REMOVAL (JN)	56.6

The calculated aerosol concentrations at prescribed sampling times were determined by interpolation of the code results. The average errors quoted in Tables 23 and 24 were determined as follows:

$$E_{av} = [(E_{rms,i})/N_s]^{0.5} \qquad (6)$$

where E_{av} = average error,

$E_{rms,i}$ = relative error at ith time,

N_s = number of sampling times.

For the error calculations during the aerosol source periods, E_{rms} values were calculated for sampling times of 480, 636, 792, 1,080, 1,380, 1,820, 2,520, 3,120, and 3,530 s (see Table 18). For the error calculations for 0 to 100,000 s, E_{rms} values were calculated for the above aerosol source times and for 5,520, 9,120, 12,200, 18,000, 24,000, 32,100, 39,700, 56,900, and 85,300 s.

Figures 16 through 22 detail the aerosol settling data including the settled-mass values determined at the end of the experiment. Table 25 lists errors in calculated overall settling values which are calculated using the formulations in Eqs. 5 and 6 with $N_s = 1$ (the final settled mass value). Table 25 also displays values of the ratio of measured-to-calculated overall settled mass. Figures 23 through 29 and Table 26 contain similar data for aerosol plateout, while Figures 30 through 36 and Table 27 present similar data for aerosol leakage from the vessel. Note that comparisons of settling and plateout were not made for the MCT-2 and AUX2.9 calculations because these codes only provided data on "retained" mass and did not have breakdown into settling and plateout.

Finally, the measured and calculated AMMD and geometric standard deviation data (for the mixed aerosol) are shown in Figs. 37 through 41, and errors in the code calculations for AMMD and standard deviation are detailed in Table 28. The errors were again calculated using equations (5) and (6), and used the aerosol-size sampling times listed in Table 22.

The major thing to note from the aerosol concentration results in Figs. 9 through 14 is that, for times greater than roughly 1,500 s, most calculated results tended to overestimate the airborne aerosol concentrations. There seems to be, based on looking at the test data, three

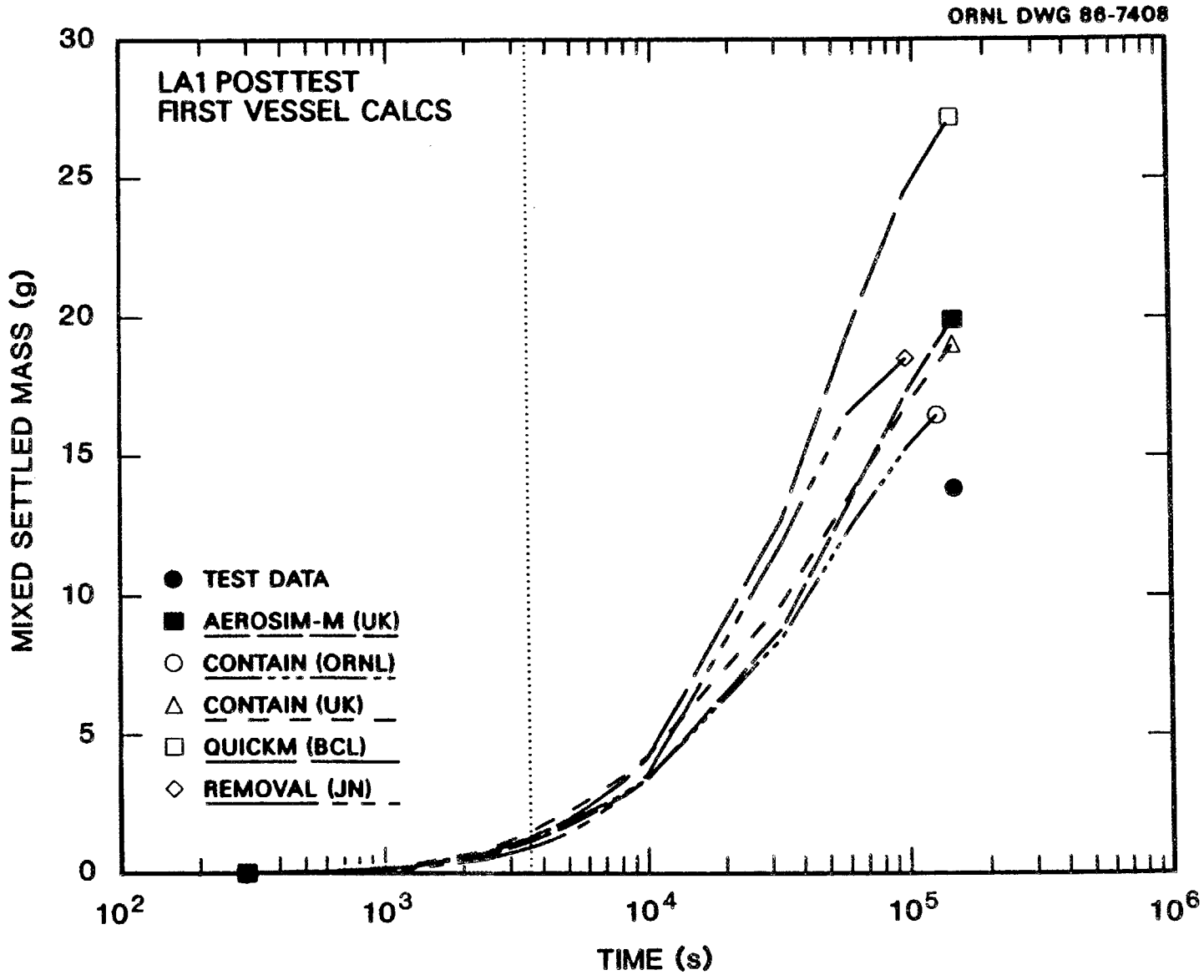

Fig. 16. LA1 "first set" vessel results: cumulative mixed aerosol settling vs time for codes other than NAUA.

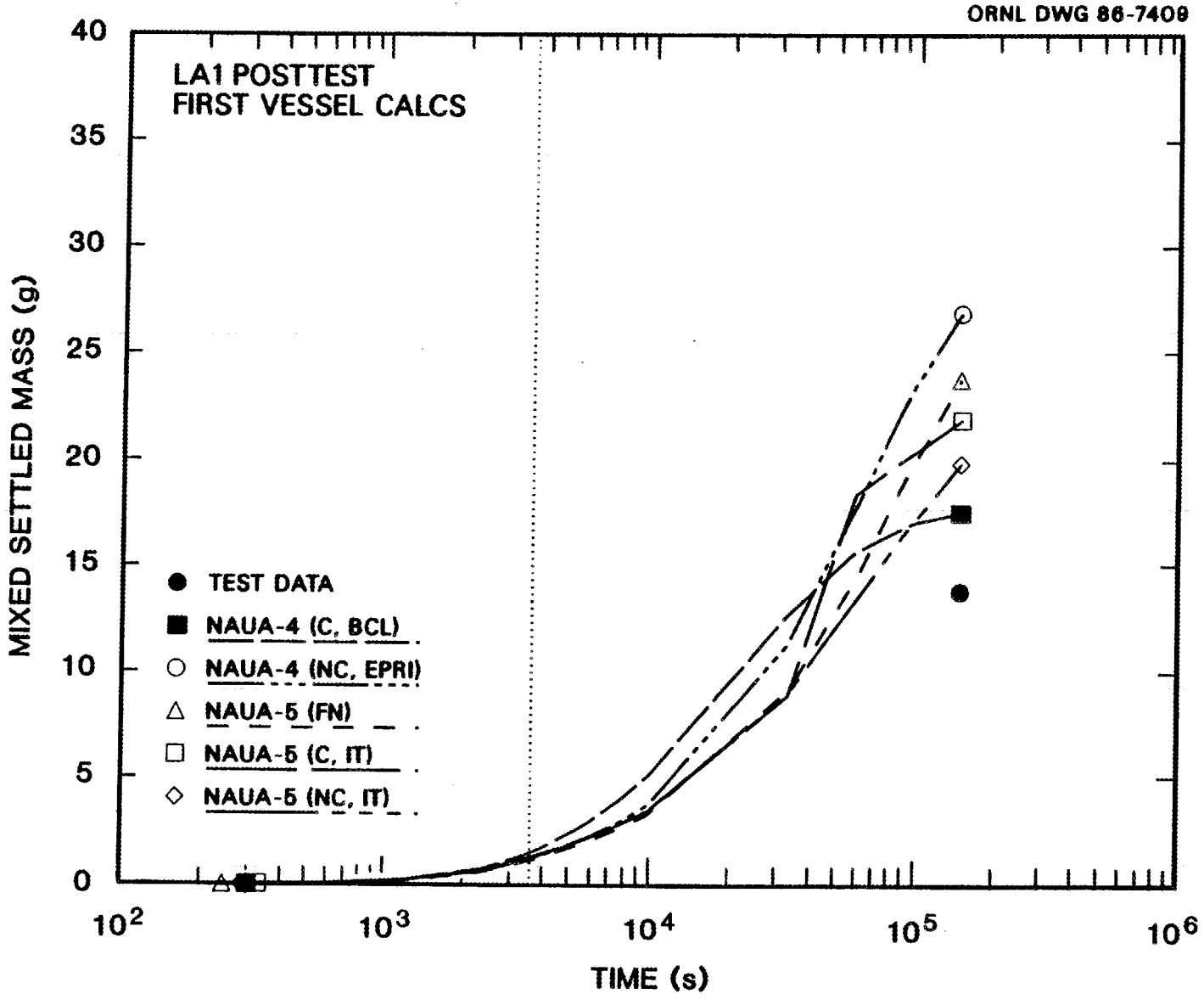

Fig. 17. LA1 "first set" vessel results: cumulative mixed aerosol settling vs time for NAUA calculations.

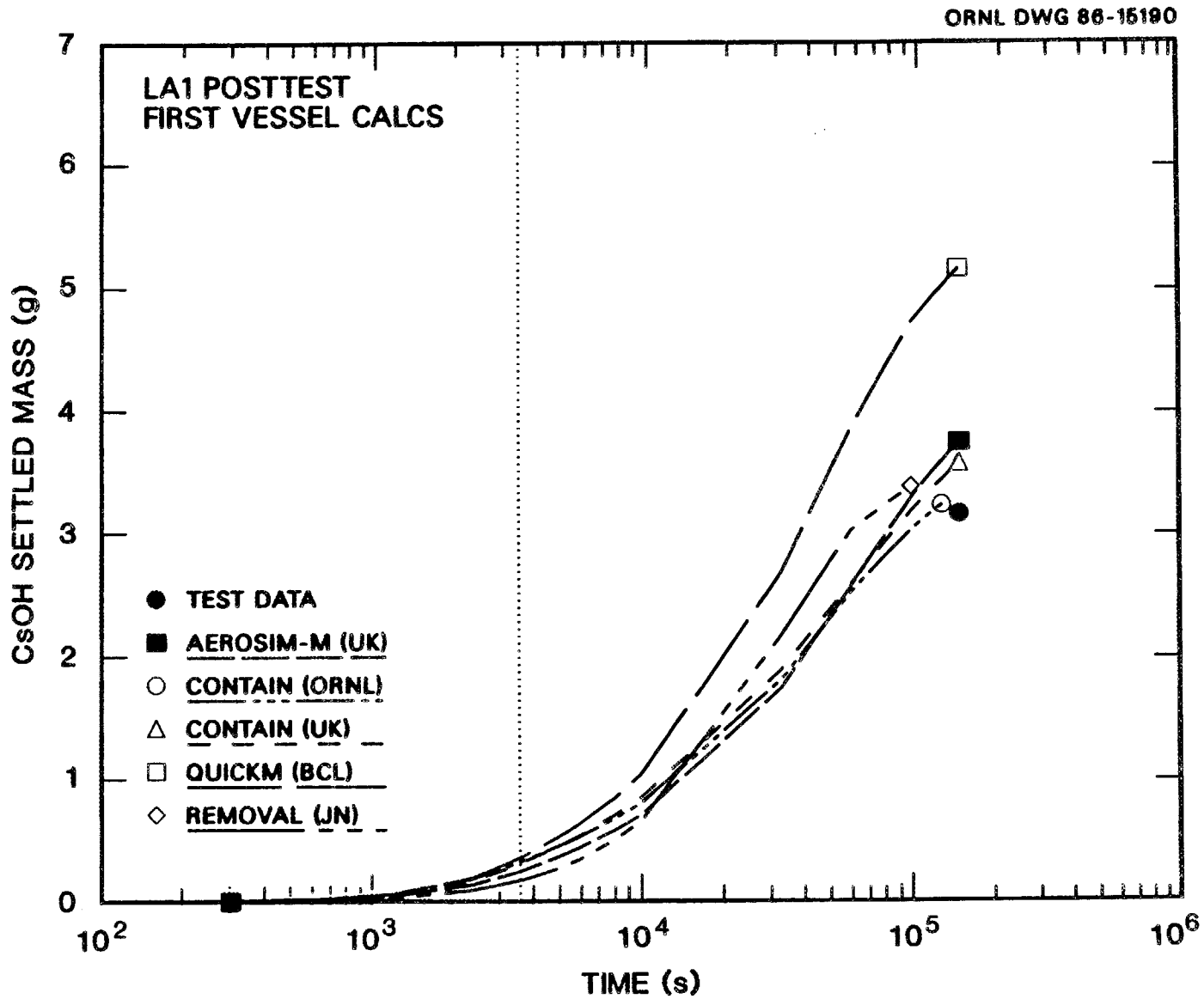

Fig. 18. LA1 "first set" vessel results: cumulative CsOH aerosol settling vs time, for codes other than NAUA.

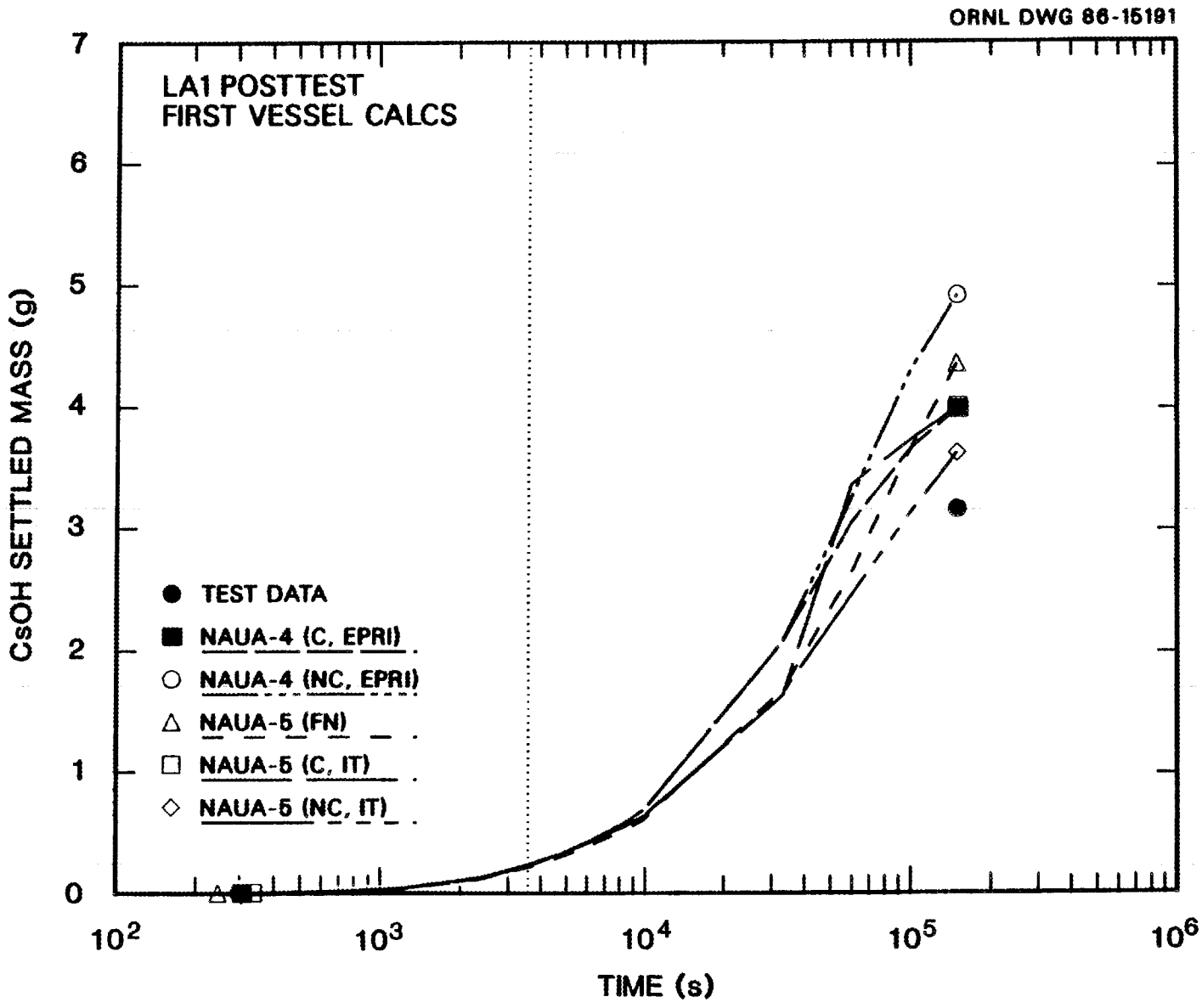

Fig. 19. LA1 "first set" vessel results: cumulative CsOH aerosol settling vs time, for NAUA calculations.

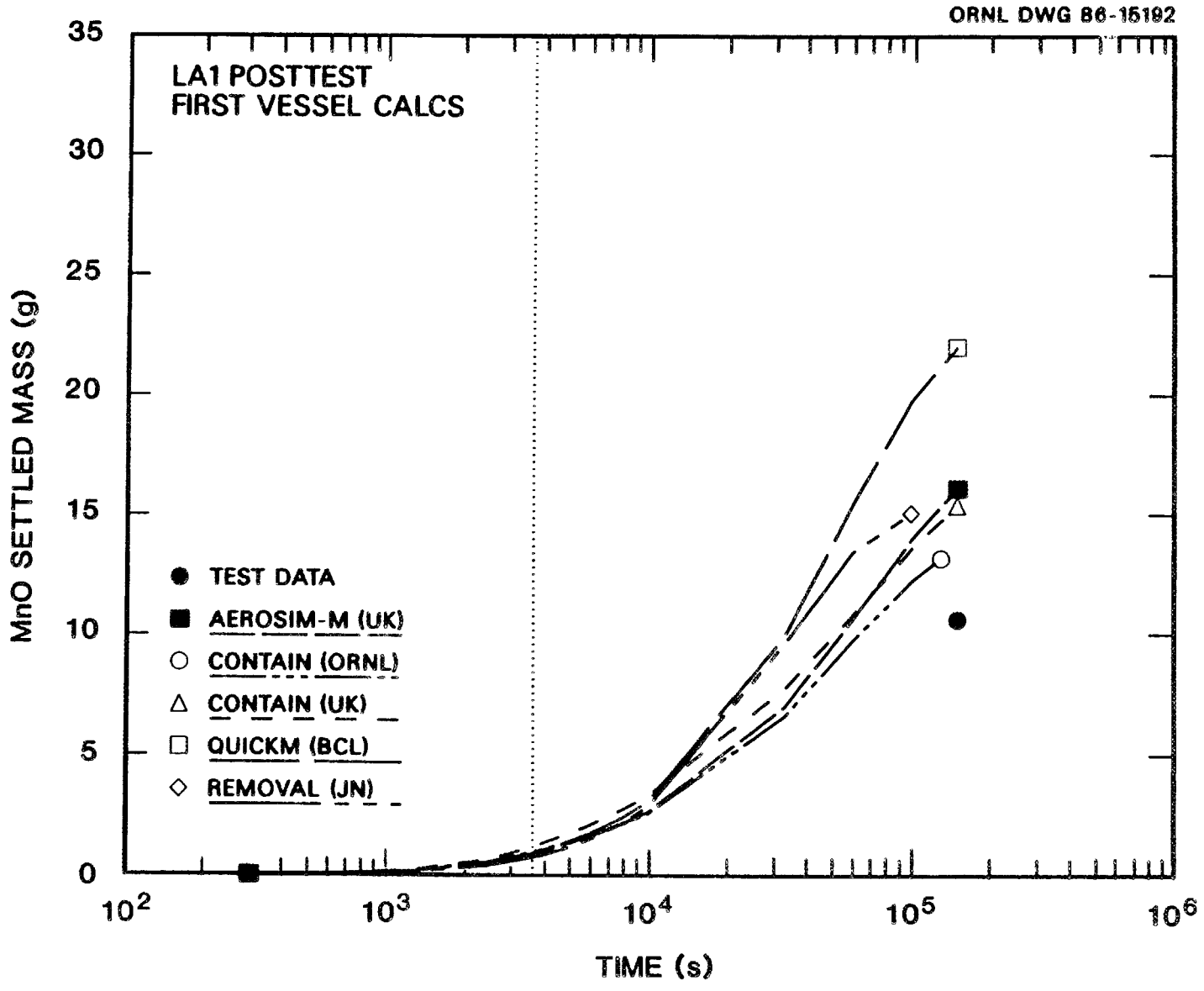

Fig. 20. LA1 "first set" vessel results: cumulative MnO aerosol settling vs time, for codes other than NAUA.

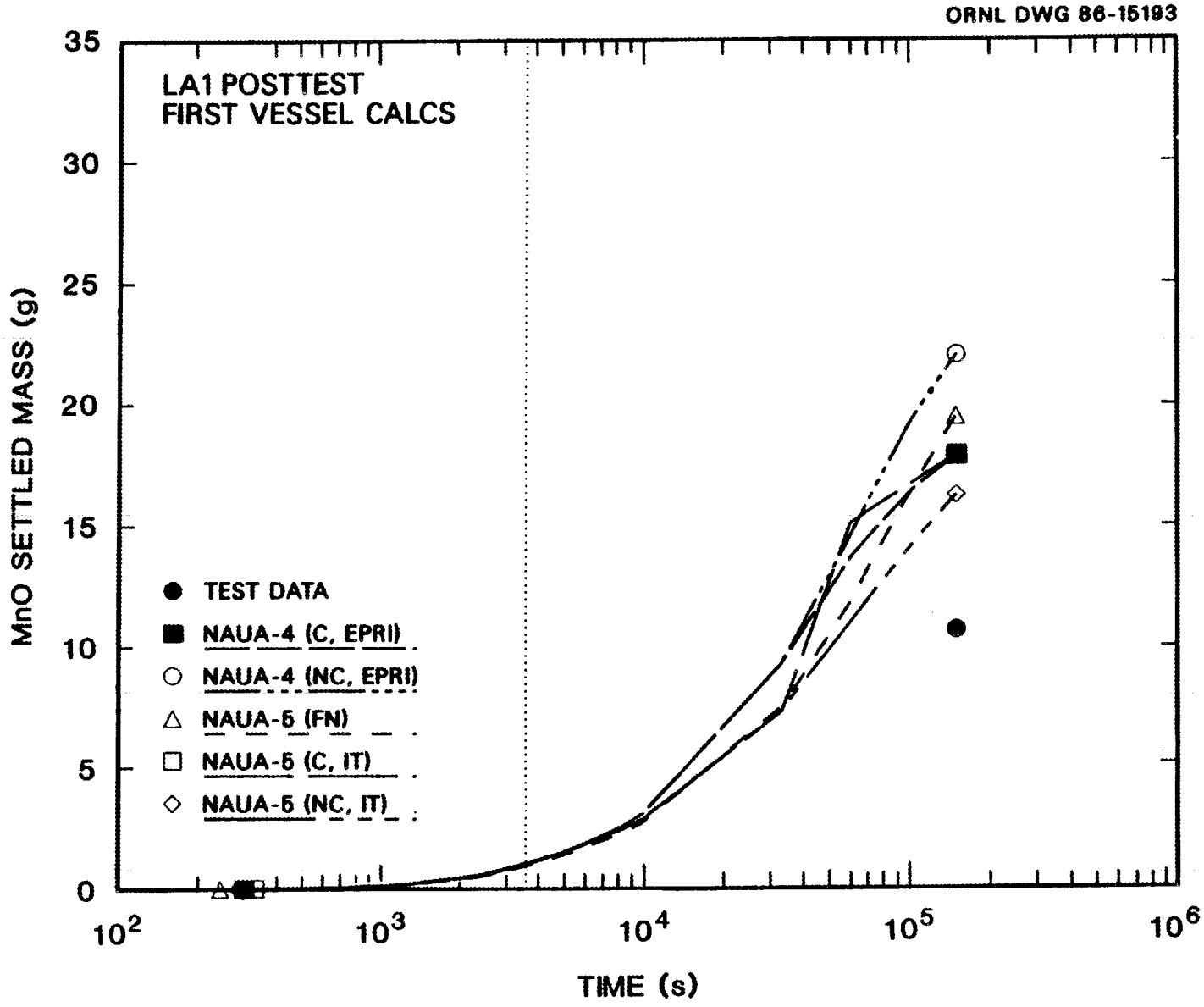

Fig. 21. LA1 "first set" vessel results: cumulative MnO aerosol settling vs time, for NAUA calculations.

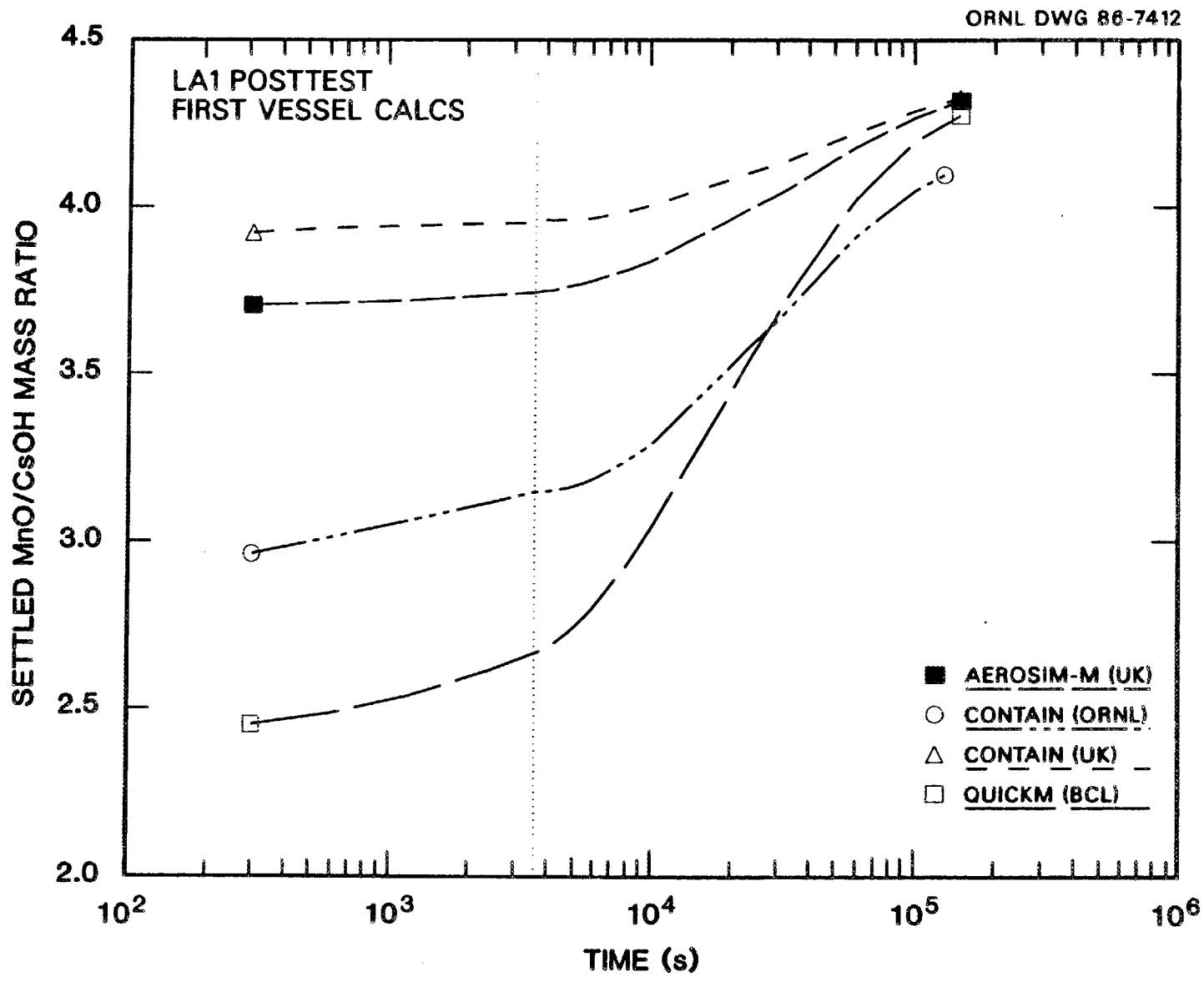

Fig. 22. LA1 "first set" vessel results: settled MnO/CsOH mass ratio vs time calculated by "multi-component" codes.

Table 25. Calculated errors in predicted aerosol settling, first set calculations

CsOH+MnO settled mass Test value = 13.86 g				CsOH settled mass Test value = 3.16 g				MnO settled mass Test value = 10.7 g			
Code	Calc settled mass (g)	Mean square error (%)	T/C[a]	Code	Calc settled mass (g)	Mean square error (%)	T/C[a]	Code	Calc settled mass (g)	Mean square error (%)	T/C[a]
AEROSIM-M (UK)	19.90	43.6	0.70	AEROSIM-M (UK)	3.74	18.4	0.84	AEROSIM-M (UK)	16.15	50.9	0.66
CONTAIN (ORNL)	16.47	18.8	0.84	CONTAIN (ORNL)	3.23	2.2	0.98	CONTAIN (ORNL)	13.24	23.7	0.81
CONTAIN (UK)	19.01	37.2	0.73	CONTAIN (UK)	3.57	13.0	0.89	CONTAIN (UK)	15.44	44.3	0.69
NAUA-4,C(EPRI)	21.80	57.3	0.64	NAUA-4,C(EPRI)	3.98	25.9	0.79	NAUA-4,C(EPRI)	17.82	66.5	0.60
NAUA-4,NC(EPRI)	26.90	94.1	0.52	NAUA-4,NC(EPRI)	4.91	55.4	0.64	NAUA-4,NC(EPRI)	21.99	105.5	0.49
NAUA-5 (FN)	23.81	71.8	0.58	NAUA-5 (FN)	4.35	37.7	0.73	NAUA-5 (FN)	19.46	81.9	0.55
NAUA-5,C (IT)	21.91	58.1	0.63	NAUA-5,C (IT)	4.00	26.6	0.79	NAUA-5,C (IT)	17.91	67.4	0.60
NAUA-5,NC (IT)	19.85	43.2	0.70	NAUA-5,NC (IT)	3.62	14.6	0.87	NAUA-5,NC (IT)	16.23	51.7	0.66
QUICK-M (BCL)	27.17	96.0	0.51	QUICK-M (BCL)	5.15	63.0	0.61	QUICK-M (BCL)	22.02	105.8	0.49
REMOVAL (JN)	18.50	33.5	0.75	REMOVAL (JN)	3.38	7.0	0.93	REMOVAL (JN)	15.12	41.3	0.71

[a]"T/C" stands for the ratio of total measured settling to total calculated settling.

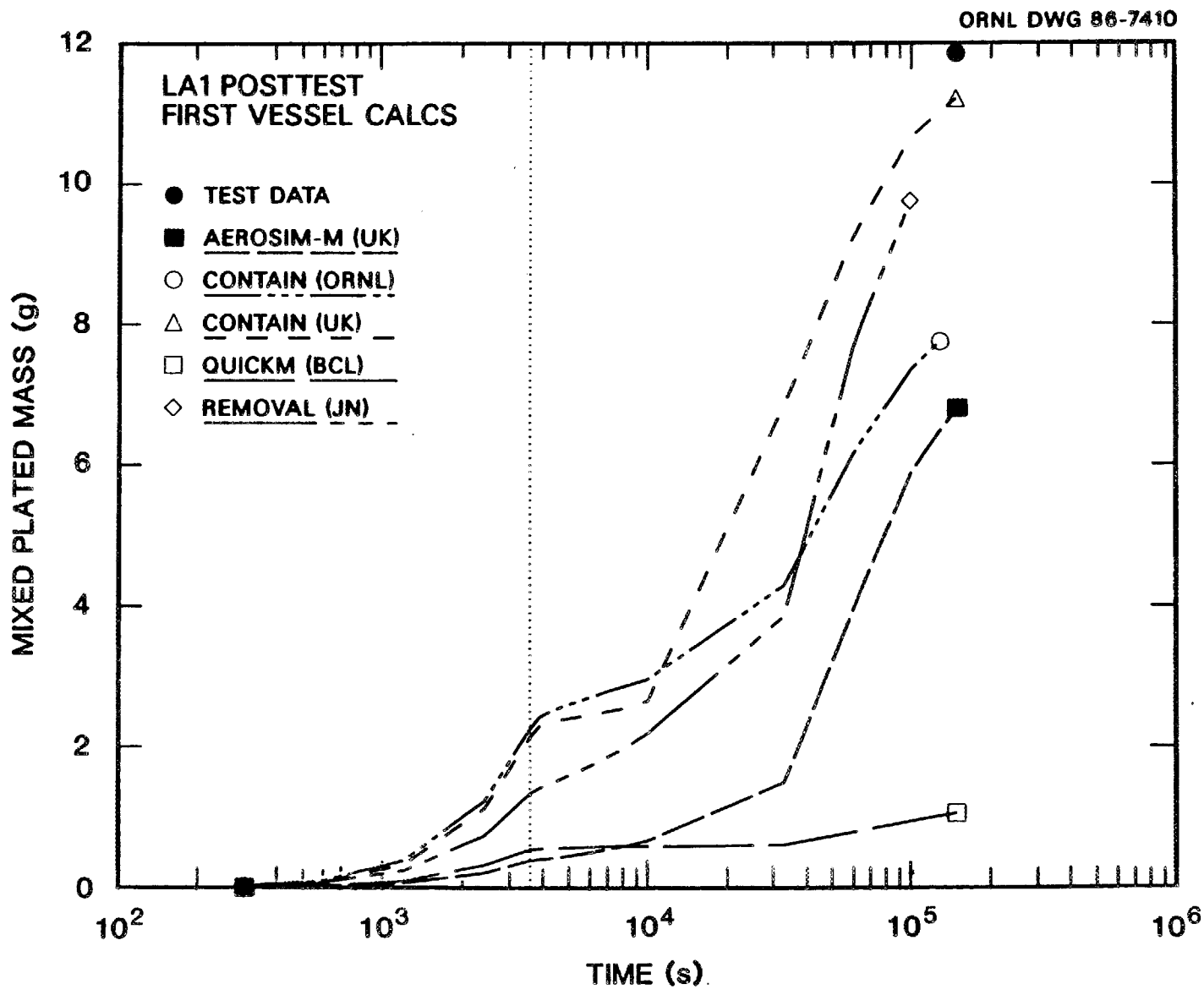

Fig. 23. LA1 "first set" vessel results: cumulative mixed aerosol plateout vs time, for codes other than NAUA.

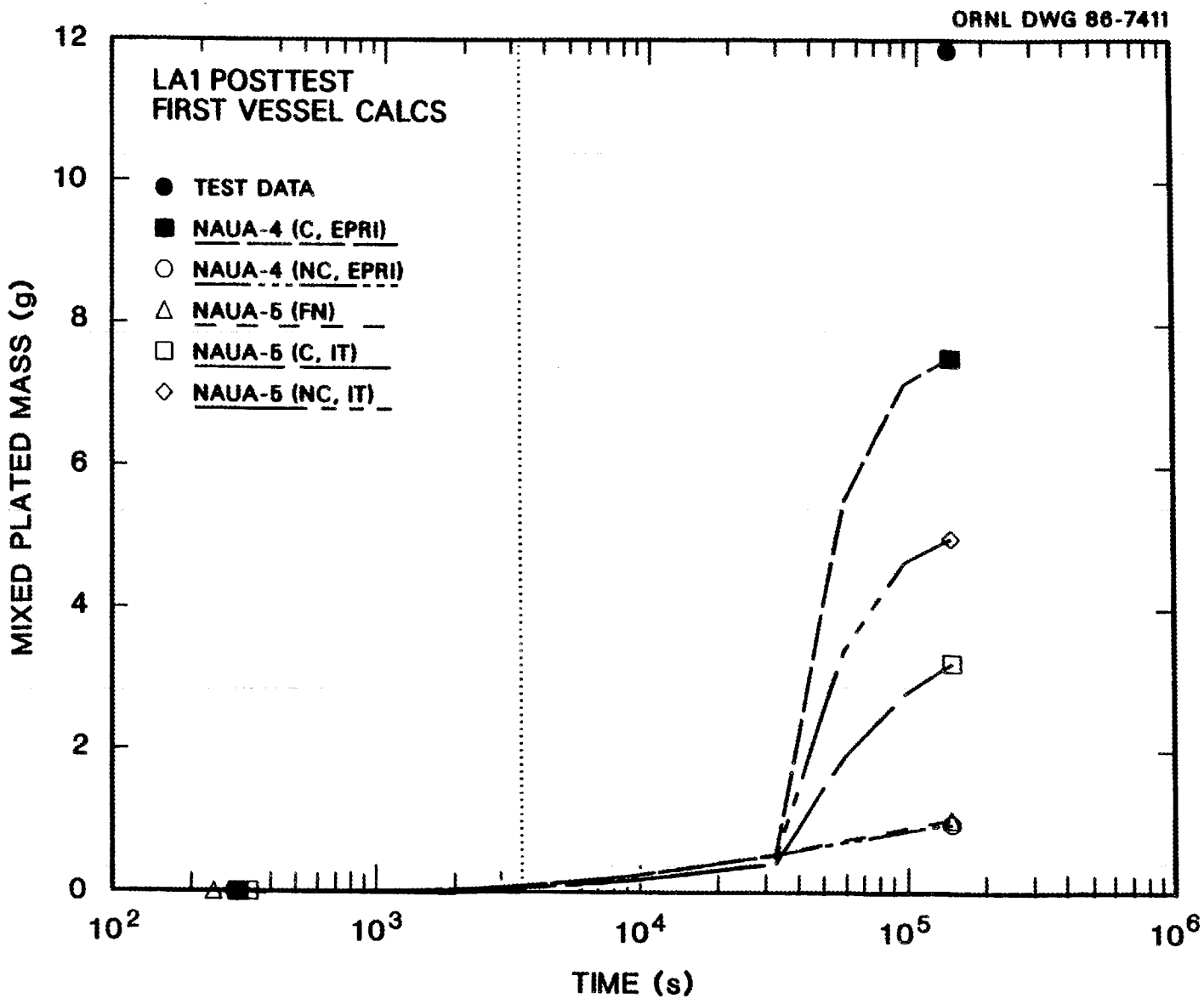

Fig. 24. LA1 "first set" vessel results: cumulative mixed aerosol plateout vs time, for NAUA calculations.

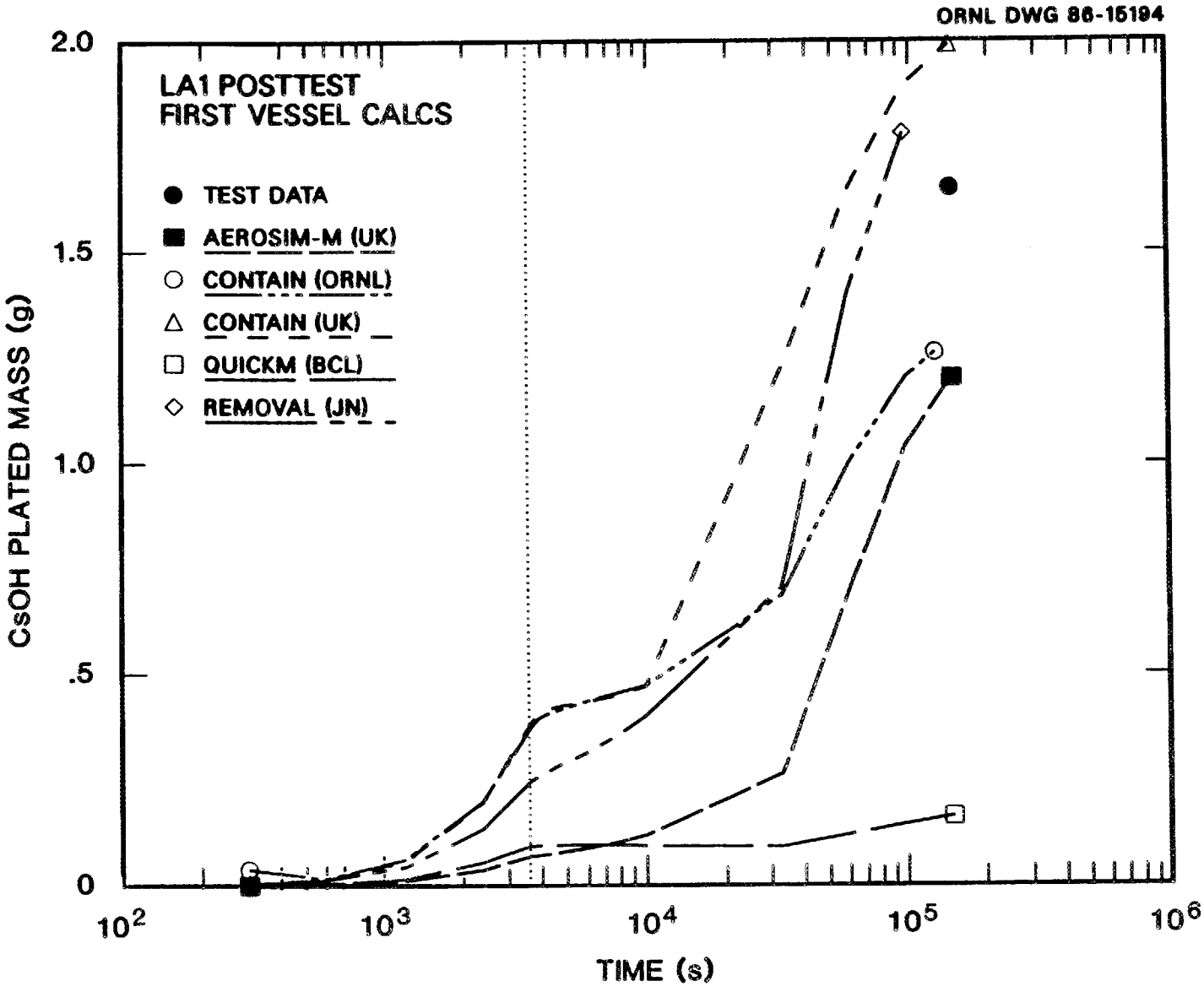

Fig. 25. LA1 "first set" vessel results: cumulative CsOH aerosol plateout vs time, for codes other than NAUA.

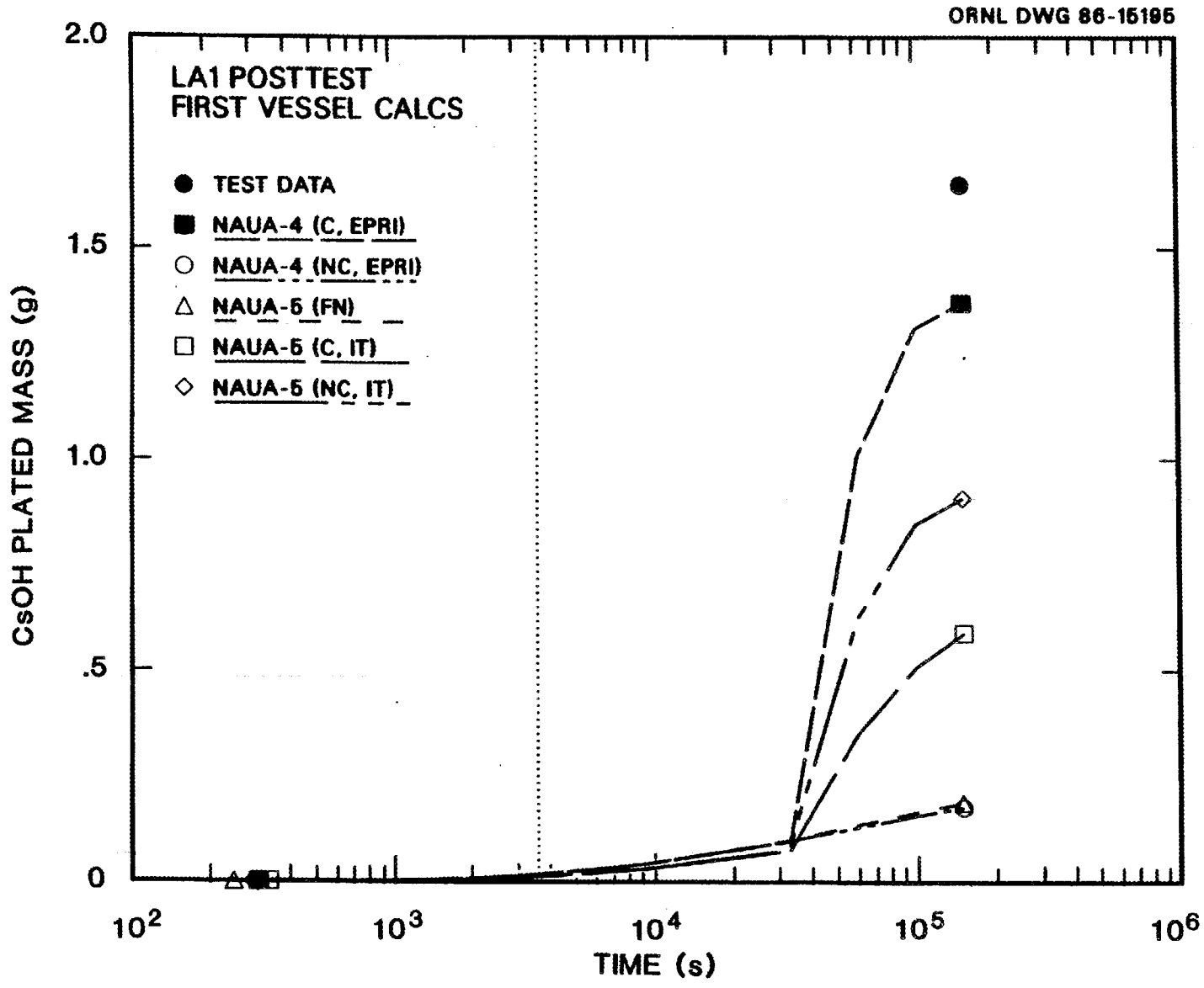

Fig. 26. LA1 "first set" vessel results: cumulative CsOH aerosol plateout vs time, for NAUA calculations.

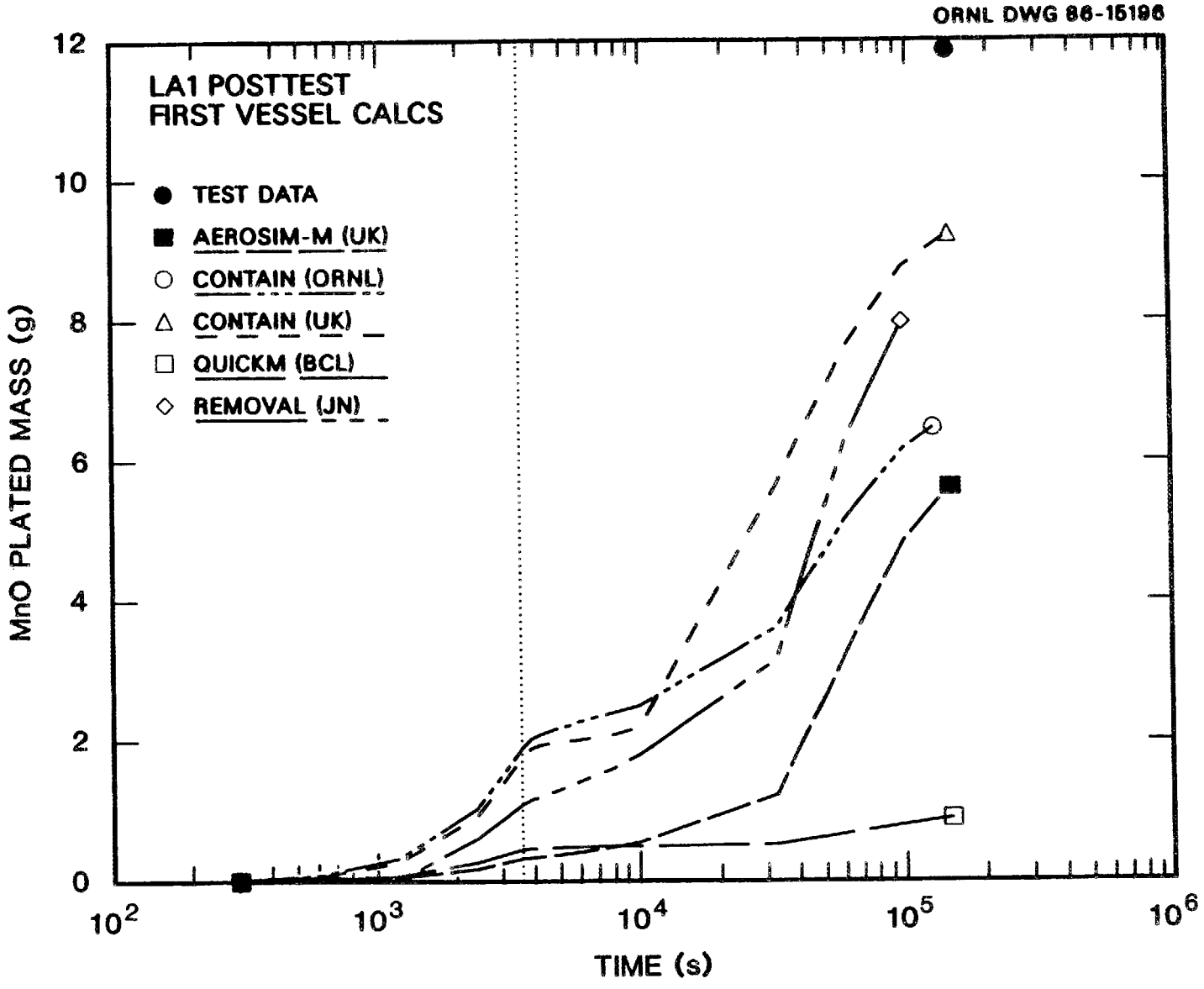

Fig. 27. LA1 "first set" vessel results: cumulative MnO aerosol plateout vs time, for codes other than NAUA.

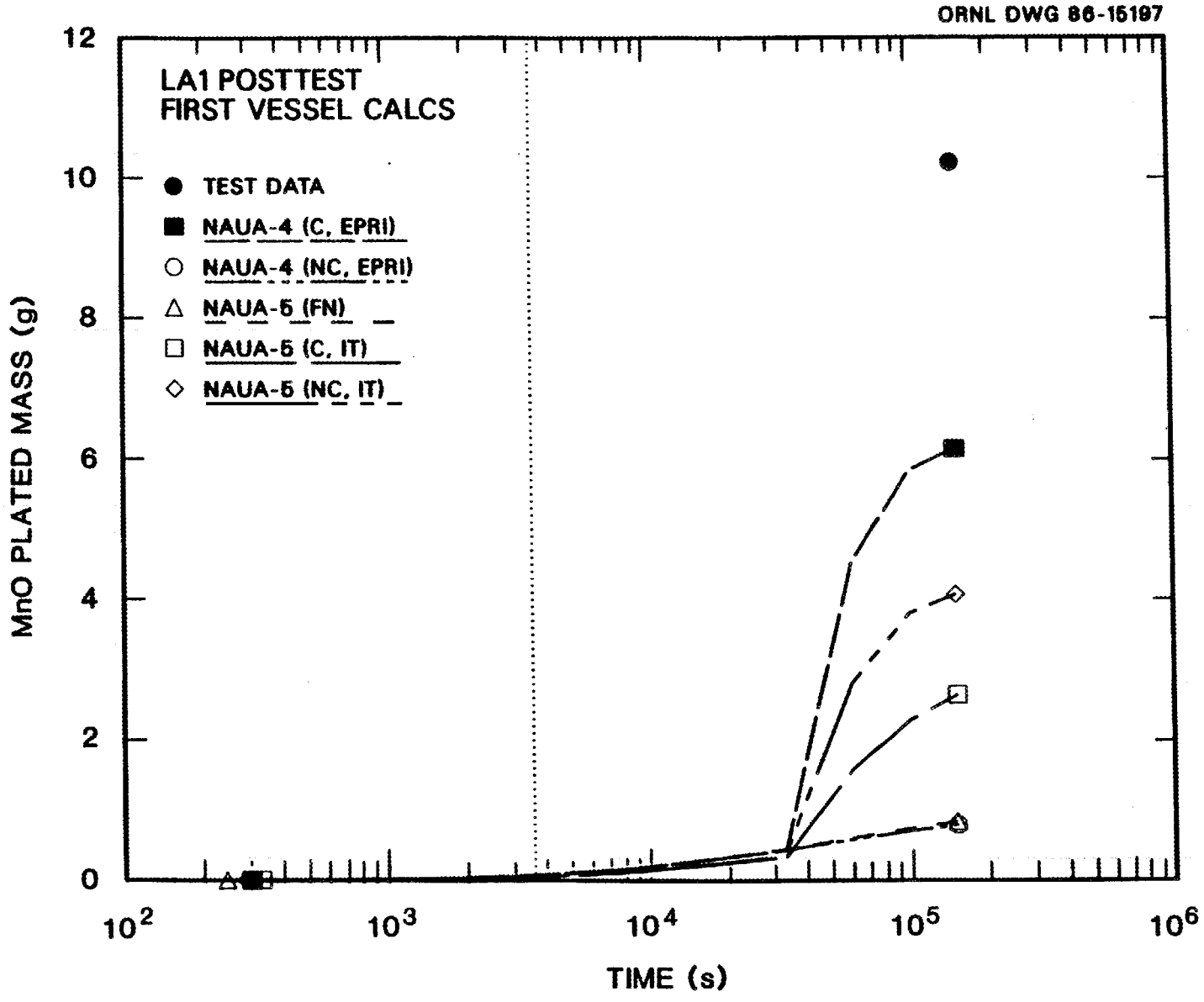

Fig. 28. LA1 "first set" vessel results: cumulative MnO aerosol plateout vs time, for NAUA calculations.

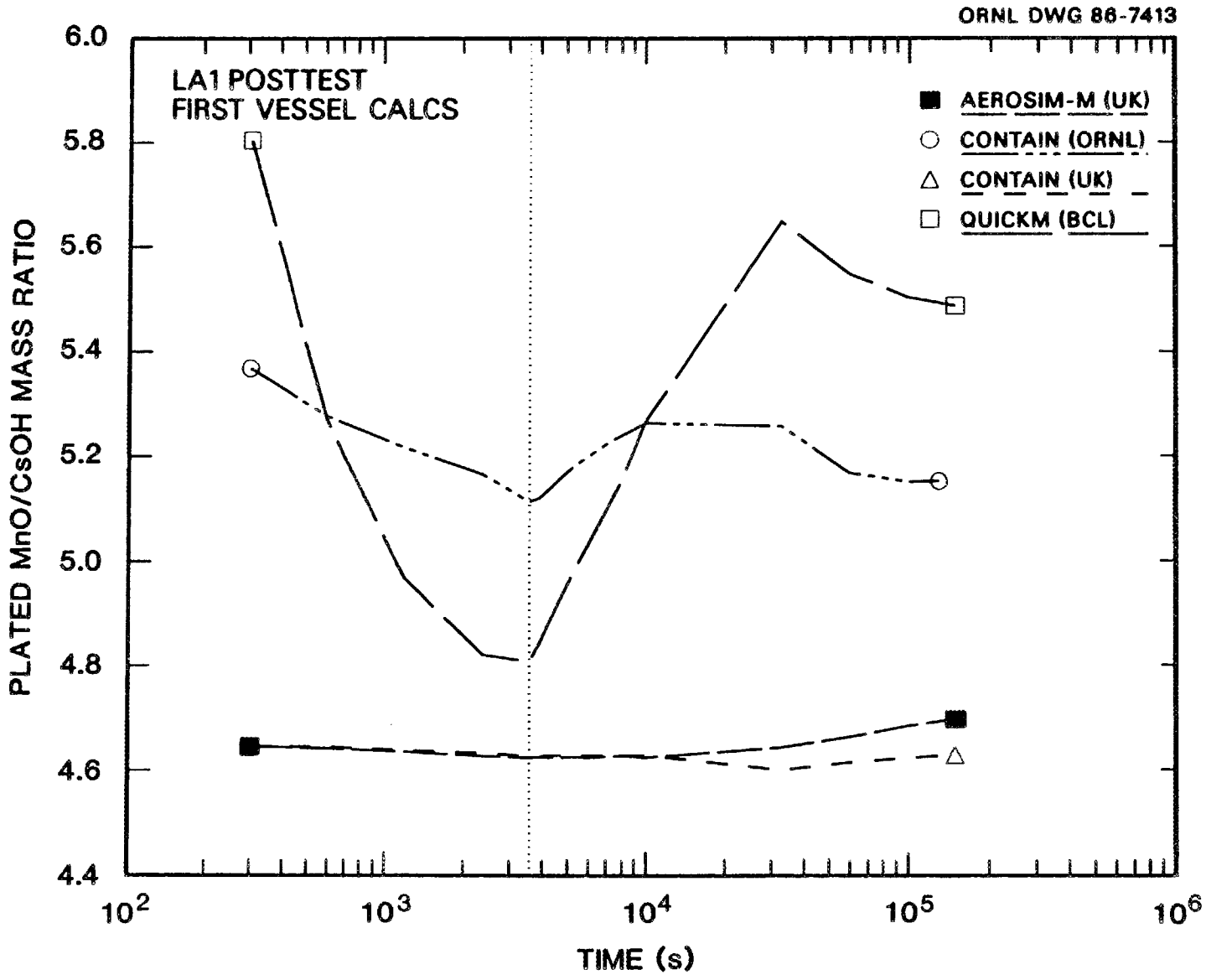

Fig. 29. LA1 "first set" vessel results: plated MnO/CsOH mass ratio vs time calculated by "multi-component" codes.

Table 26. Calculated errors in predicted aerosol plateout, first set calculations

CsOH+MnO plated mass Test value = 11.87 g				CsOH plated mass Test value = 1.65 g				MnO plated mass Test value = 10.22 g			
Code	Calc plated mass (g)	Mean square error (%)	T/C[a]	Code	Calc plated mass (g)	Mean square error (%)	T/C[a]	Code	Calc plated mass (g)	Mean square error (%)	T/C[a]
AEROSIM-M (UK)	6.81	42.6	1.74	AEROSIM-M (UK)	1.20	27.3	1.38	AEROSIM-M (UK)	5.62	45.0	1.82
CONTAIN (ORNL)	7.75	34.7	1.53	CONTAIN (ORNL)	1.26	23.6	1.31	CONTAIN (ORNL)	6.49	36.5	1.57
CONTAIN (UK)	11.21	5.6	1.06	CONTAIN (UK)	1.99	20.6	0.83	CONTAIN (UK)	9.22	9.8	1.11
NAUA-4,C(EPRI)	7.52	36.6	1.58	NAUA-4,C(EPRI)	1.37	17.0	1.20	NAUA-4,C(EPRI)	6.15	39.8	1.66
NAUA-4,NC(EPRI)	0.97	91.8	12.2	NAUA-4,NC(EPRI)	0.18	89.3	9.32	NAUA-4,NC(EPRI)	0.79	92.2	12.9
NAUA-5 (FN)	1.03	91.3	11.5	NAUA-5 (FN)	0.19	88.6	8.78	NAUA-5 (FN)	0.84	91.8	12.2
NAUA-5,C (IT)	3.24	72.7	3.66	NAUA-5,C (IT)	0.59	64.2	2.80	NAUA-5,C (IT)	2.65	74.1	3.86
NAUA-5,NC (IT)	4.99	58.0	2.38	NAUA-5,NC (IT)	0.91	44.9	1.82	NAUA-5,NC (IT)	4.08	60.1	2.50
QUICK-M (BCL)	1.06	91.1	11.2	QUICK-M (BCL)	0.16	90.1	10.1	QUICK-M (BCL)	0.89	91.3	11.4
REMOVAL (JN)	9.75	17.9	1.22	REMOVAL (JN)	1.78	7.9	0.93	REMOVAL (JN)	7.97	22.0	1.28

[a]"T/C" stands for the ratio of total measured plateout to total calculated plateout.

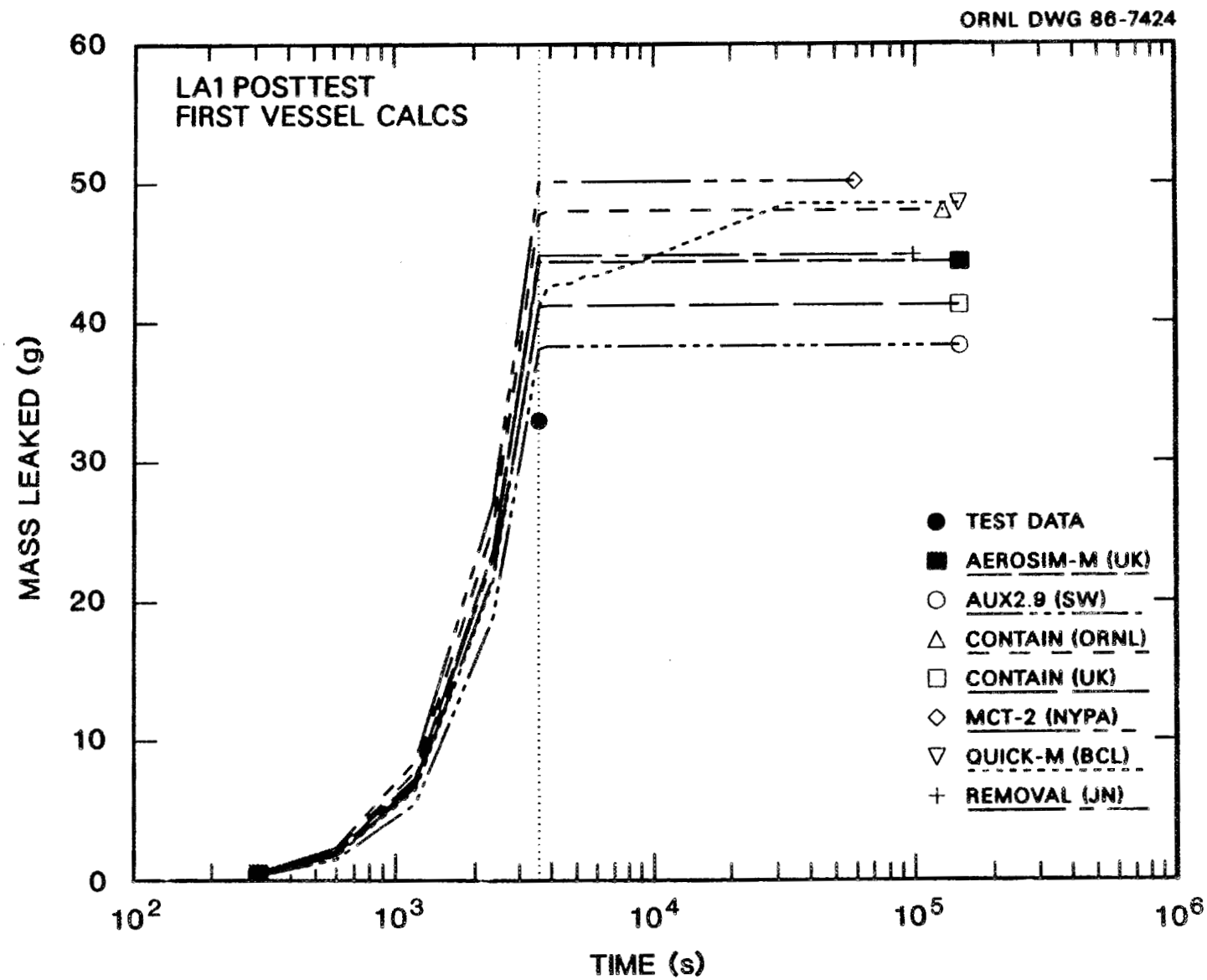

Fig. 30. LA1 "first set" vessel results: cumulative mixed aerosol leaked vs time, for codes other than NAUA.

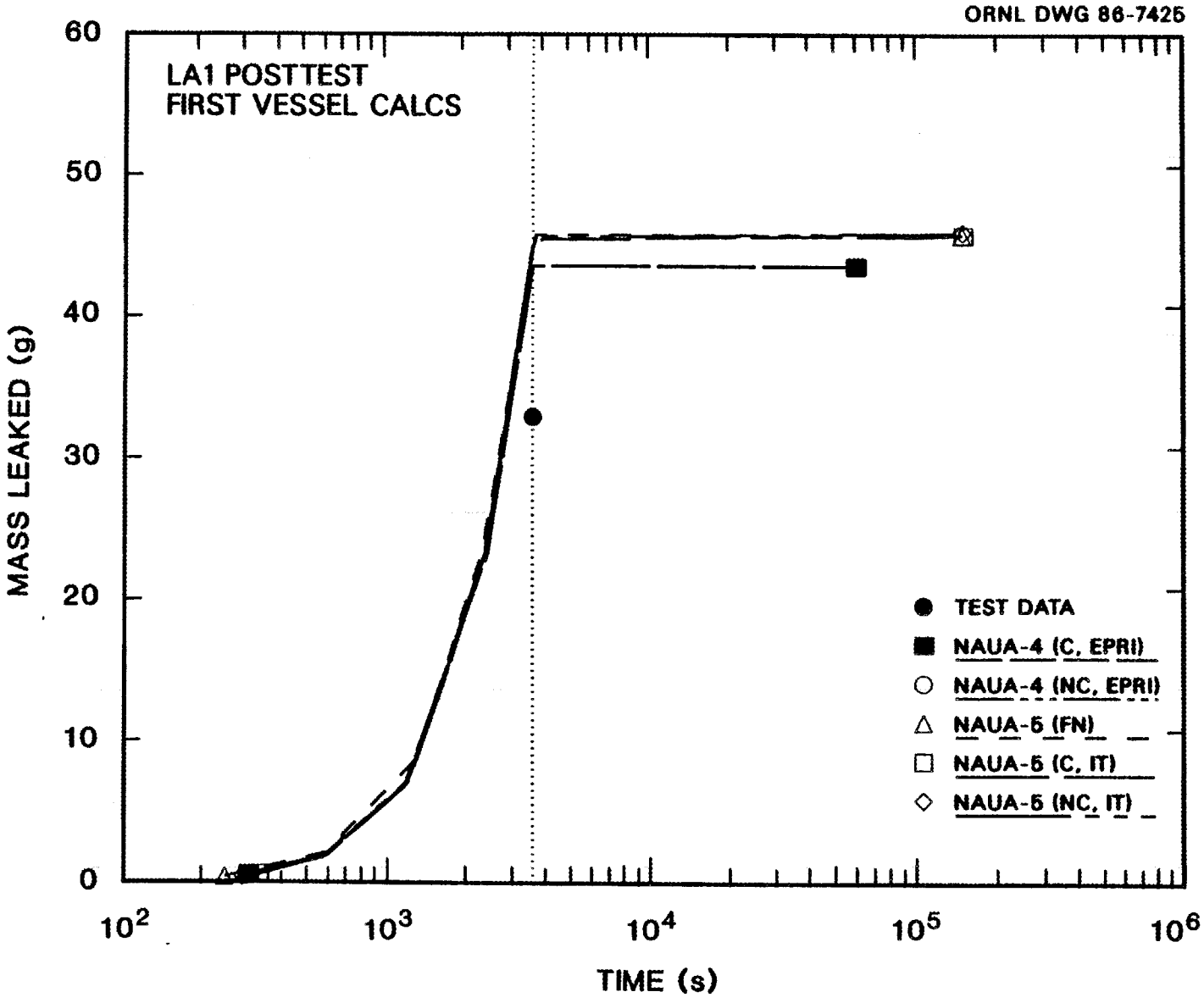

Fig. 31. LA1 "first set" vessel results: cumulative mixed aerosol leaked vs time, for NAUA calculations.

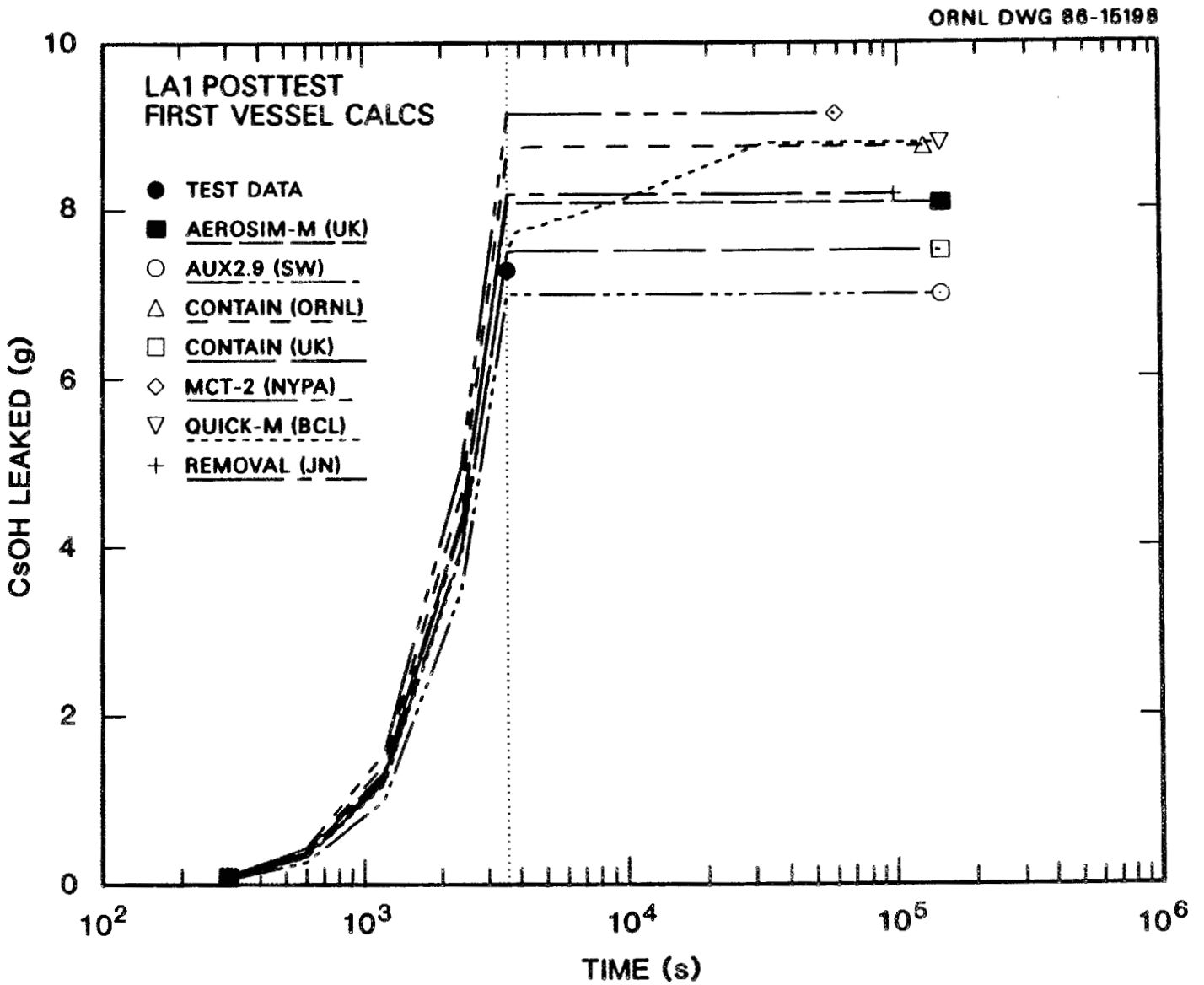

Fig. 32. LA1 "first set" vessel results: cumulative CsOH aerosol leaked vs time, for codes other than NAUA.

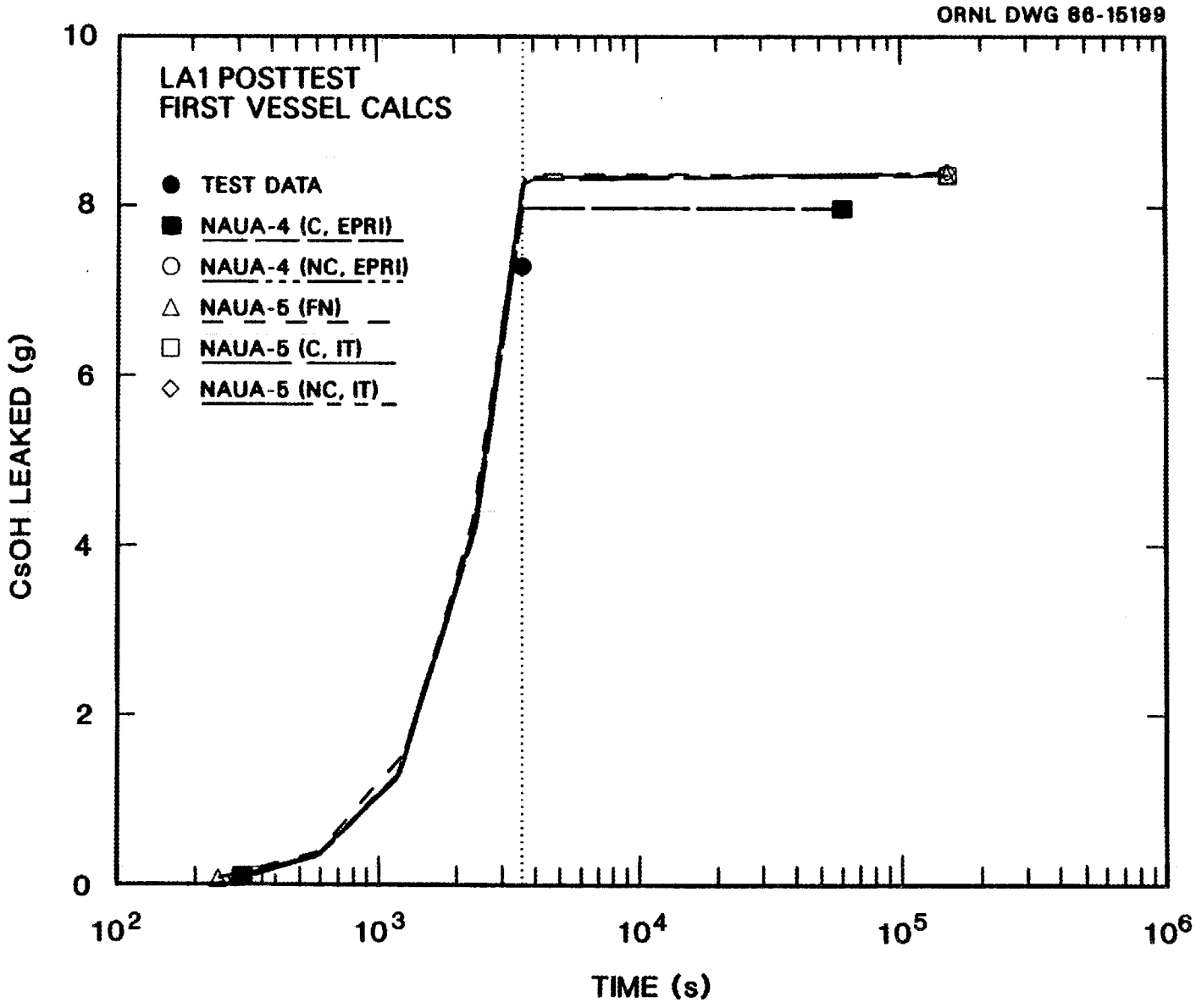

Fig. 33. LA1 "first set" vessel results: cumulative CsOH aerosol leaked vs time, for NAUA calculations.

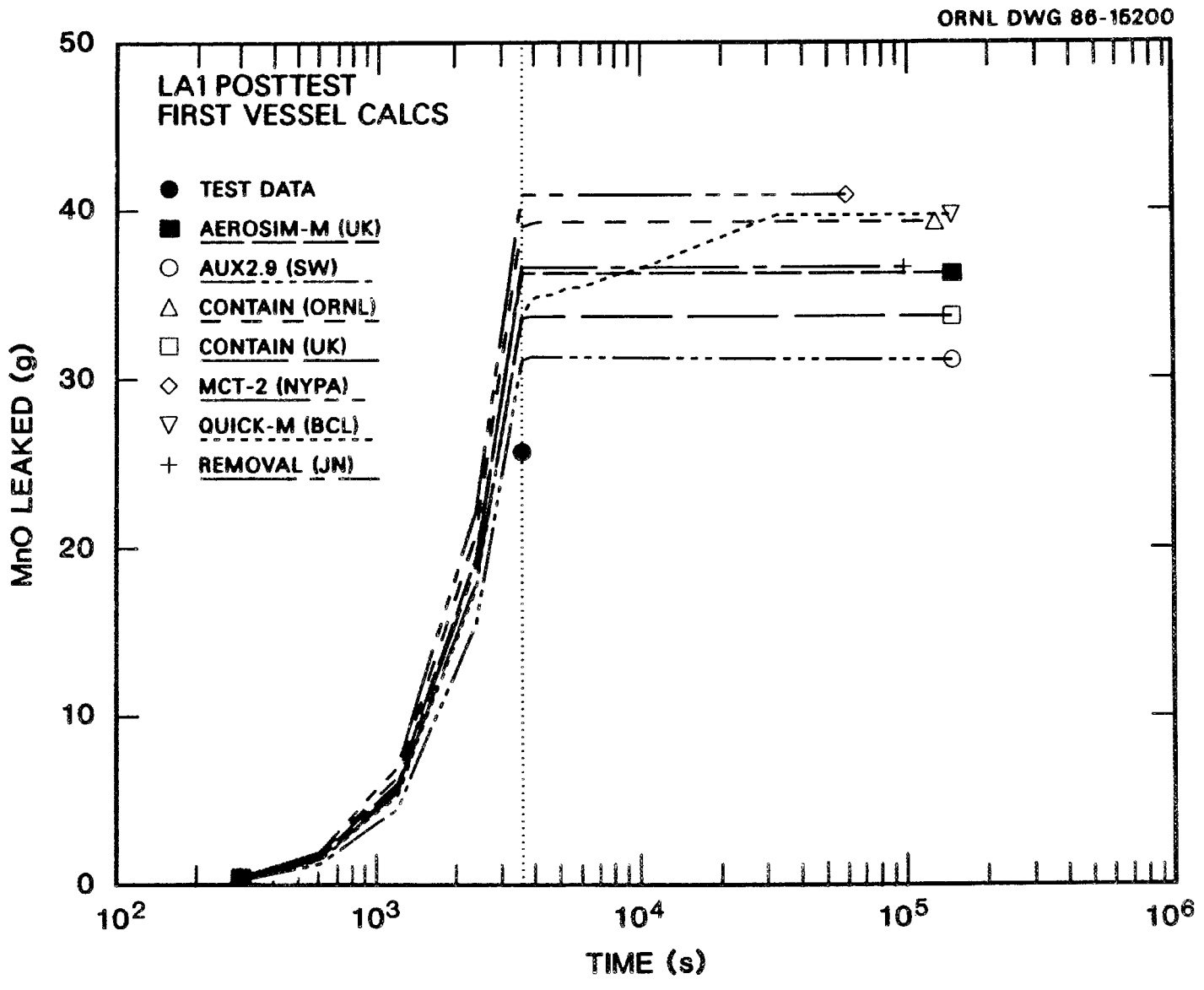

Fig. 34. LA1 "first set" vessel results: cumulative MnO aerosol leaked vs time, for codes other than NAUA.

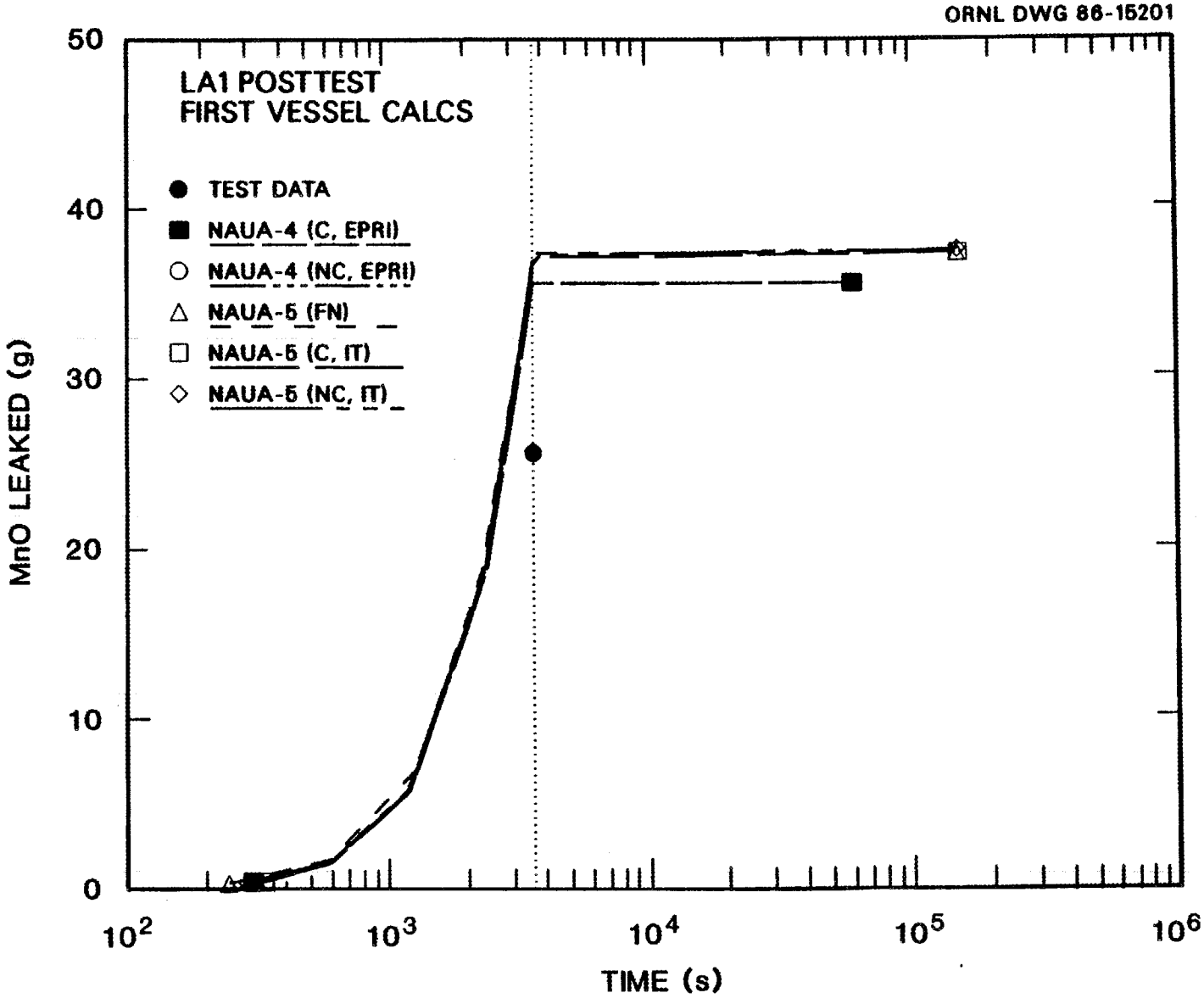

Fig. 35. LA1 "first set" vessel results: cumulative MnO aerosol leaked vs time, for NAUA calculations.

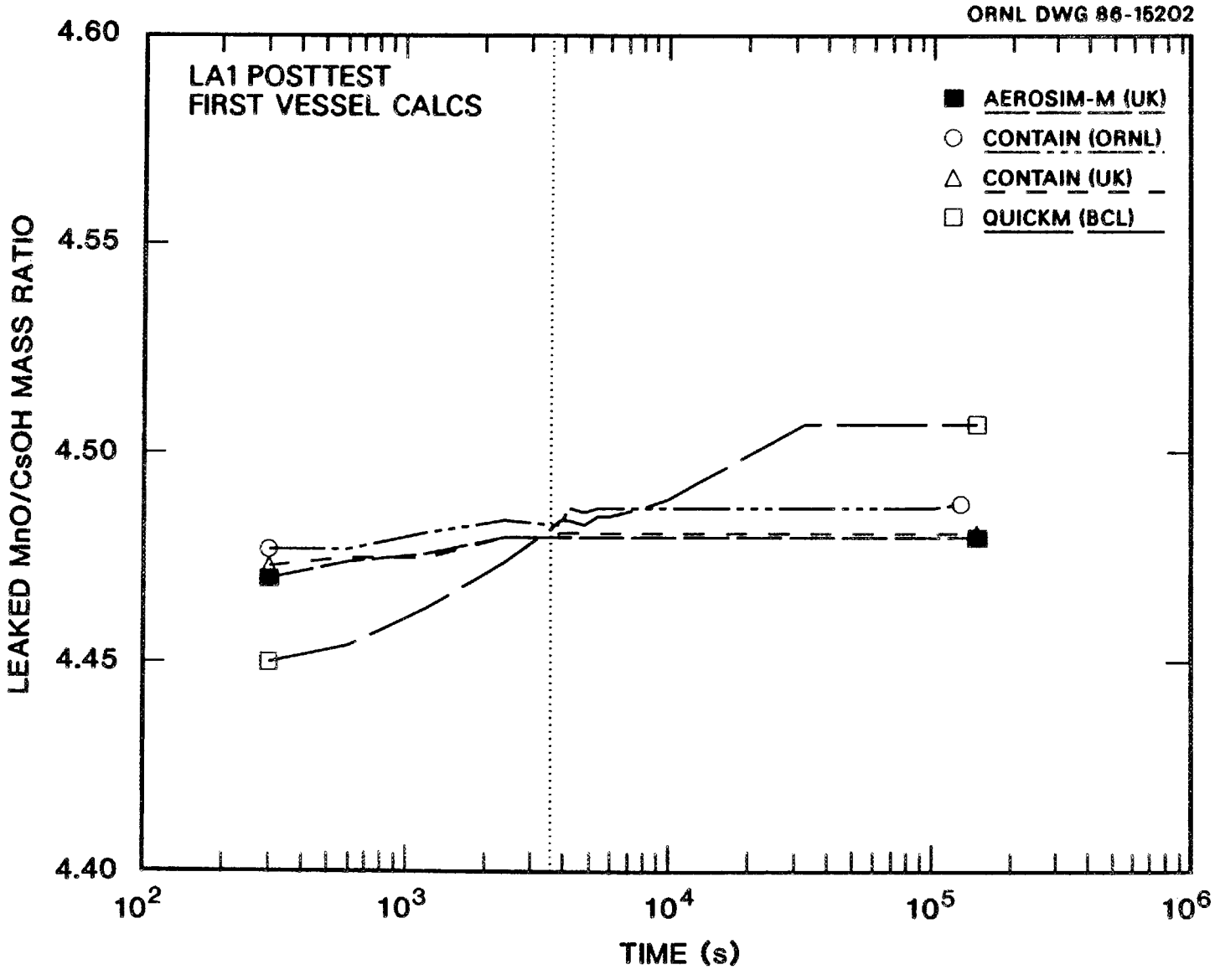

Fig. 36. LA1 "first set" vessel results: leaked MnO/CsOH mass ratio vs time calculated by "multi-component" codes.

Table 27. Calculated errors in predicted aerosol leakage from CSTF vessel; first set calculations

CsOH+MnO leaked mass Test value = 32.99 g				CsOH leaked mass Test value = 7.29 g				MnO leaked mass Test value = 25.7 g			
Code	Calc leaked mass (g)	Mean square error (%)	T/C[a]	Code	Calc leaked mass (g)	Mean square error (%)	T/C[a]	Code	Calc leaked mass (g)	Mean square error (%)	T/C[a]
AEROSIM-M (UK)	44.33	34.4	0.74	AEROSIM-M (UK)	8.09	11.0	0.90	AEROSIM-M (UK)	36.24	41.0	0.71
AUX2.9 (SW)	38.30	16.1	0.86	AUX2.9 (SW)	7.00	4.0	1.04	AUX2.9 (SW)	31.30	21.8	0.82
CONTAIN (ORNL)	48.00	45.5	0.69	CONTAIN (ORNL)	8.76	20.2	0.83	CONTAIN (ORNL)	39.30	52.9	0.65
CONTAIN (UK)	41.21	24.9	0.80	CONTAIN (UK)	7.52	3.2	0.97	CONTAIN (UK)	33.69	31.1	0.76
MCT-2 (NYPA)	50.10	51.9	0.66	MCT-2 (NYPA)	9.15	25.5	0.80	MCT-2 (NYPA)	40.90	59.1	0.63
NAUA-4,C(EPRI)	43.60	32.2	0.76	NAUA-4,C(EPRI)	7.97	9.3	0.91	NAUA-4,C(EPRI)	35.63	38.6	0.72
NAUA-4,NC(EPRI)	43.60	32.2	0.76	NAUA-4,NC(EPRI)	7.97	9.3	0.91	NAUA-4,NC(EPRI)	35.63	38.6	0.72
NAUA-5 (FN)	45.80	38.8	0.72	NAUA-5 (FN)	8.37	14.8	0.87	NAUA-5 (FN)	37.40	45.5	0.69
NAUA-5,C (IT)	45.80	38.8	0.72	NAUA-5,C (IT)	8.36	14.7	0.87	NAUA-5,C (IT)	37.60	46.3	0.68
NAUA-5,NC (IT)	46.00	39.4	0.72	NAUA-5,NC (IT)	8.40	15.2	0.87	NAUA-5,NC (IT)	37.60	46.3	0.68
QUICK-M (BCL)	48.50	47.0	0.68	QUICK-M (BCL)	8.80	20.7	0.83	QUICK-M (BCL)	39.70	54.5	0.65
REMOVAL (JN)	44.80	35.8	0.74	REMOVAL (JN)	8.19	12.3	0.89	REMOVAL (JN)	36.60	42.4	0.70

[a]"T/C" stands for the ratio of total measured leaked mass to total calculated leaked mass.

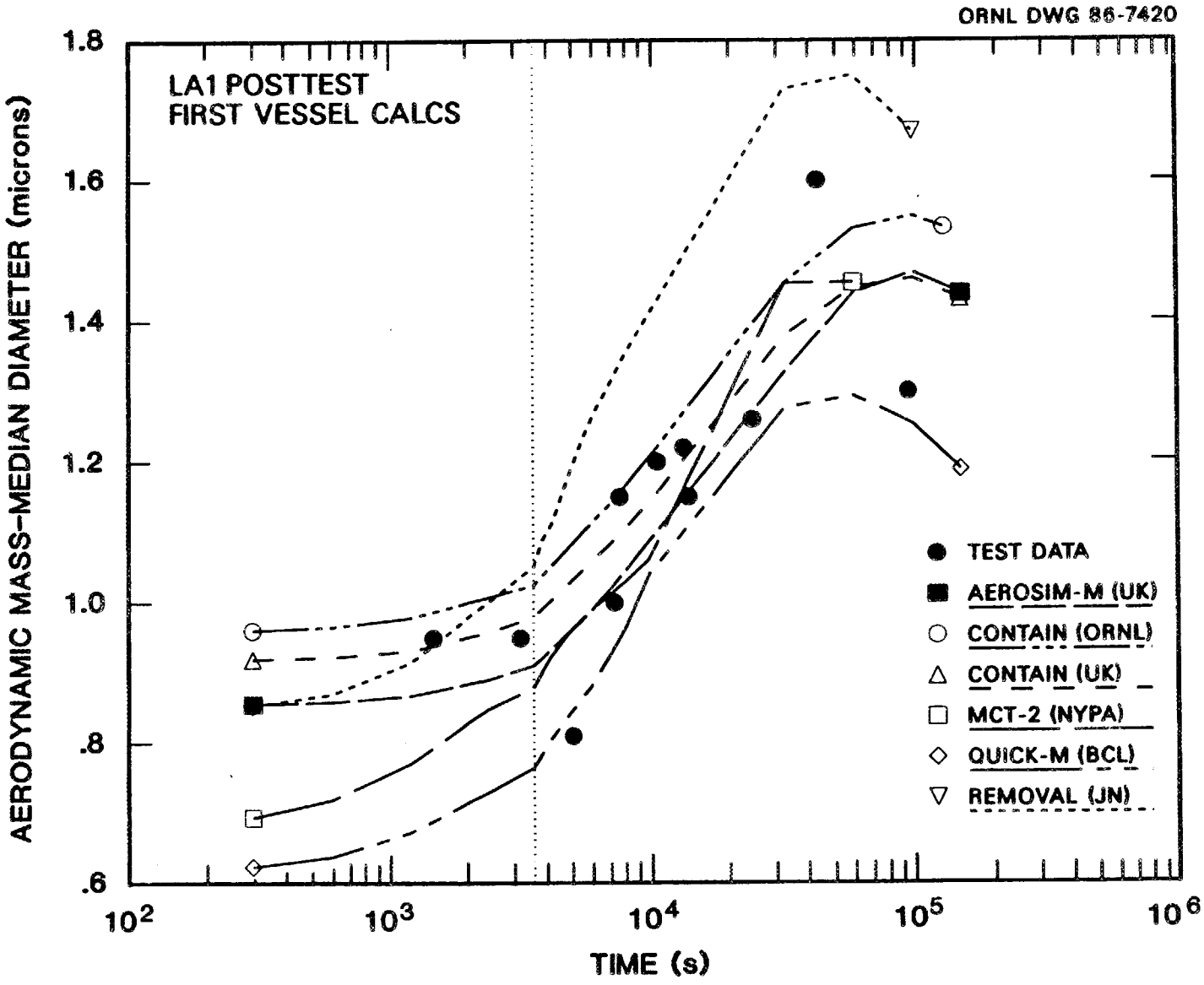

Fig. 37. LA1 "first set" vessel results: aerodynamic mass-median diameter vs time, for codes other than NAUA.

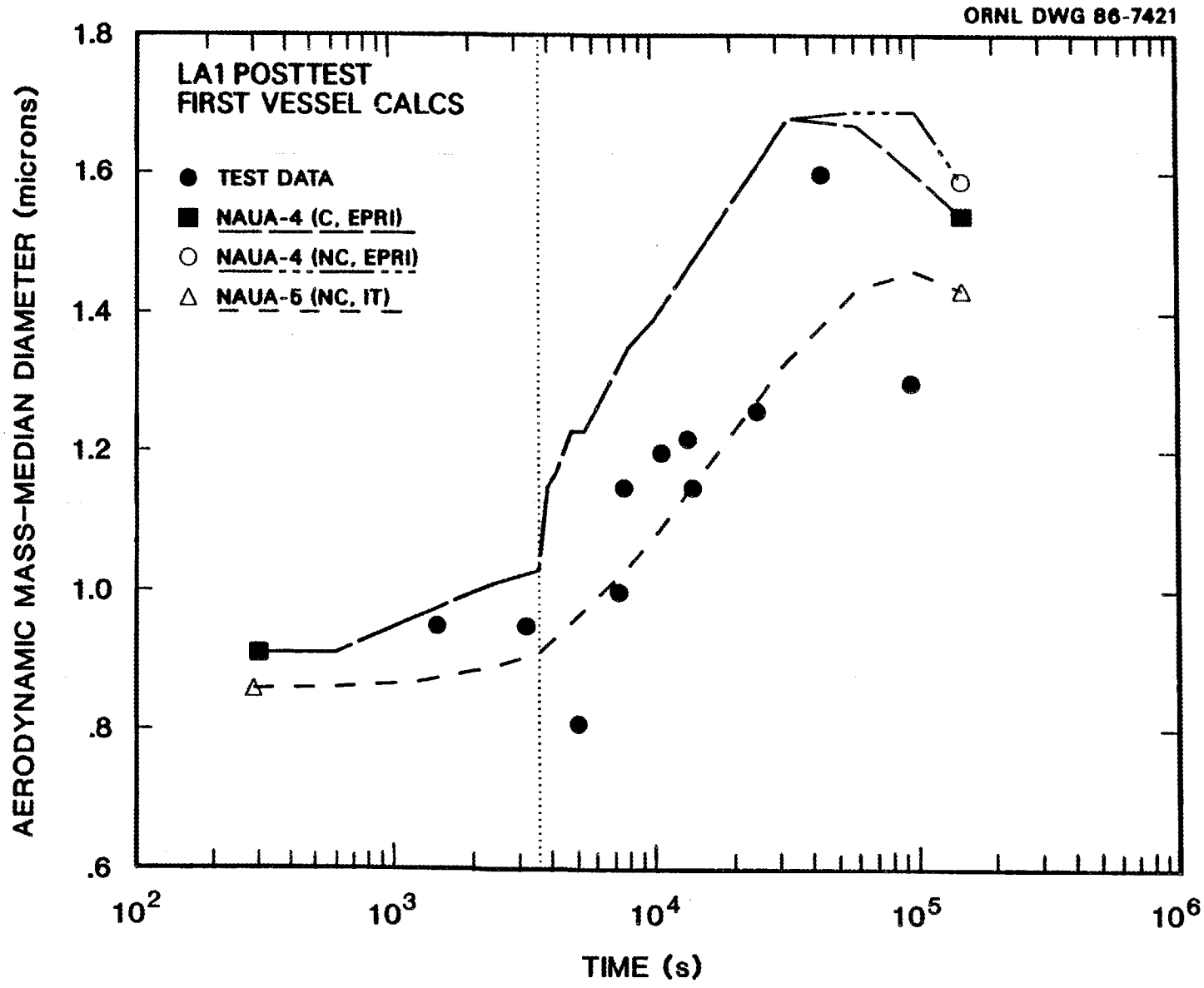

Fig. 38. LA1 "first set" vessel results: aerodynamic mass-median diameter vs time, for NAUA calculations.

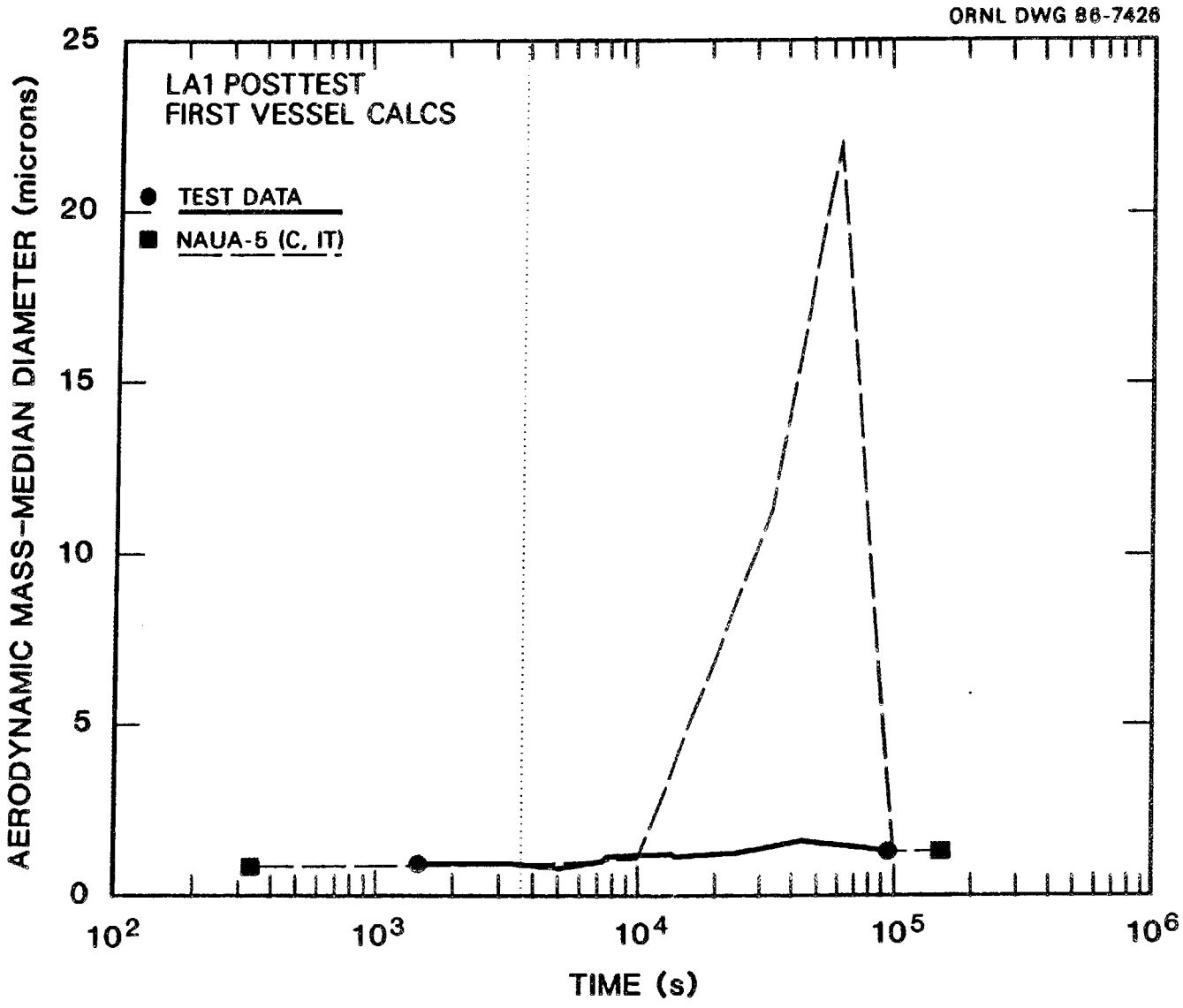

Fig. 39. LA1 "first set" vessel results: aerodynamic mass-median diameter vs time, for NAUA-5,C (IT) calculation.

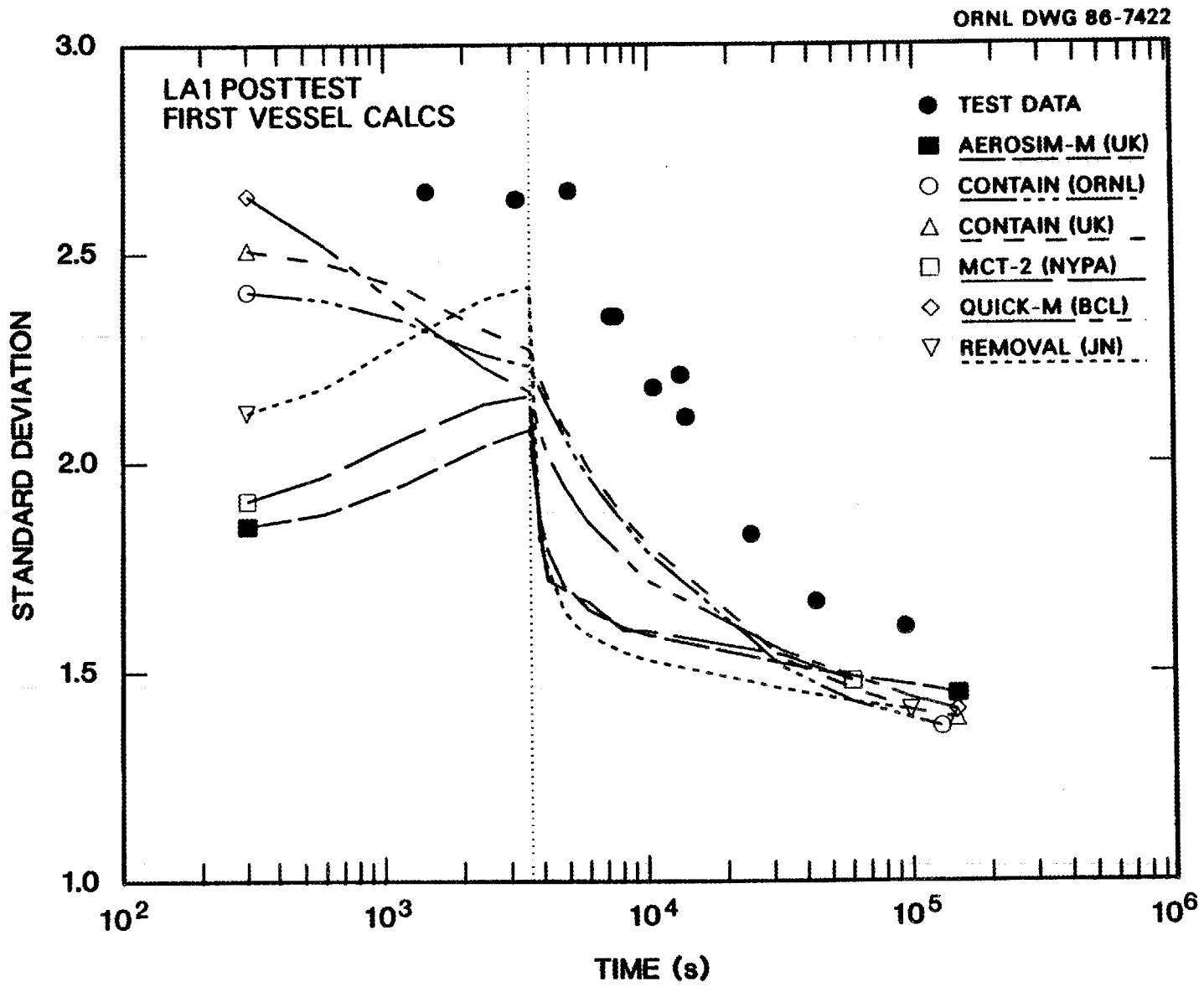

Fig. 40. LA1 "first set" vessel results: geometric standard deviation vs time, for codes other than NAUA.

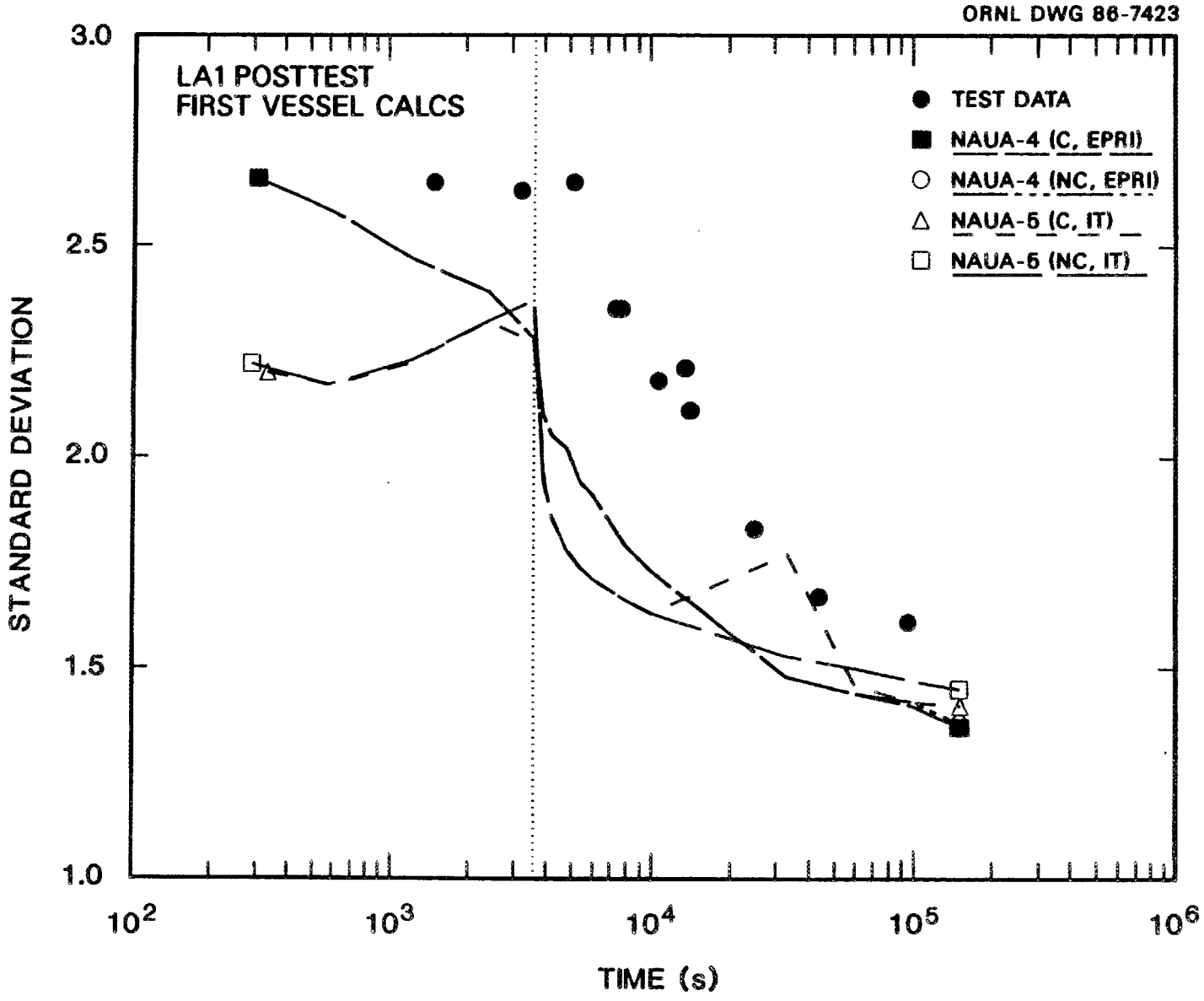

Fig. 41. LA1 "first set" vessel results: geometric standard deviation vs time, for NAUA calculations.

Table 28. Calculated errors in predicted aerosol size parameters (0-100,000 s); first set calculations

AMMD		Geometric standard deviation	
Code	Average mean square error (%)	Code	Average mean square error (%)
AEROSIM-M (UK)	9.8	AEROSIM-M (UK)	25.1
CONTAIN (ORNL)	13.4	CONTAIN (ORNL)	17.2
CONTAIN (UK)	10.4	CONTAIN (UK)	16.0
MCT-2 (NYPA)	10.4	MCT-2 (NYPA)	24.3
NAUA-4,C(EPRI)	24.3	NAUA-4,C(EPRI)	18.5
NAUA-4,NC(EPRI)	24.9	NAUA-4,NC(EPRI)	18.4
NAUA-5,NC (IT)	9.9	NAUA-5,C (IT)	21.6
QUICK-M (BCL)	14.6	NAUA-5,NC (IT)	22.3
REMOVAL (JN)	24.9	QUICK-M (BCL)	19.0
		REMOVAL (JN)	25.8

major time periods of interest: (1) a period from 0 to 1,500 s when the aerosol concentration is increasing, due to input of aerosols to the vessel; (2) a period from about 1,500 to 30,000 s, during which the aerosol concentration seems to be dropping; and (3) a period for t> 30,000 s, where the aerosol decay rate increases. What may be occurring for times between 1,500 and 3,600 s is that the aerosol release from the test pipe may have been greatly reduced. The behavior during the third period is likely to be due to steam condensation in the vessel. The drop in concentration at roughly 1,500 s was not noticed when the aerosol source conditions for test calculations were prescribed.

The code error results in Tables 23 and 24 illustrate the fact that, in spite of inaccuracies in the definition of the aerosol source, the codes calculated the aerosol concentration behavior during the source period (0-3,600 s) better than they did for the source plus depletion periods. For the source period, the calculated CsOH concentrations were more accurate than those calculated for MnO (as expected, since the prescribed MnO source was too high).

The airborne MnO/CsOH mass ratio results in Fig. 15 show that none of the codes did a good job of tracking the airborne aerosol mass ratio. However, this may be misleading, because the aerosol source mass ratio from 0 to 3,600 s was prescribed as a constant value of 4.47 (since the vessel source could not be measured); this condition was not likely to have been true. Note that the aerosol source mass ratio based on the sum of aerosol settling, plateout, and leakage was 3.85, somewhat less than the mass-balance value. Of particular interest in Fig. 15 is the fact that there was a significant increase in the MnO/CsOH airborne mass ratio for t>30,000 s. This increase indicates that when steam condensation conditions existed CsOH was removed more rapidly than MnO.

Some of the reasons for the over-predictions of aerosol concentration can be explained by evaluation of the aerosol settling, plateout, and leakage results. In terms of aerosol settling, all the codes calculated greater settling than was measured in test LA1. As illustrated in Table 25, calculated settling errors were larger for CsOH than for MnO, once more probably because the MnO source used was too large. Table 25 also shows that roughly half of the calculations predicted the measured measured settling within 50%. The results in Fig. 22 show that the multi-component codes calculate that CsOH is settled more rapidly than MnO. The final measured MnO/CsOH settled mass ratio was 3.39, less than predicted by all of the codes. However, this value is less than the "true" source value of 3.85 (see Table 6), which would seem to indicate that MnO was actually settled more rapidly in the test.

The aerosol plateout calculations differed from the settling results in that most calculations under-predicted the measured aerosol plateout. Plateout would be expected to occur by thermophoresis throughout the test, and by diffusiophoresis for t>33,000 s (when steam saturation conditions existed). The NAUA code does not model thermophoresis and, as seen from the graphical results and from the plateout error results in Table 26, tends to under-predict plateout by large amounts for calculations where diffusiophoresis was not modeled ("NC" calculations). The code error results show, however, that roughly half of the calculations predicted the measured plateout values within 50%.

Figure 29 gives the calculated MnO/CsOH plated mass ratio results. The final measured value was 6.19, significantly greater than predicted by all but the CONTAIN (ORNL) calculation. This situation corresponds to more effective removal of CsOH by wall plateout and may be consistent with the large measured increase in airborne aerosol mass ratio for t>30000 s that is illustrated in Figure 15.

Figures 30 through 35 display the aerosol leakage results. Aerosol leakage was overestimated in most calculations, probably because the MnO aerosol source assumed was too large. However, as illustrated in Table 27, all codes predicted the measured leakage within 50%.

The leaked mass ratio results shown in Figure 36 show that the multi-component codes predict essentially no change in the mass ratio from that assumed for the source. The measured leaked mass ratio was 3.52. Although this was less than the codes calculated, it was within 10% of the aerosol source value of 3.85 based on the sum of settling, plateout, and leakage.

The AMMD results illustrated in Figures 37-39 and Table 28 illustrate that the aerosol size predictions for LA1 were quite good. This should be expected, since the LA1 aerosol concentrations in the CSTF vessel were low. The figures show that, for the most part, the NAUA calculations tended to overestimate the measured AMMD values more than the other calculations. This result is consistent with the fact that, as illustrated in Table 25, the NAUA calculations also tended to calculate more settling than the other calculations. Overall, however, the measured AMMD results were predicted quite well.

The test AMMD results show a large increase in AMMD shortly after 30,000 s. If this is not simply due to the uncertainty in measuring AMMD, it might have been due to water condensation onto the airborne aerosols.

The comparisons of geometric standard deviation (σ_g) illustrated in Figs. 40 and 41 show some puzzling trends. First of all, some codes predicted that σ_g decreased during the source period, while others predicted that it increased; at present, we cannot explain this behavior.

Figure 41 shows that the EPRI version of NAUA predicted a decreased σ_g during the source time, while the other versions predicted an increase. The other puzzling result is that shortly after the end of the source period many codes predicted a very rapid drop in σ_g; the measured decrease was not as severe as that predicted. Finally, all of the codes under-predicted the measured standard deviation. Table 28 illustrates that the overall error in the calculated σ_g was not large. However this is deceiving, because small variations in standard deviation correspond to large variations in particle-size distribution. We will come back to a further discussion of calculated σ_g results in Sect. 5 of this report; there we will illustrate that some of the codes are incorrectly calculating the geometric standard deviation.

The code-input parameters that seem to have the major influence on differences in code results are: (1) the vessel leakage rate, (2) how steam condensation for t>33,000 s (when steam saturation conditions occurred) was modeled; and, (3) to a lesser extent, the gas-wall temperature gradients driving thermophoretic deposition (when modeled). Table 29 presents a summary of the assumptions and values used in modeling these parameters for the first set of LA1 vessel calculations. Below, we discuss how these parameters influenced the different code calculations. We also discuss any other interesting aspects of the calculations that have not previously been mentioned.

AEROSIM-M (UK)

This calculation was performed with leakage rates and steam wall-condensation rates similar to those that we presented in Tables 10 and 11. In addition, the dynamic and collision shape factors were assumed to be equal to 1.5, and a turbulent energy dissipation rate of 10.38 m^2/s^3 was assumed for t>3,600 s. Plateout results indicated that 3.2 g of aerosol was removed by thermophoresis and diffusion, and 3.7 g was removed by diffusiophoresis.

Table 29. Summary of major code-input assumptions for first set of vessel calculations

Code	Leak rate to scrubber t=0-3600 s	Modeling of steam condensation in vessel	Wall temperature gradients
AEROSIM-M (UK)	5423 vol %/d	Condensation on wall modeled: steam removal rate of 2.5 g/s for 33,000 to 86,700 s, 1.4 g/s for t > 86,700 s	7°C/cm for 0 to 3600 s, 2°C/cm for t > 3600 s
AUX2.9 (SW)	As given in Table 5	a	a
CONTAIN (ORNL)	0.4 kg/s	Wall condensation calculated to start slightly before 28,000 s. Average steam removal rate for 28,000 to 80,000 s was 2.4 g/s; Average steam removal rate for t > 80,000 s was 0.5 kg/s	a
CONTAIN (UK)	About 0.35 kg/s for 0-3600 s	Water condensation calculated to start at 10,000 s. Average steam removal rates were 4.3 g/s for 10,000 to 20,000 s, 3.9 g/s for 20,000 to 33,000 s, 2.6 g/s for 33,000 to 80,000 S, 0.12 g/s for 80,000 to 150,000 s.	a
MCT-2 (NYPA)	As given in Table 5	No steam condensation	a
NAUA-4 (NC,EPRI)	5190 vol %/d	No steam condensation	None
NAUA-4 (C,EPRI)	5190 vol %/d	Wall condensation assumed to start at 33,000 s. Removal rates calculated similar to those in Table 11	None
NAUA-5 (FN)	5749 vol %/ d	No steam condensation	None

Table 29 (continued)

Code	Leak rate to scrubber t=0-3600 s	Modeling of steam condensation in vessel	Wall temperature gradients
NAUA-5 (NC,IT)	Varies from 1.9E-4 to 1E-3 s^{-1} (similar to Table 10)	Steam condensation only on walls, starting at 33,000 s. Based on vessel heat-flux data. Steam removal rates of 6.8 g/s at 33,000 s, 2.6 g/s at 72,600 s, 0.06 g/s at 135,000 s	None
NAUA-5 (C,IT)	Varies from 1.9E-4 to 1E-3 s^{-1} (similar to Table 10)	Steam condensation on walls and particles, starting at 33,000 s. Wall condensation rates of 3.4 g/s at 33,000 s, 2.1 g/s at 72,600 s. Condensation rates on particles of 3.4 g/s at 33,000 s, 0.5 g/s at 72,600 s. No condensation after about 75,000 s.	None
QUICK-M (BCL)	Varies from 3.3E-4 to 1.6E^{-3} s^{-1} for t=0 to 3600 s; in the range of 1E-4 s^{-1} for times up to 80,000 s.	No steam condensation	a
REMOVAL (JN)	Varies from 1.9E-4 to 1E-3 s^{-1}	Condensation on wall modeled, starting at 33,000 s. Based on wall heat-flux data. Wall condensation rates of 3.3 g/s at 33,000 s, 1.5 g/s at 100,800 s.	8.6 °C/cm at t = 0 s, 4 °C/cm at t = 3660 s, 0.25 °C/cm at t = 100,080 s

[a]Data not provided for this parameter.

CONTAIN (ORNL)

The CONTAIN code is a coupled thermal-hydraulics and aerosol transport code. For this calculation, a constant leak rate of 0.4 kg/s for t<3,600 s was assumed; this rate is comparable to the values in Table 5. However, a gas injection rate to the test vessel of 0.35 kg/s was assumed for t<3,600 s. The consequence of this assumption is that the calculated pressure in the vessel dropped during the injection period; the pressure at t=0 was 107.9 kPa, while the calculated pressure at 3,600 s was 87.1 kPa. Because of this pressure drop (which did not occur in the test) a small "back-flow" of gas from the surroundings to the test vessel started at roughly 4,800 s. In looking at the code output, this back-flow corresponded to the time when small amounts of water aerosols became airborne in the test vessel. We believe this water came from water airborne in "cell 2" (the control volume modeling the environment outside the test vessel) in the calculation. We do not believe, however, that this slight in-flow of water influenced the calculated results.

The wall (steam) condensation rates calculated by CONTAIN compare reasonably well with those calculated from the decrease in airborne water in the vessel (Table 11). However, CONTAIN calculated that steam condensation started at roughly 28,000 s, about 5,000 s earlier than the vessel atmosphere reached saturation conditions. At 28,000 s in the CONTAIN calculation the gas-steam saturation ratio was about 0.8; relative to the wall temperatures, though, the steam was saturated and condensation was calculated to occur.

Finally, it should be noted that, other than the small amount of water that became airborne due to back-flow from cell 2, the CONTAIN (ORNL) predicted no condensation of water onto the airborne aerosols.

CONTAIN (UK)

The calculated gas leak rate of about 0.35 kg/s was slightly lower than the values shown in Table 5, and the predicted vessel pressures predicted were better than those in the CONTAIN (ORNL) calculation. However,

steam condensation was predicted to start at about 10,000 s rather than at 33,000 s. Because of this and the fact that relatively high condensation rates were predicted for 10,000 to 33,000 s, aerosol deposition by diffusiophoresis was probably overestimated in this calculation.

We should also note that this calculation also predicted a small "back-flow" of gas into the CSTF vessel for t>3,600 s; however, the flow rates were negligible compared to those from the CONTAIN (ORNL) calculation.

Finally, as for the CONTAIN (ORNL) calculation, no condensation of water onto airborne aerosols was predicted in the CONTAIN (UK) calculation.

MCT-2 (NYPA)

The MCT-2 code is also a coupled thermal-hydraulics and aerosol transport code; however, the measured test thermal-hydraulic conditions were used as input for this calculation. The MCT-2 calculation was performed for times up to 60,000 s; we had requested calculations to be performed for 150,000 s. Up to 60,000, a total of 17.5 g of aerosol was calculated to be "retained" in the vessel, and 7.3 g of aerosol was calculated to still be airborne. In looking at the code outputs provided to us, we found that the calculated thermophoretic deposition velocities were about 100 times less than those calculated for settling; therefore, essentially all calculated aerosol retention was due to settling. This means that we might estimate that the code would have calculated a total settled mass (in 150,000 s) of 17.5+7.3 = 24.8 g, about twice the measured value.

In looking at the MCT-2 AMMD results presented in Fig. 37, we note that the calculated AMMD at 300 s (0.69 μm) was less than the aerosol source value of 0.89 μm. This would suggest, as was discussed previously in the LA2 pretest results report,[12] that the MCT-2 code incorrectly calculates the AMMD. At 300 s, we recalculated the AMMD and found a value of 0.88 μm, about 20% greater than the code value and comparable to the source value (as it should be for short times after the start of aerosol generation). This error has been pointed out to the code analyst.

NAUA-4 [NC,C (EPRI)]

About 7 g of aerosol was calculated to deposit by diffusiophoresis ("C"); this amount was about 7 g more plateout than was predicted in the "NC" calculation. However, in the LA2 pretest calculations, it was discovered that the form of the diffusiophoresis model used in the EPRI version of NAUA had an error that would cause it to over-calculate diffusiophoresis by about a factor of 2 for the LA1 conditions.[11]

NAUA-5 [NC,C (IT)]

The meaning of the "NC" and "C" results for the Italian NAUA calculations was somewhat different than for the other NAUA calculations. In the Italian "NC" calculation, steam condensation onto the walls was modeled; and heat-flux measurements were used to obtain steam condensation rates onto the walls. In the Italian "C" calculation, steam condensation onto walls and particles was modeled. The change in the total airborne steam was attributed to total steam condensation, and the difference between this and the wall condensation rates represented the condensation rate onto particles. The mass deposited by diffusiophoresis in the "NC" calculation was about 4.5 g, while the diffusiophoretic deposit for the "C" calculation was about 3 g. The most interesting result from the Italian calculations is illustrated in Fig. 39, the AMMD results for the calculation including water condensation onto the aerosols. The condensing water caused the calculated AMMD to increase by roughly a factor of 20. Although an increase of this magnitude was not measured, two things are of note: (1) as illustrated in Fig. 38, there was a large (although not as large as calculated) increase in AMMD measured at 43,800 s which may have been due to water condensation, (2) the measured AMMD data is for the "dry" aerosol only, while the calculated AMMD data includes water on the aerosols; therefore, it is not really appropriate to compare the two results. All of the Italian AMMD results (when water was condensed onto the aerosols) could not be corrected to produce "dry" AMMD values; therefore, calculated AMMD errors for the "C" calculation are not given in Table 28. However, we could correct the data for one of the code output times, t=60,577 s. At that time, the AMMD calculated by

the code (including the water) was 20.6 μm; the AMMD we calculated for the "dry" aerosol mass, however, was 1.32 μm. These values show that AMMD comparisons must be done with care for conditions where water condenses onto aerosols.

QUICK-M (BCL).

As shown in Fig. 34, QUICK-M calculated aerosol leakage for t>3,600 s; this occurred because leak rates used were greater than zero for times up to about 80,000 s. QUICK-M also calculated very little diffusiophoretic deposition because the calculated steam saturation ratio never rose above 0.45. Finally, as for the MCT-2 calculations, the calculated AMMD at 300 s was 0.62 μm, significantly less than the source value of 0.89 μm. Using the code output provided to us, we recalculated a value of 0.88 μm at 300 s which indicates that AMMD is being calculated incorrectly in QUICK-M (this conclusion has been discussed with the code analysts). Since the aerosol physics models in QUICK-M, MCT-2, and TRAP-MELT2 all derive from those in the original QUICK code (developed at BCL), we expect that all of these are incorrectly calculating the AMMD.

REMOVAL (JN)

REMOVAL calculated plateout by thermophoresis of 3.7 g, and diffusiophoretic plateout of 5.2 g. However, as for the EPRI version of NAUA, the version of REMOVAL used for this calculation included a diffusiophoresis modeling error that caused diffusiophoresis to be overcalculated by a factor of 2.

5. SUMMARY OF "SECOND SET" OF LA1 VESSEL CODE-EXPERIMENT COMPARISON RESULTS

Table 30 illustrates that eleven "second set" calculations were performed to model the aerosol vessel behavior in test LA1. All of the codes used were discrete size-distribution codes. Two CONTAIN and five NAUA calculations were performed. In terms of the NAUA calculations, some investigators again chose to perform two calculations: one ("NC") with no modeling of water condensation effects after 33,000 s, and the

Table 30. Summary of codes used for second set of LA1 vessel calculations

Code[a]	Code analyst	Affiliation
AEROSIM-M (UK)	S. Ramsdale	United Kingdom, Atomic Energy Authority, Safety and Reliability Directorate
CONTAIN (ORNL)	M. Tobias	United States, Oak Ridge National Laboratory
CONTAIN (UK)	P. Smith	United Kingdom, Atomic Energy Authority, AEE Winfrith
MCT-2 (NYPA)	P. Bieniarz	United States, New York Power Authority
NAUA-4 (NC,EPRI) NAUA-4 (C,EPRI)	R. Sher	United States, Electric Power Research Institute
NAUA-5 (FN)	J. Makynen	Finland, Technical Research Centre
NAUA-5 (NC,IT) NAUA-5 (C,IT)	M. Valisi	Italy, ENEL-Thermal and Nuclear Research Centre
QUICK-M (BCL)	V. Kogan	United States, Battelle Columbus Laboratories
REMOVAL (JN)	N. Yamano	Japan, Atomic Energy Research Institute

[a]Initials in parentheses indicate country or organization.

other ("C") where water condensation effects were modeled. As for the first set of calculations, the designations for the NAUA-5 (IT) calculations were slightly different: the NAUA-5,NC (IT) calculation considered only water condensation onto wall surfaces, while the NAUA-5,C (IT) calculation considered water condensation onto walls and aerosols.

Figures 42 through 48 graph the aerosol concentration comparison results for the second set of vessel calculations. As for the first set of calculations, MnO/CsOH mass ratio data are shown only for the AEROSIM-M, CONTAIN, and QUICK-M results; for all other codes the mass ratio was fixed throughout the calculation at a value of 2.43. Table 31 gives calculated errors for the code-data comparisons of aerosol concentrations. These were calculated using Eqs. 5 and 6 for measurement times of 5,520, 9,120, 12,200, 18,000, 24,000, 32,100, 39,700, 56,900, and 85,300 s.

Figures 49 through 54 present calculated results for aerosol settling and plateout for t>3,600 s. Note that no experimental data is shown, because settling and plateout measurements were made for the total experiment time. Because of this, only plots of the total aerosol settling and plateout, and of settling and plateout mass ratios, are shown.

Finally, Figs. 55 through 59 present the AMMD and geometric standard deviation results for the second set of vessel calculations, and calculated errors for these parameters are shown in Table 32.

As for the first set of calculations, the aerosol concentration results shown in Figs. 42 to 47 show that most calculations tended to overpredict the airborne concentrations at long times. Note though, that in Fig. 42 the difference in mass airborne between the results of all calculations at 150,000 s is only about 2.5 g, a small value. The results in Table 31, when compared to those in Table 24, show that the comparisons of total and MnO airborne concentrations are improved for the second set of calculations. However, none of the codes did an adequate job of predicting the CsOH concentrations for the second set of calculations. Figures 44 and 45 show that a drop in CsOH concentration occurred

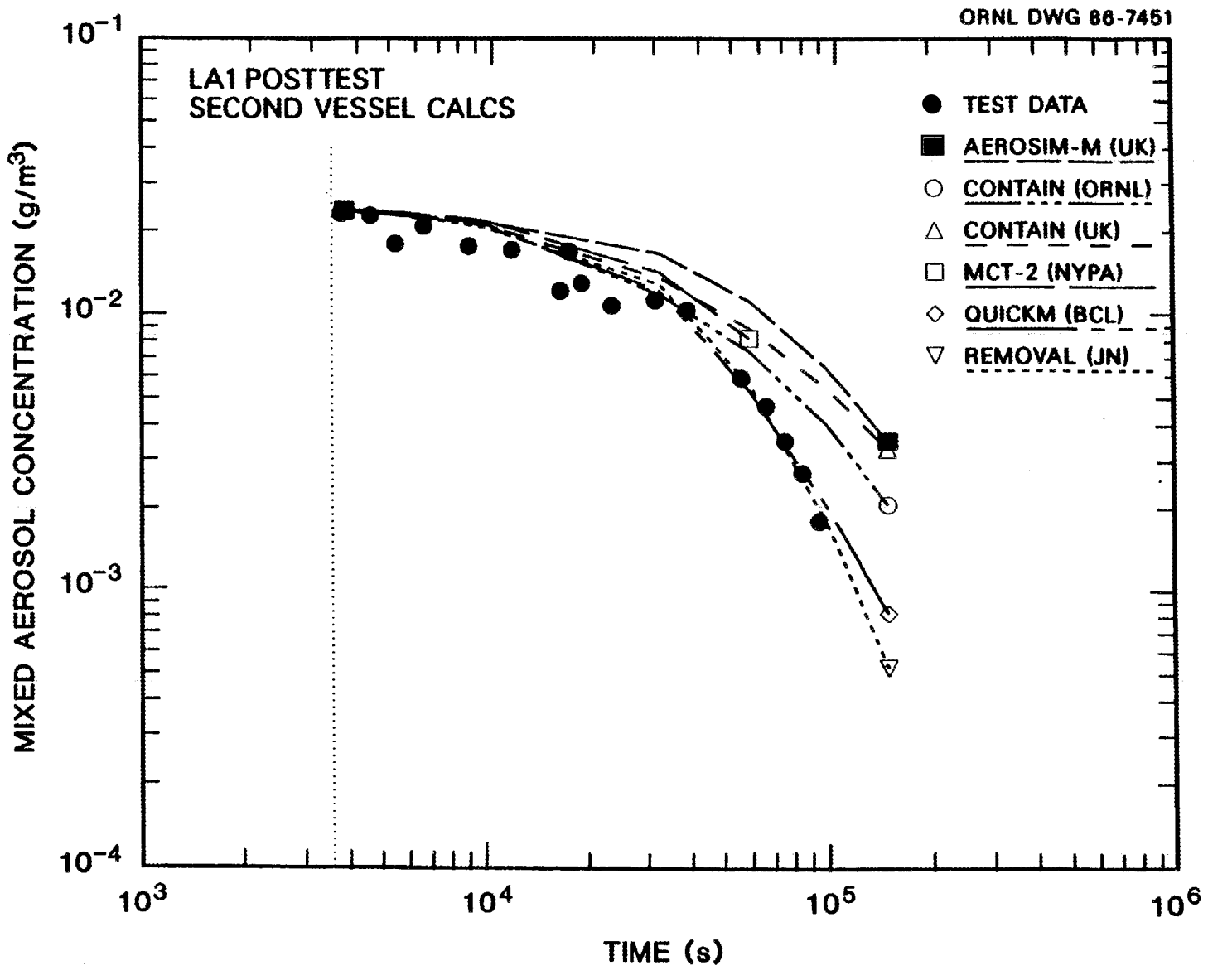

Fig. 42. LA1 "second set" vessel results: airborne mixed aerosol concentration vs time for codes other than NAUA.

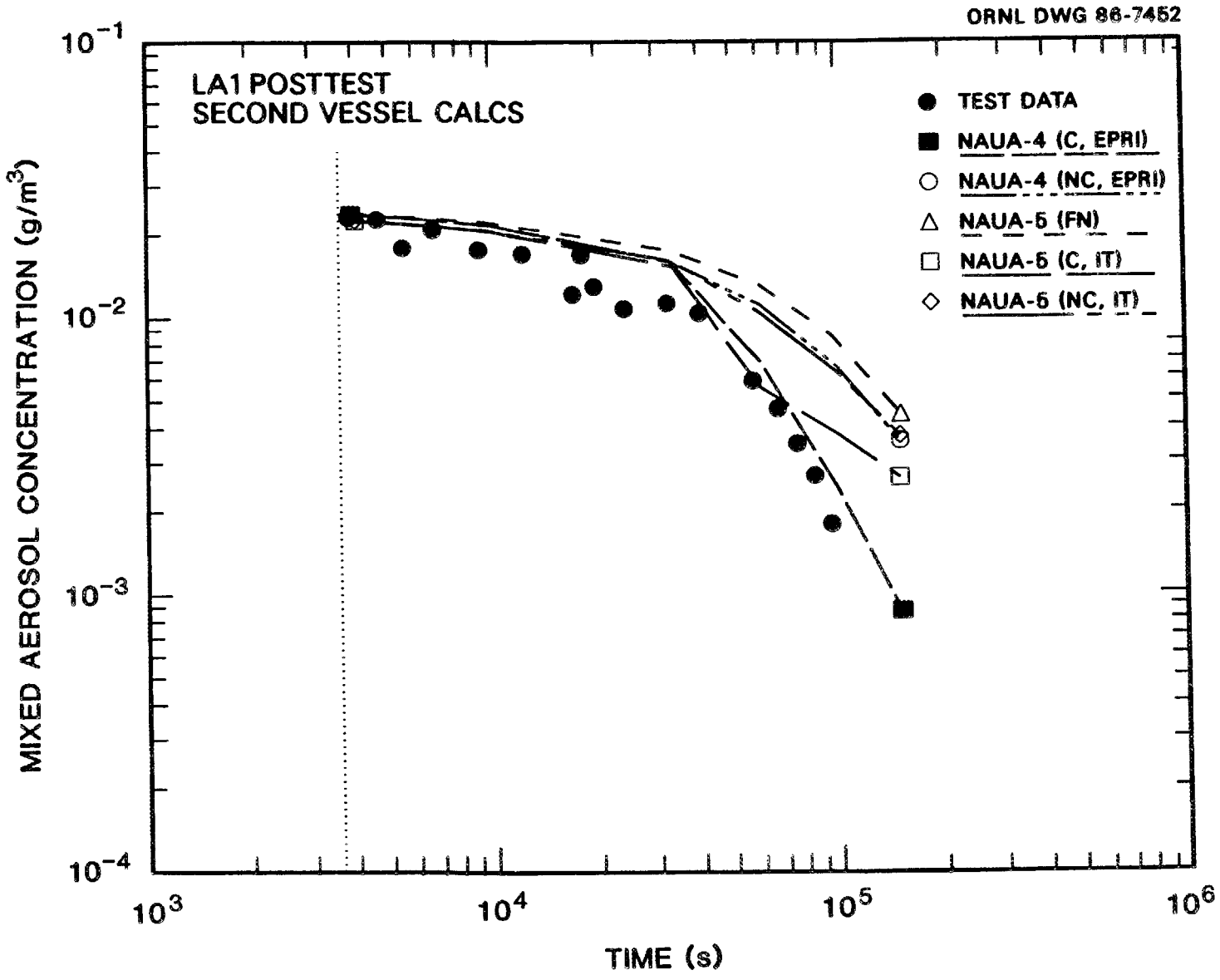

Fig. 43. LA1 "second set" vessel results: airborne mixed aerosol concentration vs time for NAUA calculations.

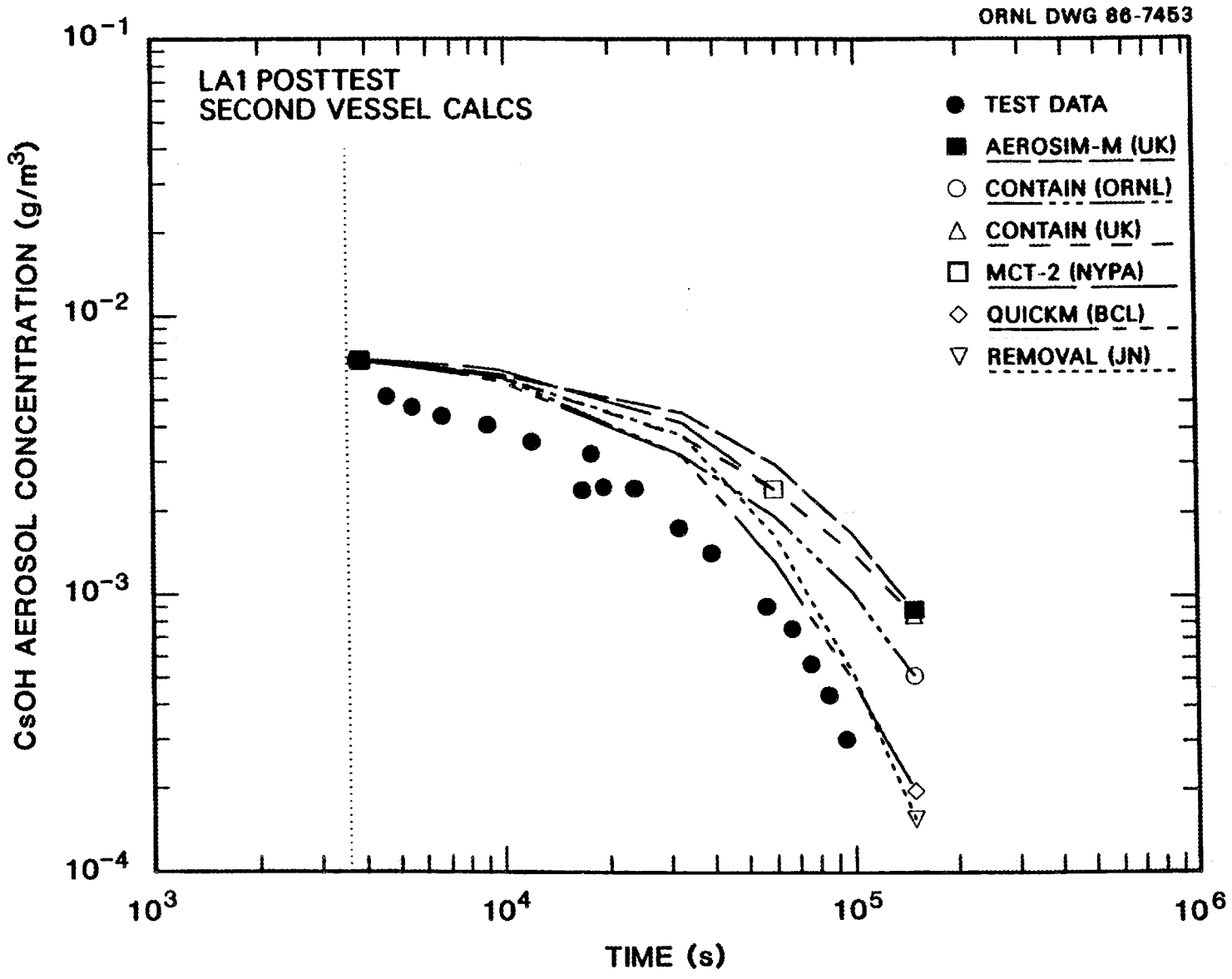

Fig. 44. LA1 "second set" vessel results: airborne CsOH aerosol concentration vs time for codes other than NAUA.

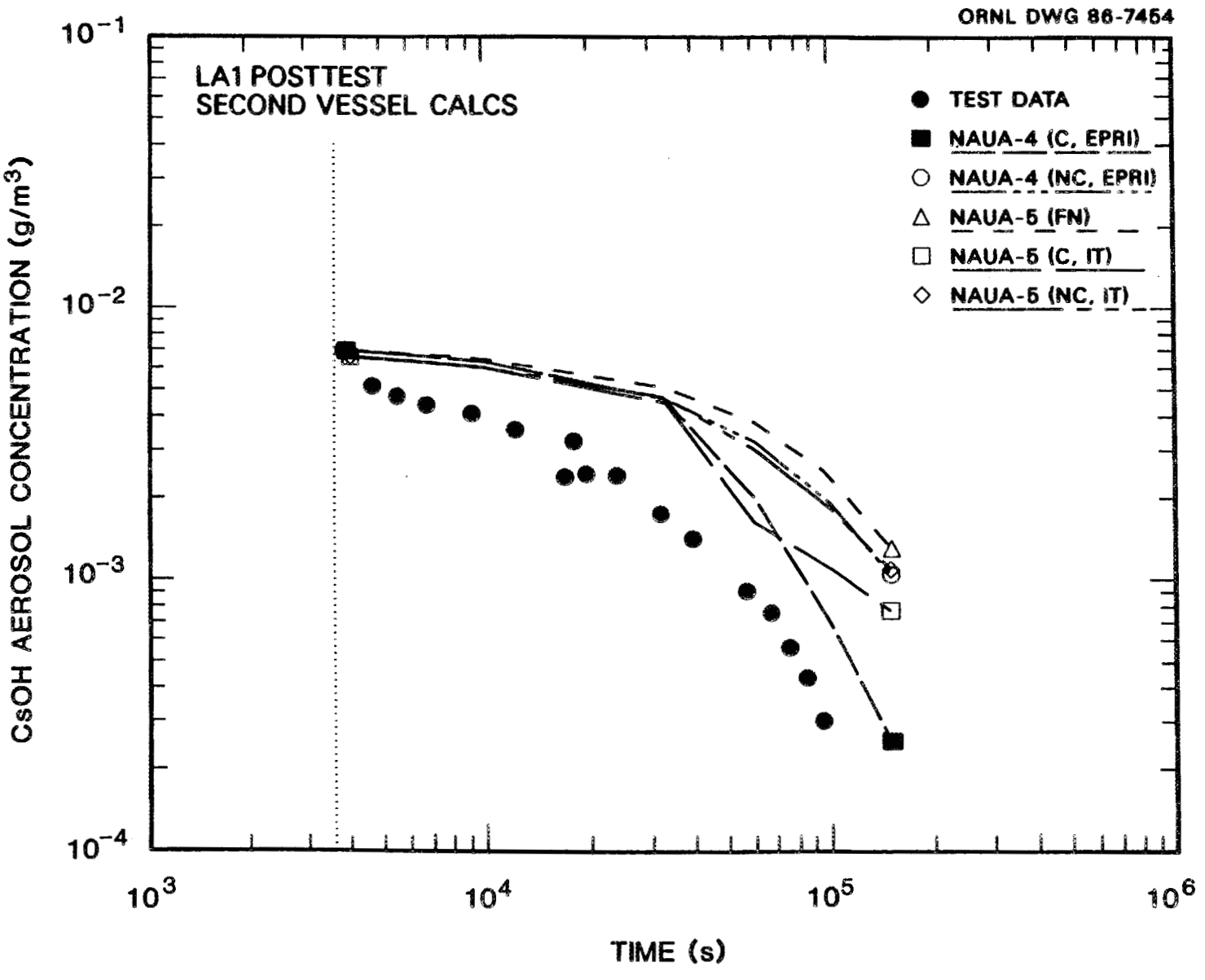

Fig. 45. LA1 "second set" vessel results: airborne CsOH aerosol concentration vs time for NAUA calculations.

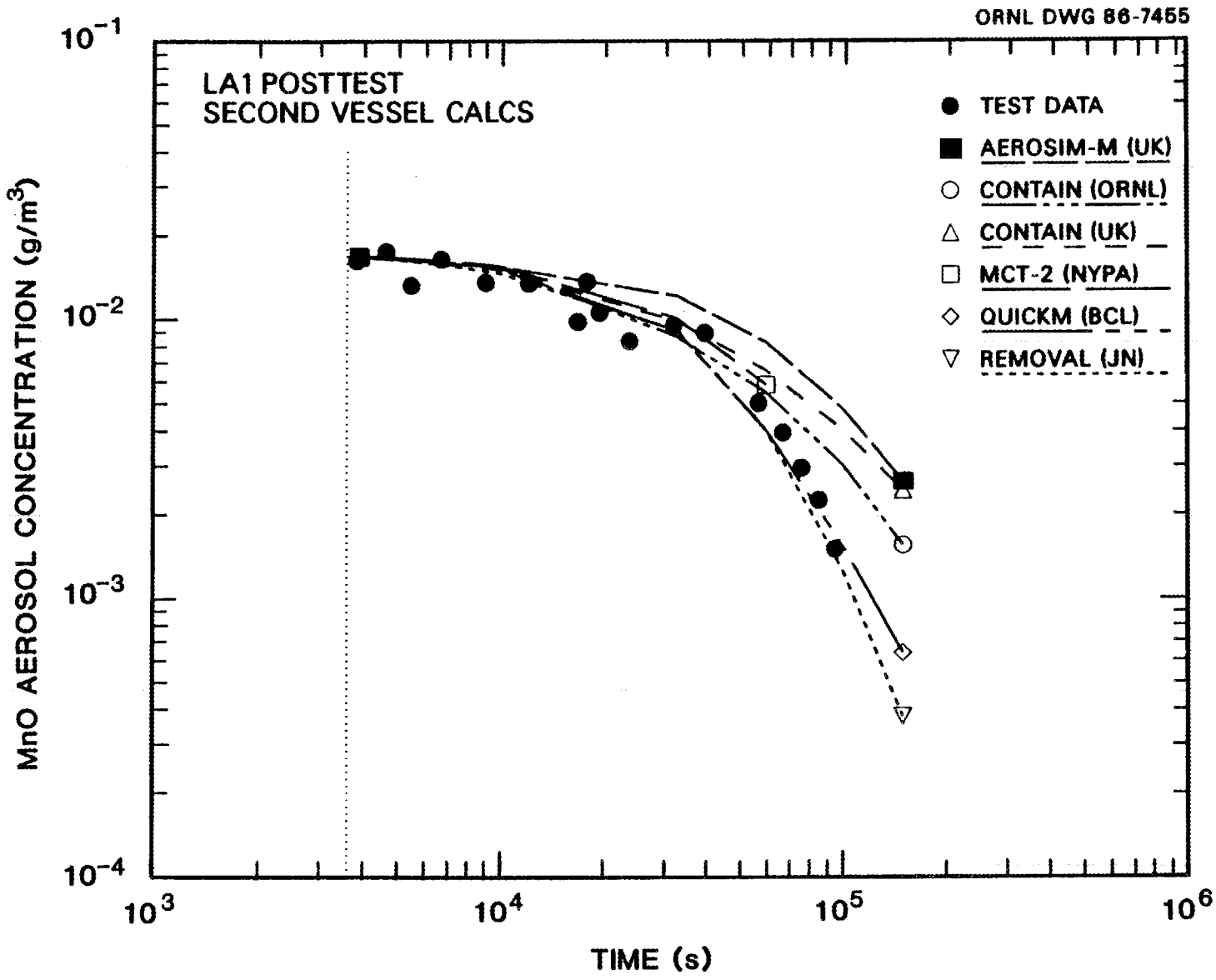

Fig. 46. LA1 "second set" vessel results: airborne MnO aerosol concentration vs time for codes other than NAUA.

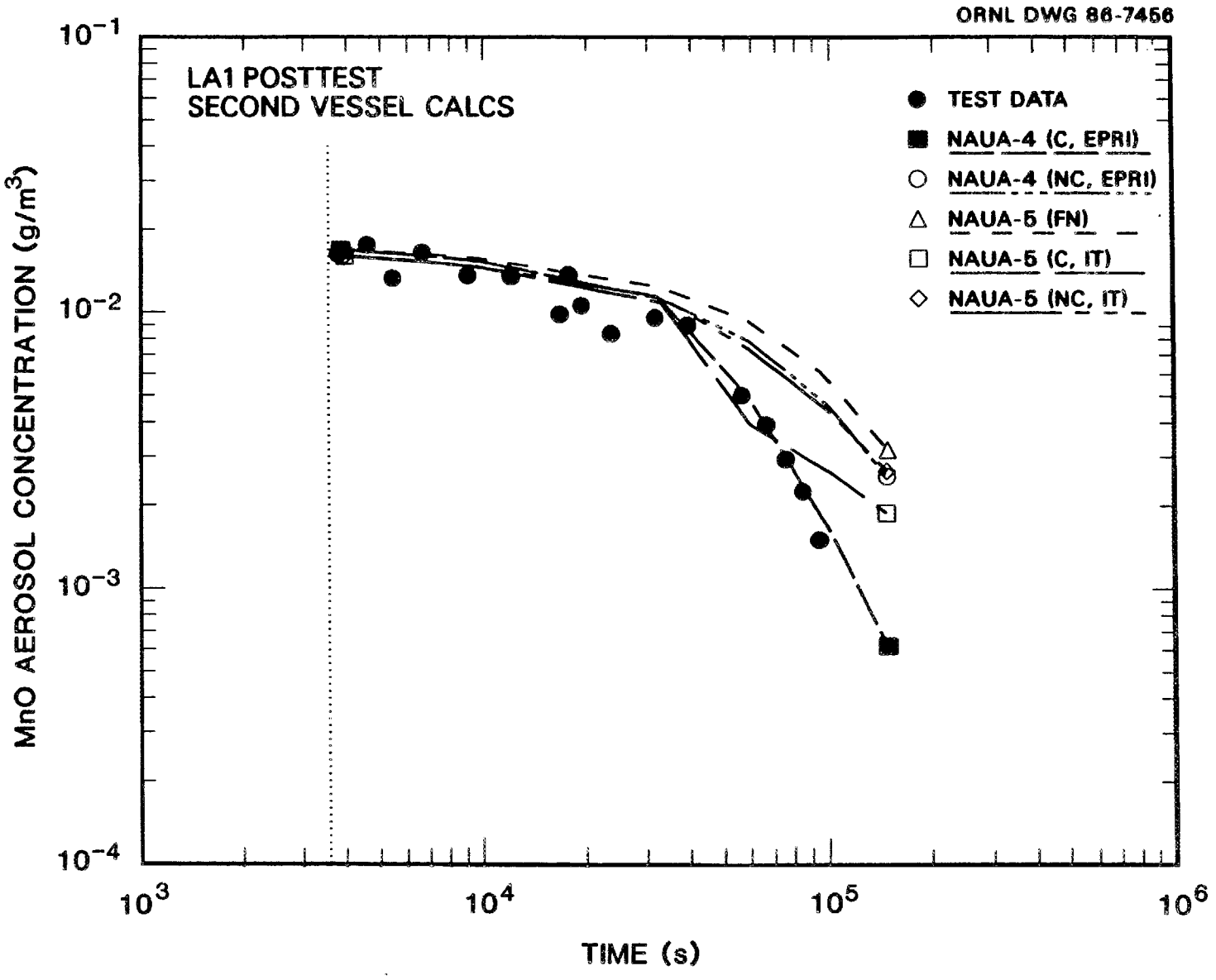

Fig. 47. LA1 "second set" vessel results: airborne MnO aerosol concentration vs time for NAUA calculations.

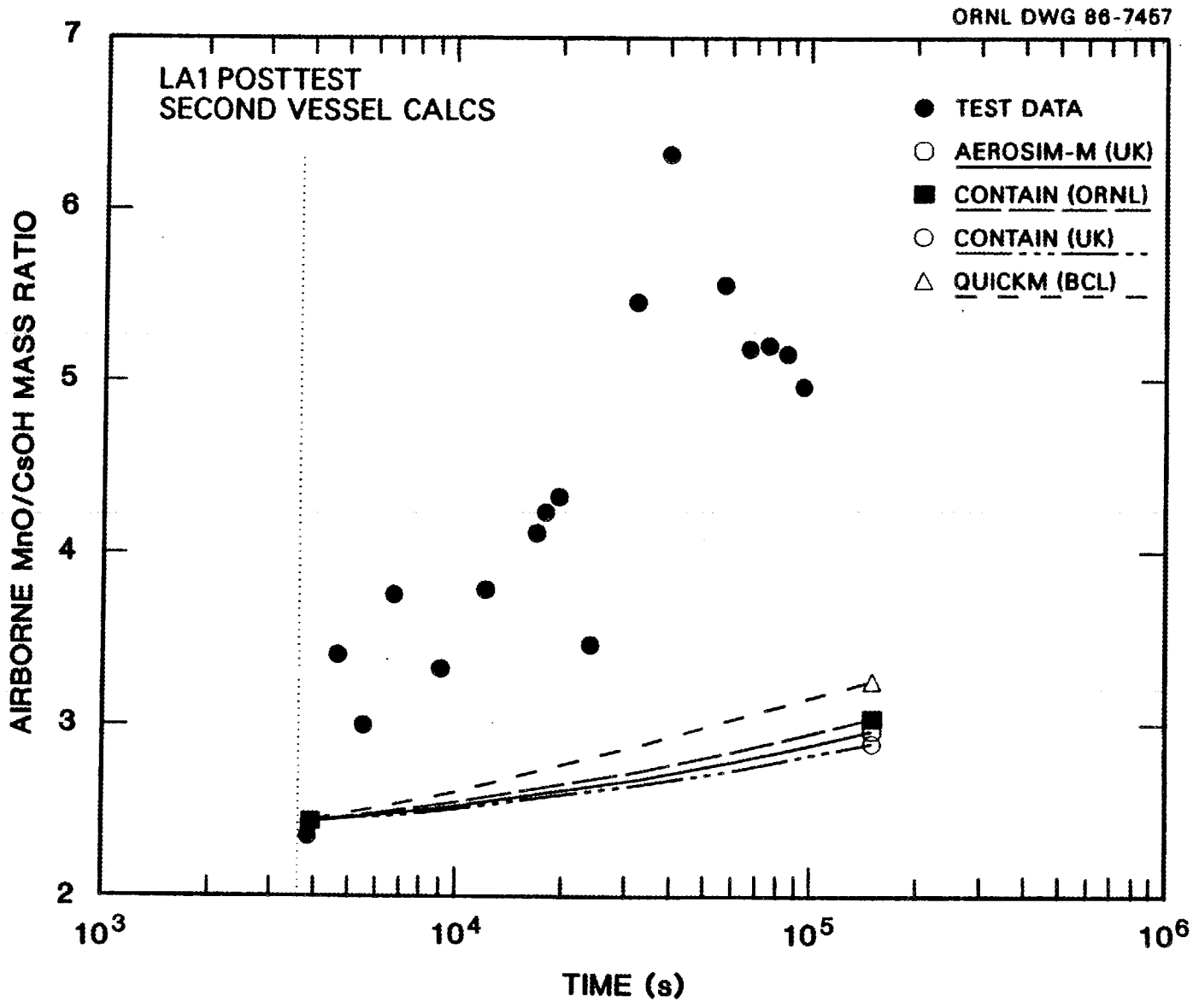

Fig. 48. LA1 "second set" vessel results: airborne MnO/CsOH mass ratio vs time calculated by "multi-component" codes.

Table 31. Calculated errors in predicted aerosol concentrations (3600 to 100,000 s); second set calculations

CsOH+MnO		CsOH		MnO	
Code	Average mean square error (%)	Code	Average mean square error	Code	Average mean square error (%)
AEROSIM-M (UK)	84.2	AEROSIM-M (UK)	183.3	AEROSIM-M (UK)	66.4
CONTAIN (ORNL)	39.0	CONTAIN (ORNL)	102.8	CONTAIN (ORNL)	29.1
CONTAIN (UK)	58.9	CONTAIN (UK)	141.5	CONTAIN (UK)	44.7
MCT-2 (NYPA)	50.9	MCT-2 (NYPA)	146.3	MCT-2 (NYPA)	34.4
NAUA-4,C(EPRI)	37.8	NAUA-4,C(EPRI)	126.4	NAUA-4,C(EPRI)	22.8
NAUA-4,NC(EPRI)	82.7	NAUA-4,NC(EPRI)	204.3	NAUA-4,NC(EPRI)	60.8
NAUA-5 (FN)	107.4	NAUA-5 (FN)	249.0	NAUA-5 (FN)	81.5
NAUA-5,C (IT)	35.3	NAUA-5,C (IT)	120.3	NAUA-5,C (IT)	21.8
NAUA-5,NC (IT)	76.0	NAUA-5,NC (IT)	193.0	NAUA-5,NC (IT)	55.1
QUICK-M (BCL)	20.7	QUICK-M (BCL)	68.0	QUICK-M (BCL)	15.5
REMOVAL (JN)	21.5	REMOVAL (JN)	91.7	REMOVAL (JN)	14.1

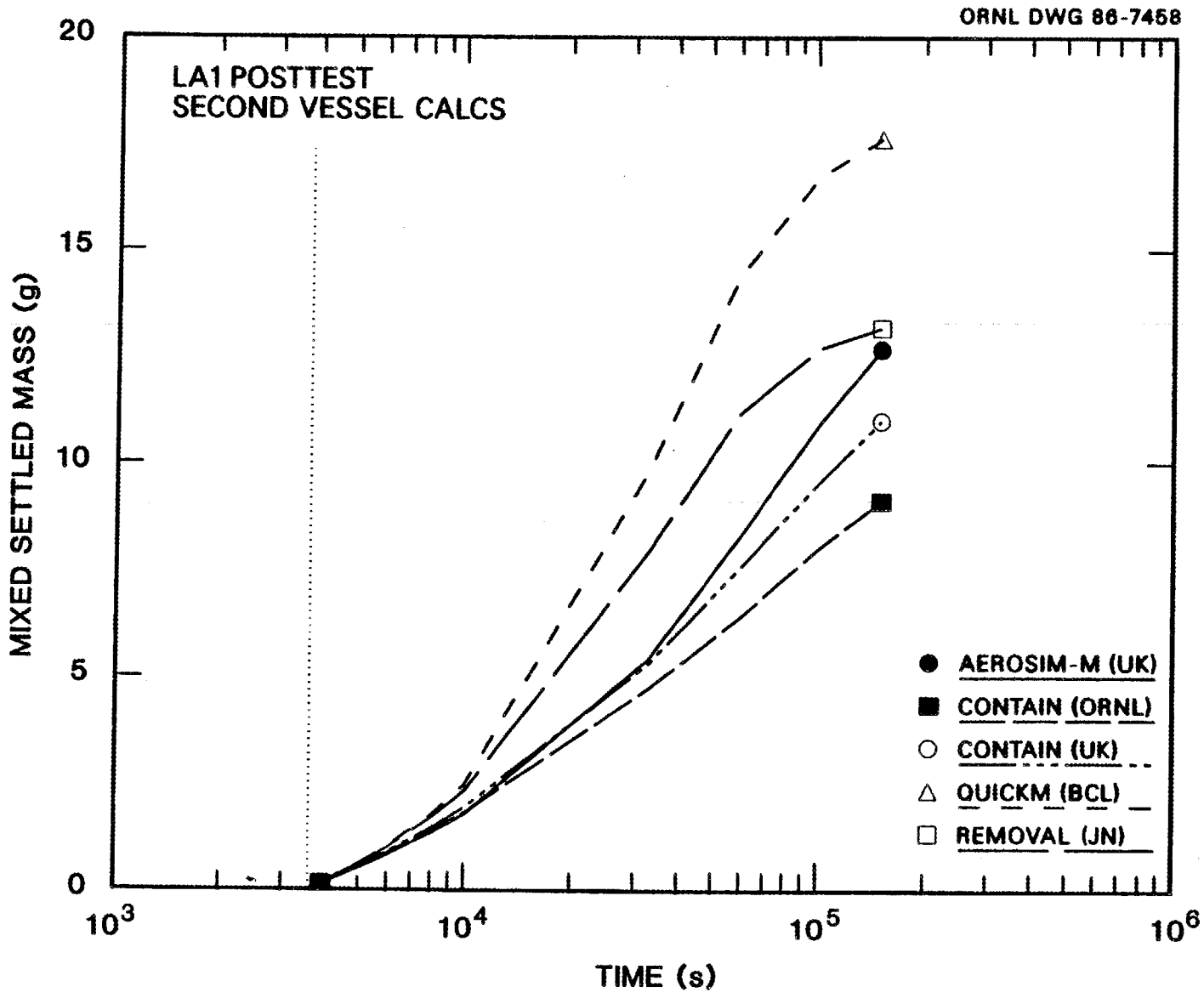

Fig. 49. LA1 "second set" vessel results: cumulative mixed aerosol settling vs time for codes other than NAUA.

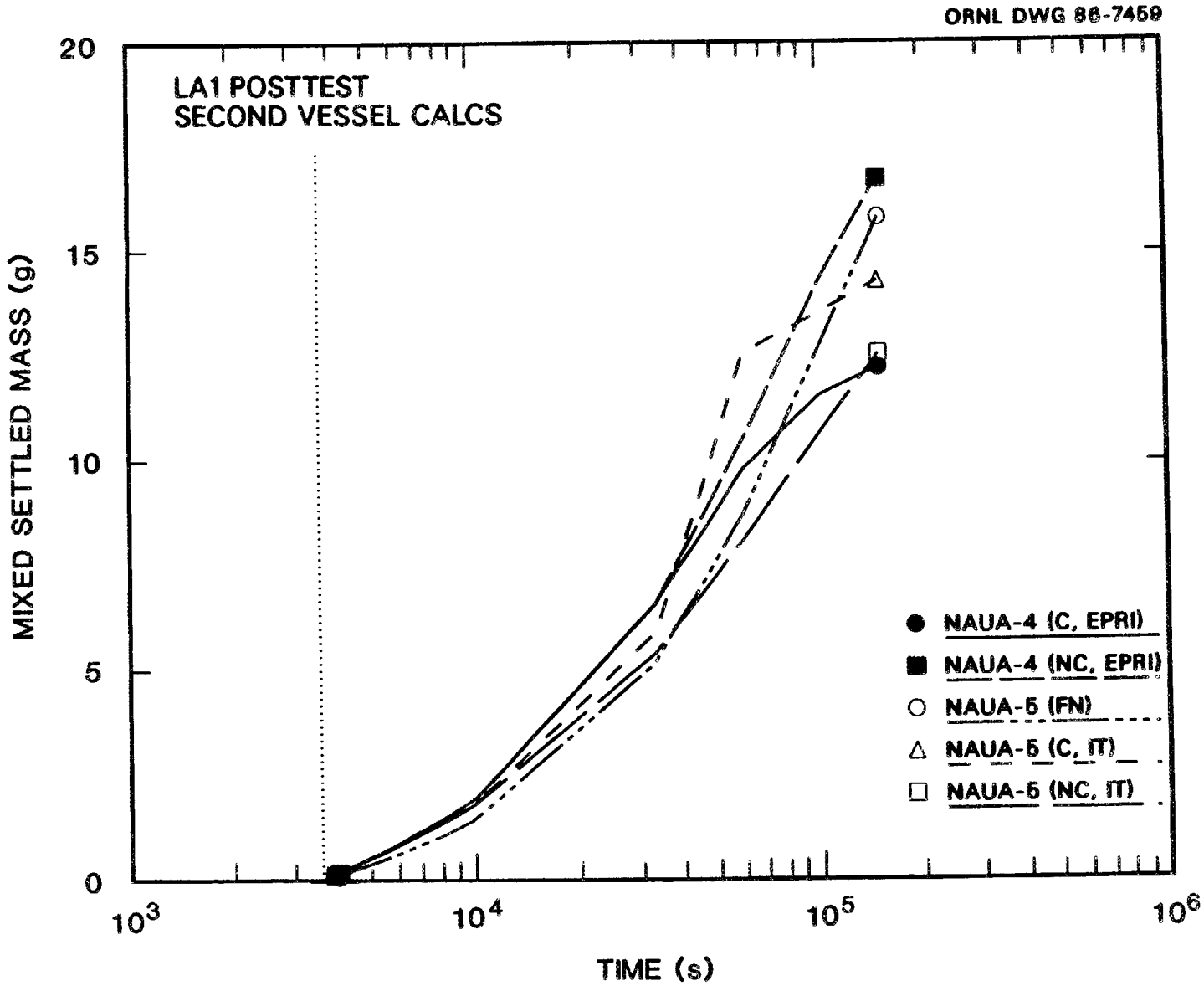

Fig. 50. LA1 "second set" vessel results: cumulative mixed aerosol settling vs time for NAUA calculations.

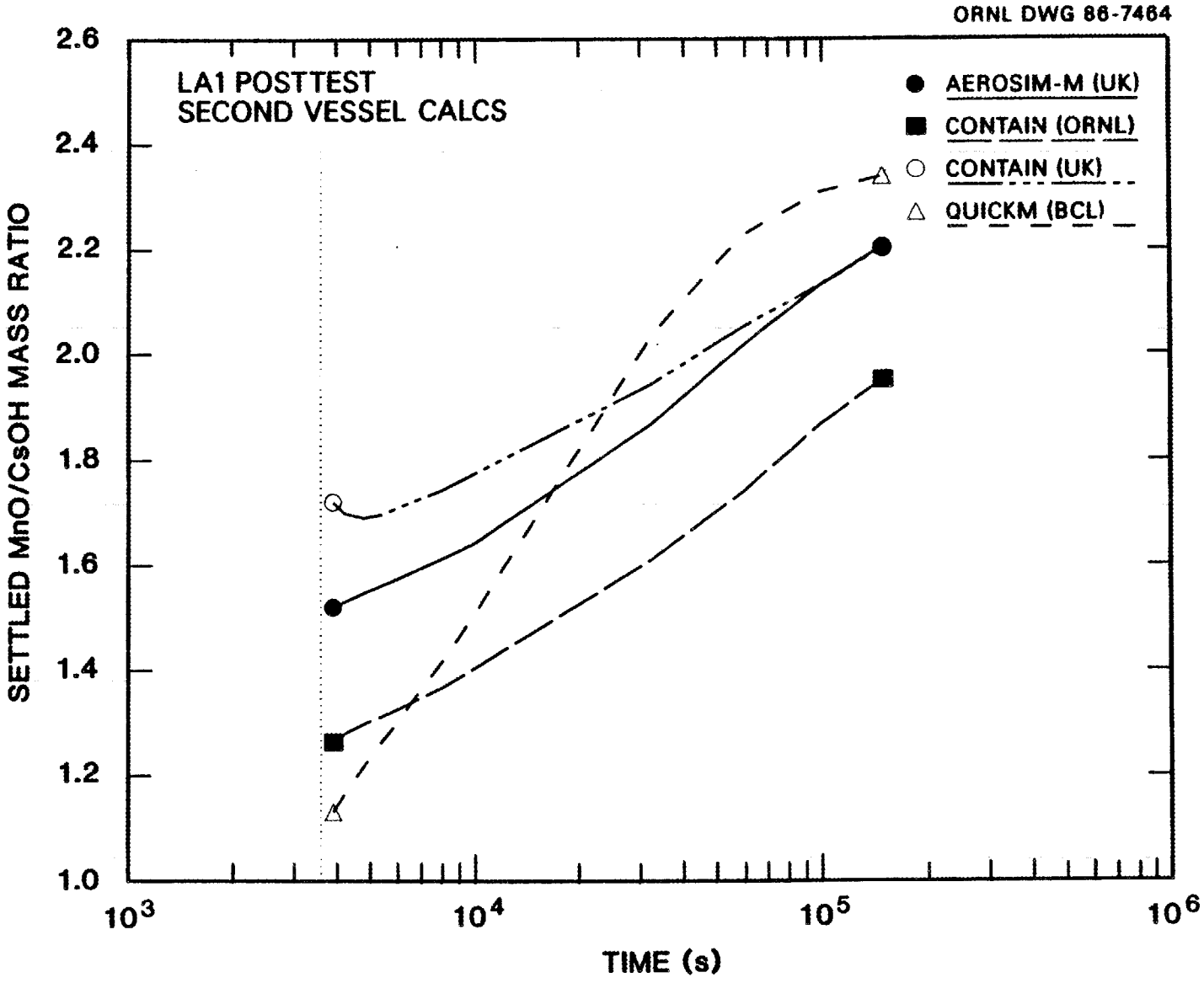

Fig. 51. LA1 "second set" vessel results: settled MnO/CsOH mass ratio vs time calculated by "multi-component" codes.

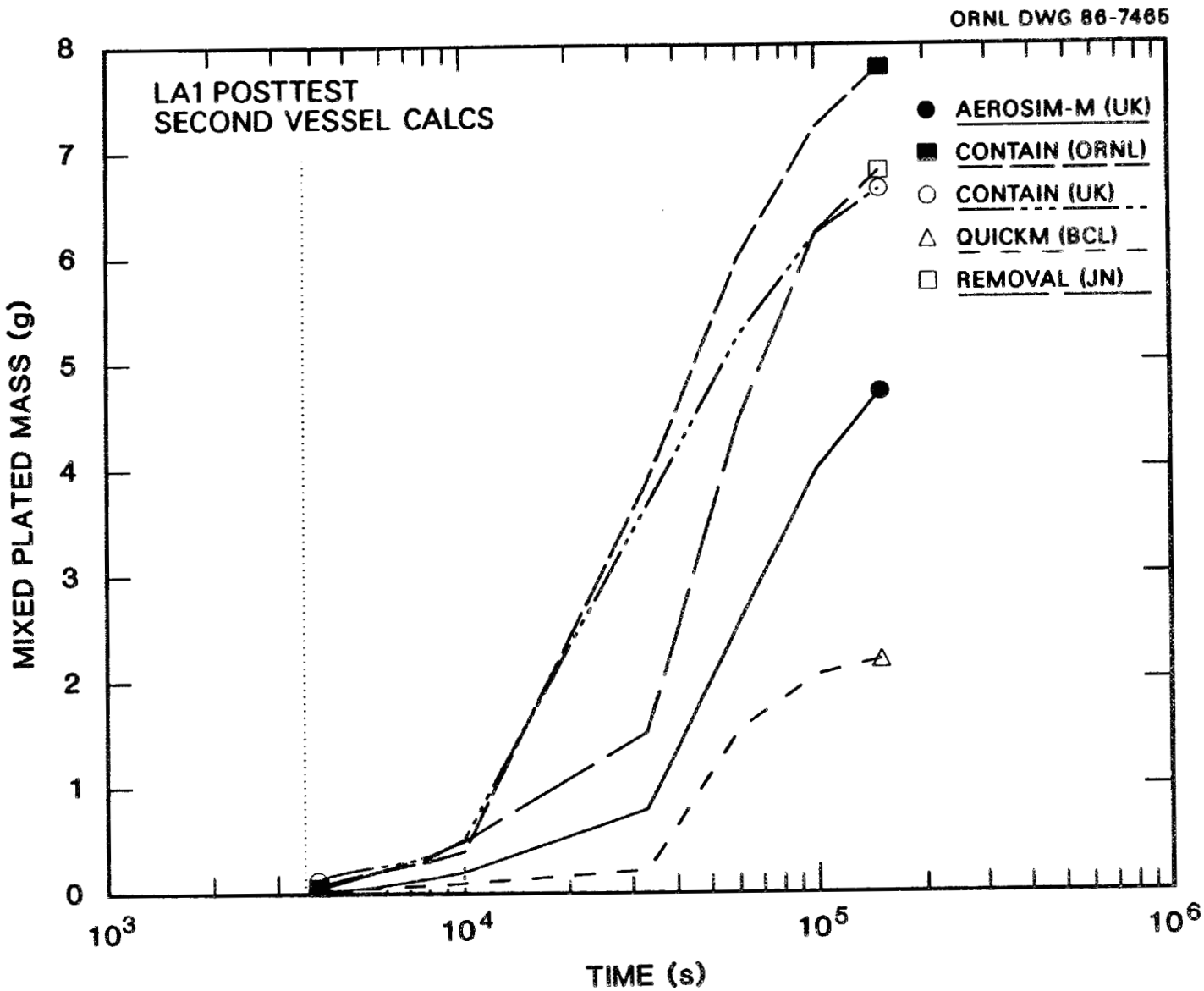

Fig. 52. LA1 "second set" vessel results: cumulative mixed aerosol plateout vs time for codes other than NAUA.

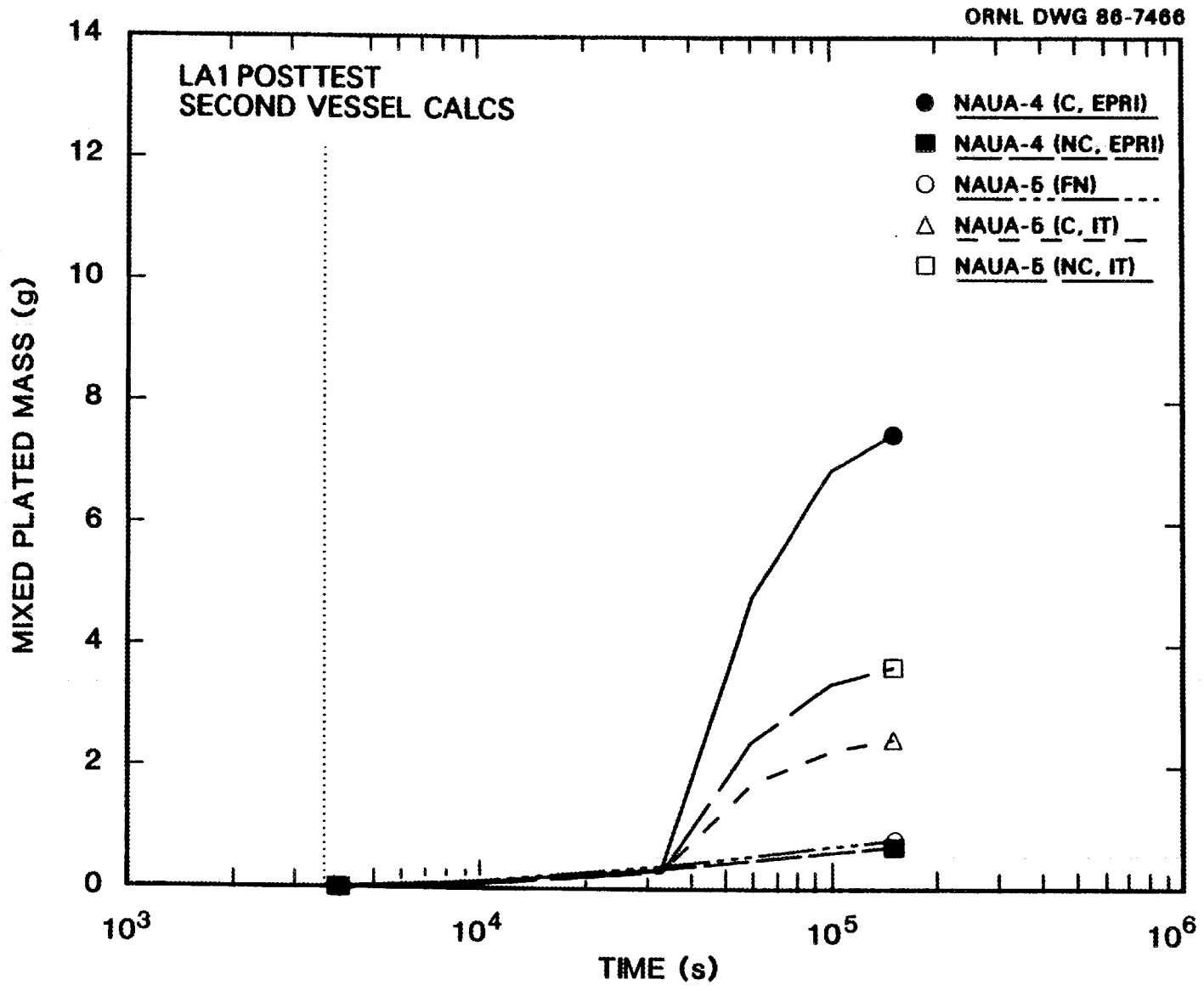

Fig. 53. LA1 "second set" vessel results: cumulative mixed aerosol plateout vs time for NAUA calculations.

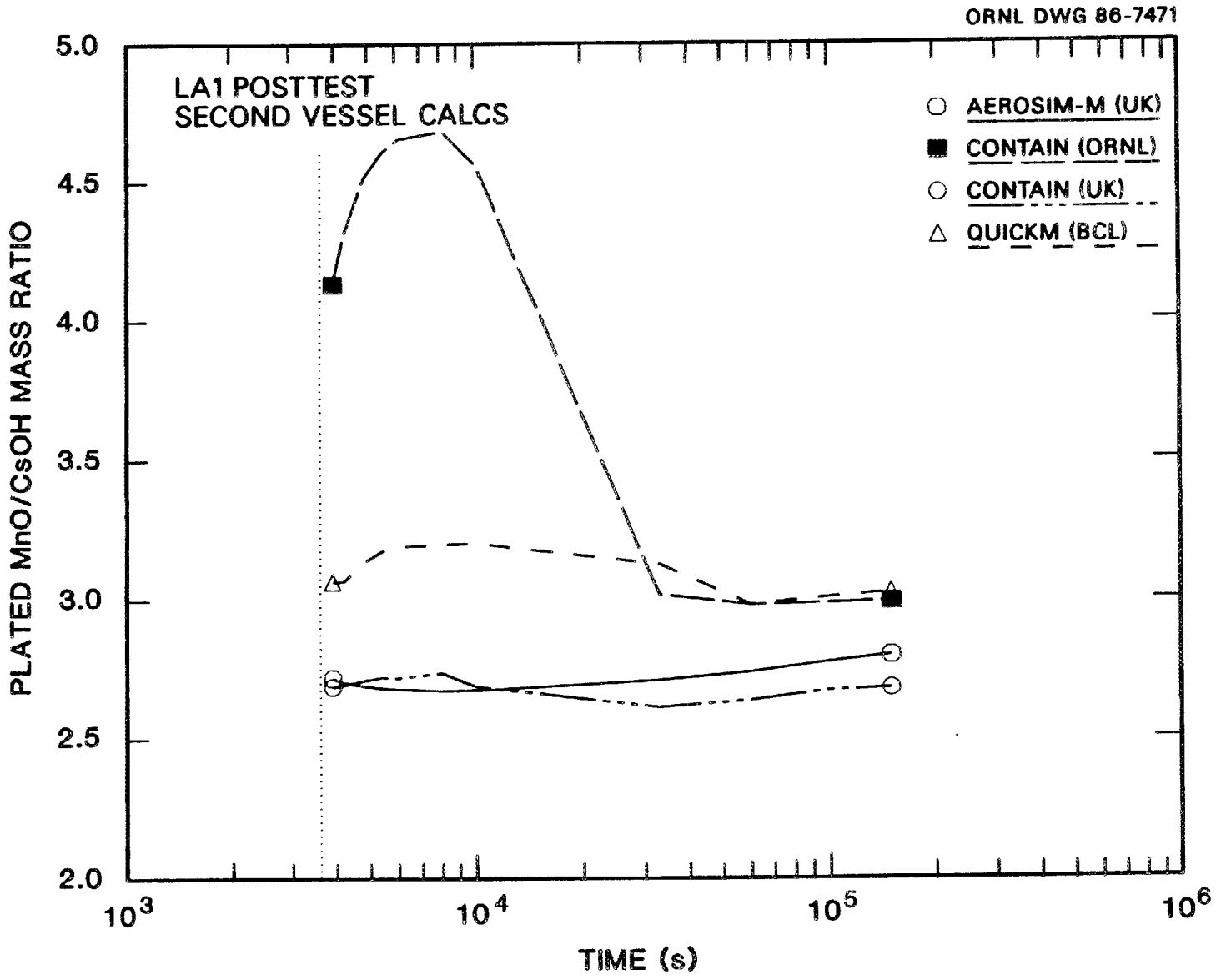

Fig. 54. LA1 "second set" vessel results: plated MnO/CsOH mass ratio vs time calculated by "multi-component" codes.

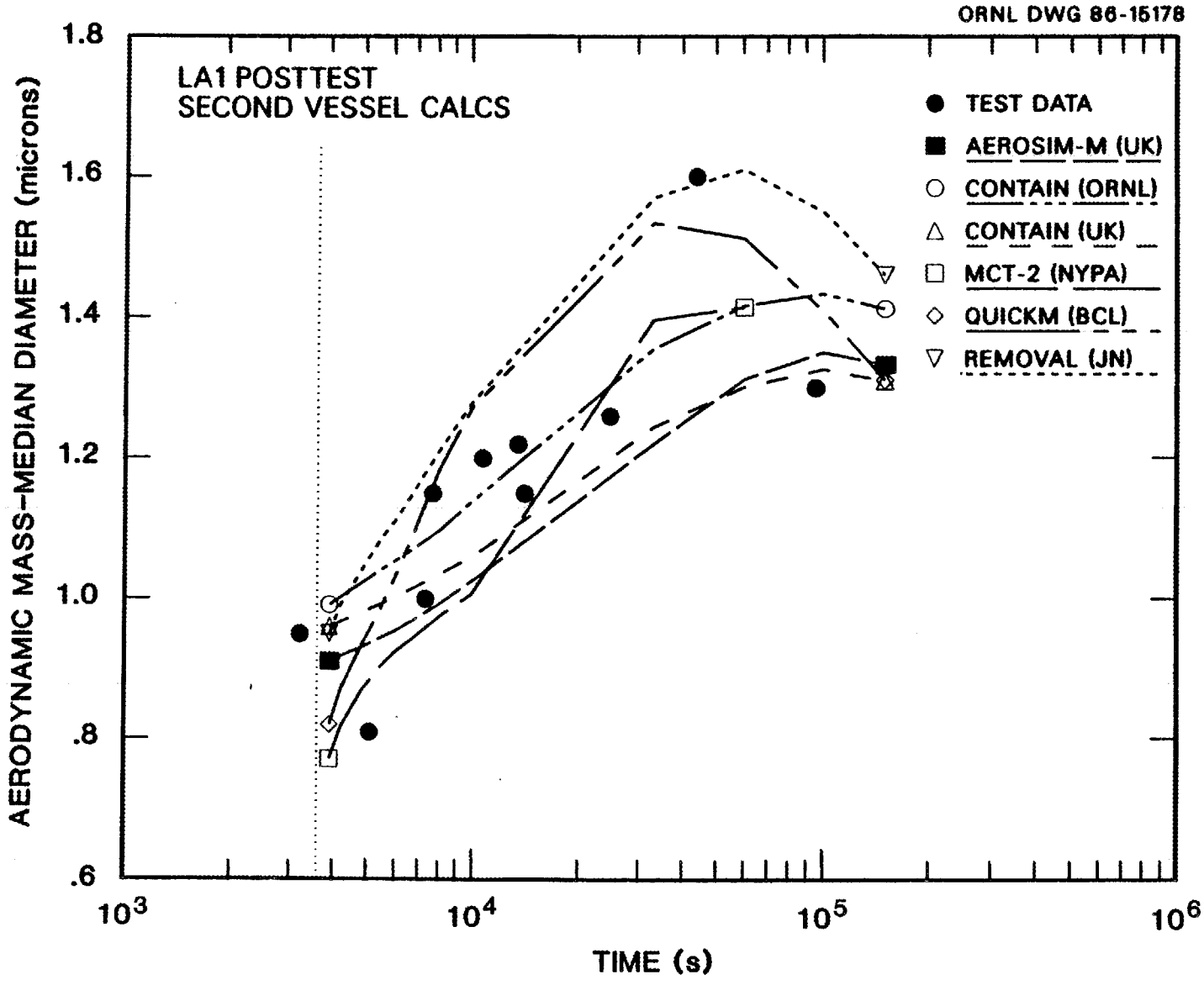

Fig. 55. LA1 "second set" vessel results: aerodynamic mass-median diameter vs time for codes other than NAUA.

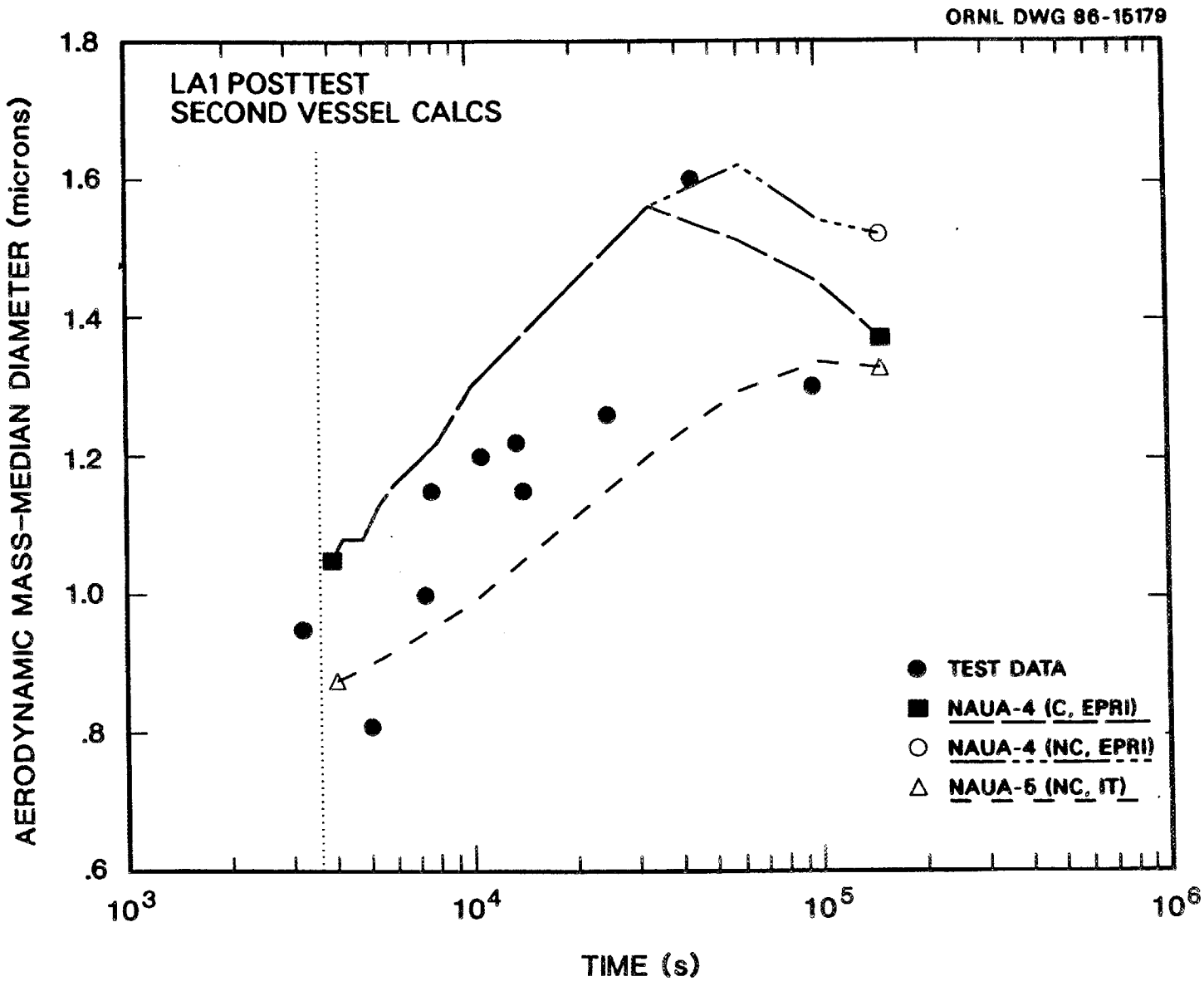

Fig. 56. LA1 "second set" vessel results: aerodynamic mass-median diameter vs time for NAUA calculations.

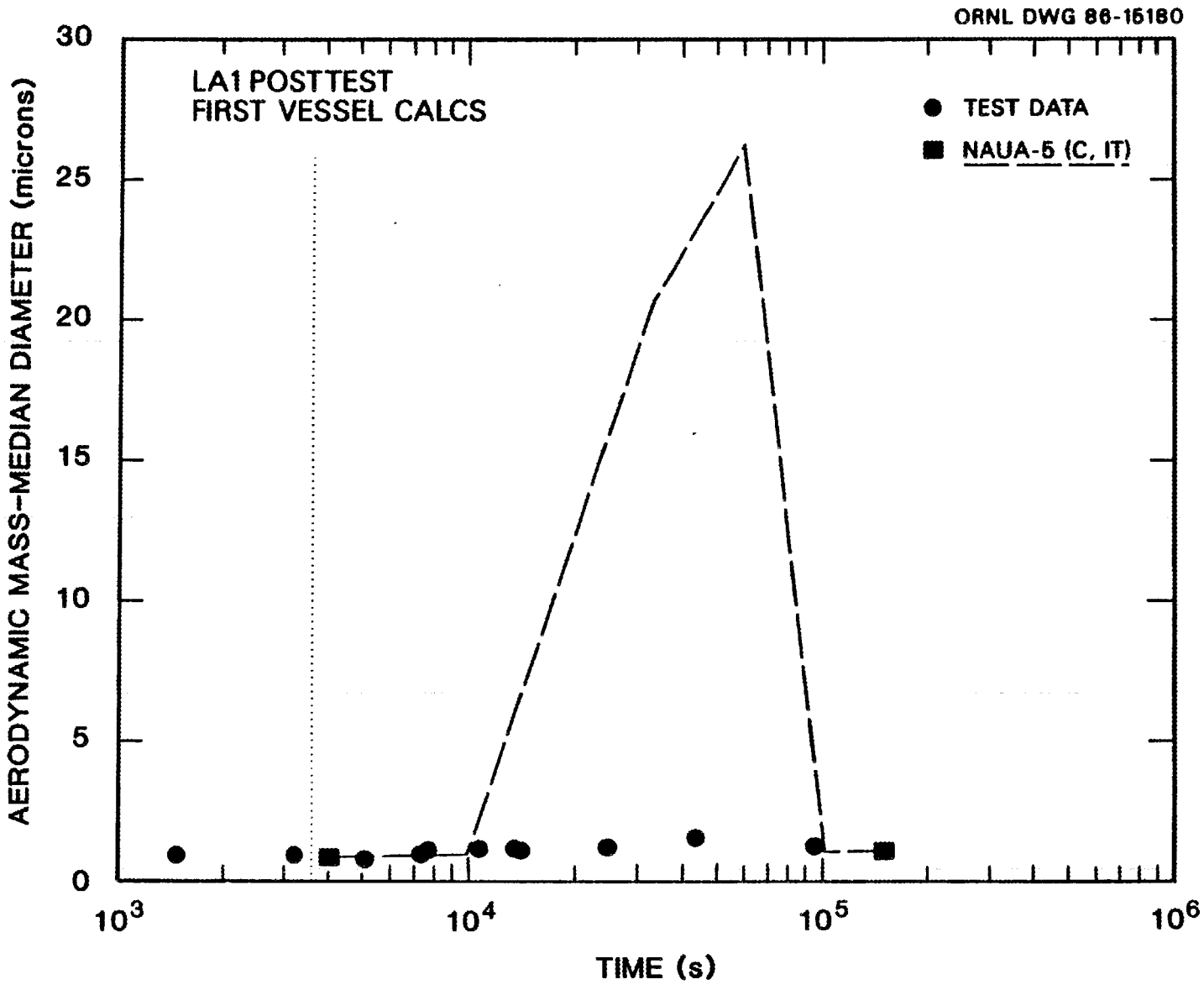

Fig. 57. LA1 "second set" vessel results: aerodynamic mass-median diameter vs time for NAUA-5,C (IT) calculation.

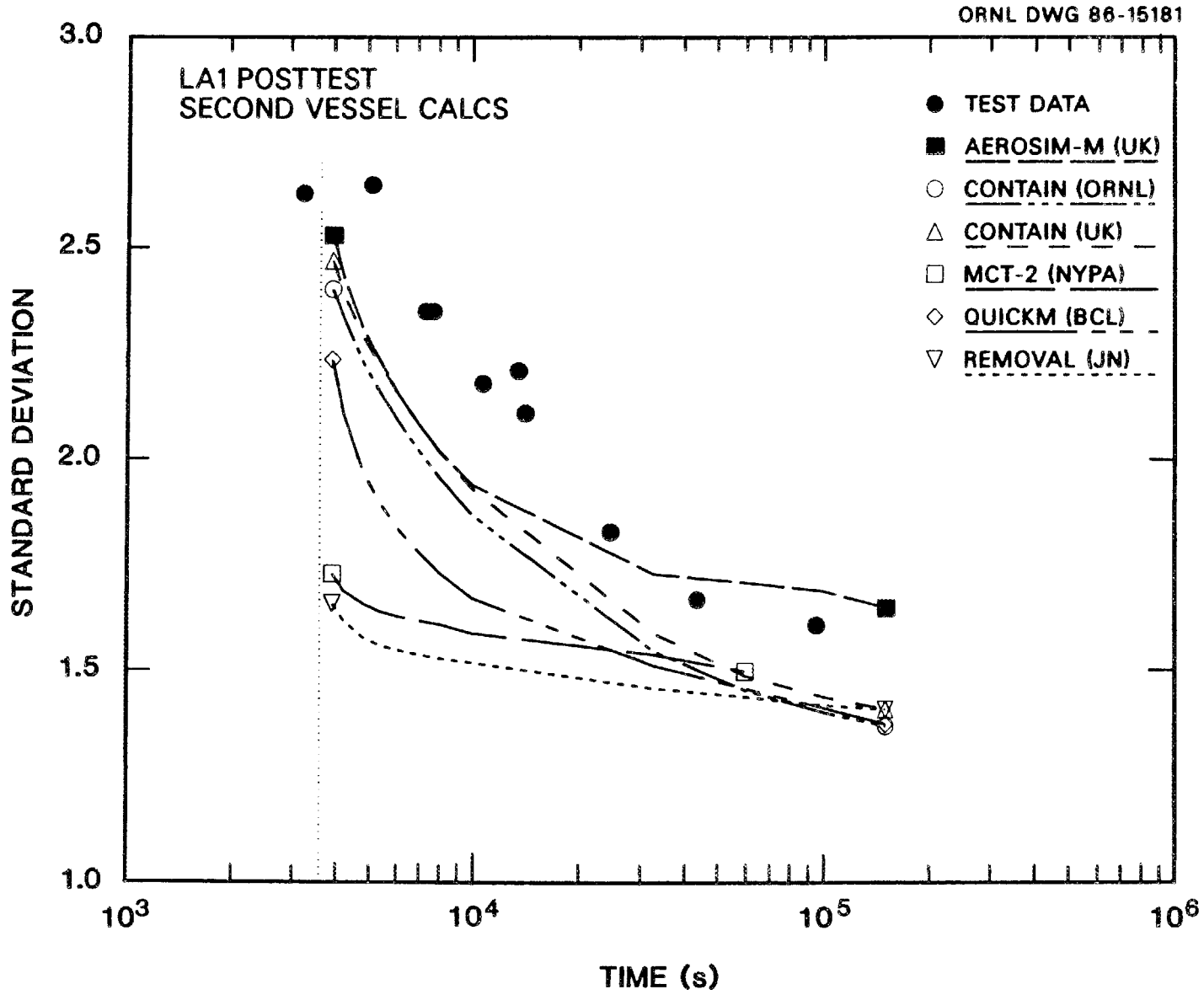

Fig. 58. LA1 "second set" vessel results: geometric standard deviation vs time for codes other than NAUA.

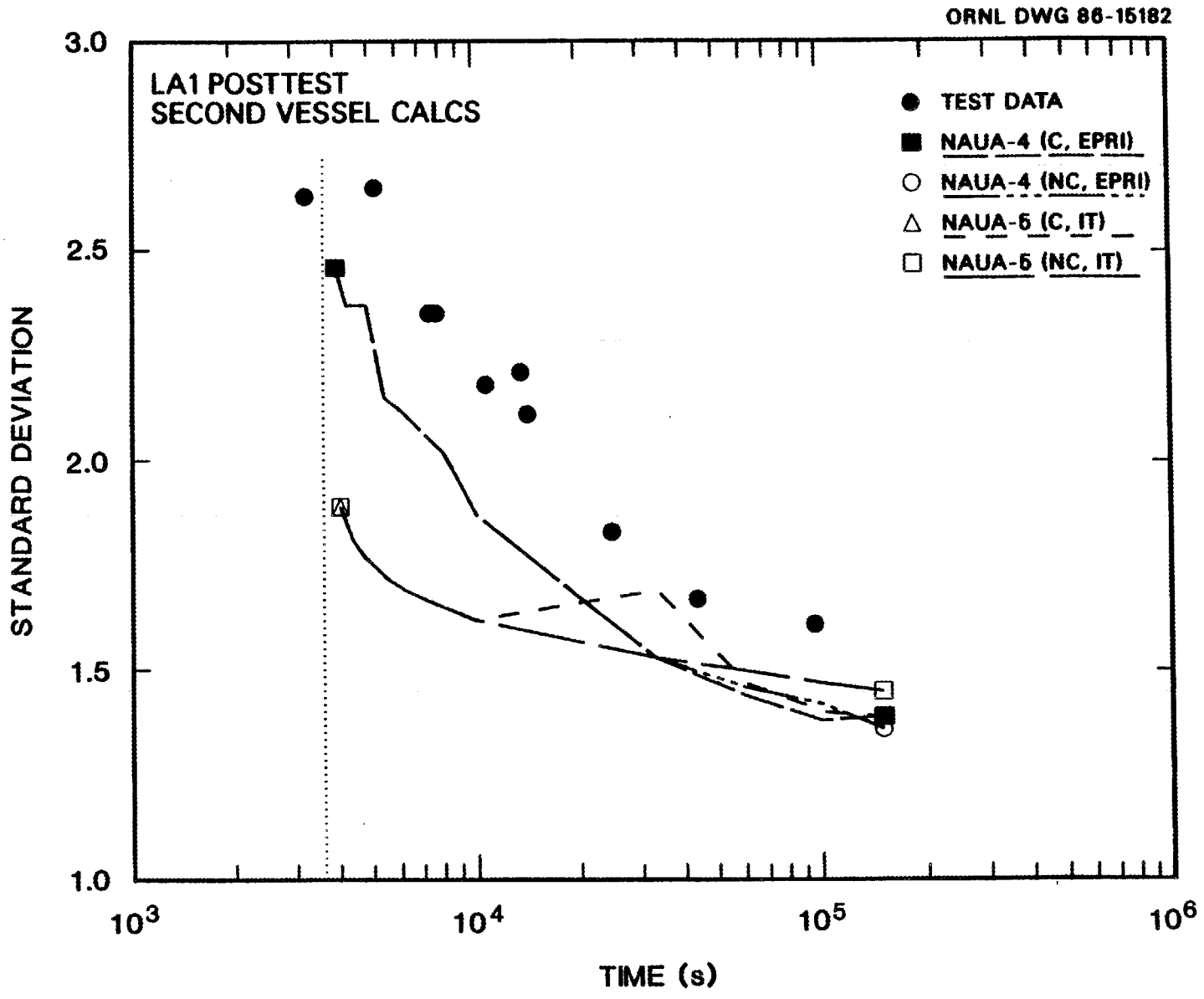

Fig. 59. LA1 "second set" vessel results: geometric standard deviation vs time for NAUA calculations.

Table 32. Calculated errors in predicted aerosol size parameters (3,600 to 100,000 s); second set calculations

AMMD		Geometric standard deviation	
Code	Average mean square error	Code	Average mean square error
AEROSIM-M (UK)	12.7	AEROSIM-M (UK)	10.3
CONTAIN (ORNL)	11.4	CONTAIN (ORNL)	14.2
CONTAIN (UK)	12.2	CONTAIN (UK)	11.7
MCT-2 (NYPA)	10.5	MCT-2 (NYPA)	25.7
NAUA-4,C(EPRI)	17.1	NAUA-4,C(EPRI)	13.6
NAUA-4,NC(EPRI)	17.8	NAUA-4,NC(EPRI)	13.4
NAUA-5,NC (IT)	14.0	NAUA-5,C (IT)	23.6
QUICK-M (BCL)	11.2	NAUA-5,NC (IT)	24.2
REMOVAL (JN)	16.0	QUICK-M (BCL)	21.4
		REMOVAL (JN)	28.8

shortly after 3,600 s; this drop was not predicted by any of the codes. Because of this, as illustrated in Table 31, most of the CsOH concentration calculations differed from the measured results by more than 100%.

Figure 48 shows comparisons of calculated and measured airborne aerosol mass ratios for the AEROSIM-M, CONTAIN, and QUICK-M calculations (all other code calculations held the mass ratio fixed at a value of 2.43). Although these results are better than those illustrated in Figure 15 for the first set of calculations, none of the codes accurately predicted the measured mass ratios.

Figures 49 to 51 are plots of total settled mass vs time for t>3,600 s (assuming that at t=3,600 s, the settled mass = 0), and of the settled mass ratio vs time. The amount of aerosol settling for t>3,600 s was not measured; therefore, only the calculated values for total settled mass are shown. If we compare the results in Figures 49 and 50 with those in Figures 16 and 17, we note that the total calculated settled mass for the second set of calculations was about half that calculated for the first set. This is explained by the fact that, for the first set of calculations, aerosol concentrations at t=3,600 s were over-predicted by about a factor of 2.

The code results illustrated in Figures 16 and 17 predicted that very little settling occurred during the aerosol source period. If we assume this to be true, then most of the final calculated settled mass values shown in Figs. 49 and 50 compare quite well with the overall measured value of 13.86 g.

Figures 52 to 54 are plots of calculated total plated mass and of the plated mass ratio for t>3,600 s. These results are similar to those in Figs. 24 and 25. If we again assume, based on code results in Figs. 24 and 25, that plateout was minimal for t<3,600 s; then, as for the first set of calculations, most of the codes under-predicted the measured total plateout of 11.87 g.

Figures 55 to 59 and Table 32 show the AMMD and geometric standard deviation (σ_g) results. Comparing the ranking results in Table 30 with

those in Table 26, we see that code predictions for AMMD and σ_g improved for the second set of calculations. However, the MCT-2, REMOVAL, and all NAUA results (except those from EPRI) showed sharp drops in calculated σ_g shortly after 3,600 s (for each of the codes the first data point shown on the plots is at 3,900 s); these drops do not correlate with the measured values.

For this set of calculations, we had sufficient data from the MCT-2 (NYPA), NAUA-5 (IT), and REMOVAL (JN) calculations to recalculate values of the geometric standard deviation (GSD) for times shortly after 3,600 s. There are a number of ways that the GSD can be determined,[13] but the generalized analytical formula used to calculate it is:

$$\ln(GSD) = [\sum_i (m_i(\ln d_i - \ln d_m)^2)/M]^{0.5} \qquad (7)$$

where

GSD = geometric standard deviation
m_i = the mass of particles with diameter d_i
d_m = logarithmic mass-mean diameter = $w_i \ln d_i$
w_i = mass fraction of aerosol with diameter d_i
M = total airborne aerosol mass

This method to calculate the GSD is being used to analyze the impactor data and to determine the code-calculated GSDs for the LA2 posttest code comparisons.[14]

If the aerosol size distribution is log-normal, the GSD can be determined from either of the following two formulas:

$$GSD = d_{50}/d_{15.8} \qquad (8)$$

or

$$GSD = d_{84.13}/d_{50} \qquad (9)$$

where

$d_{15.8}$: 15.8% of the aerosol mass consists of particles having sizes less than this diameter

d_{50} : 50% of the aerosol mass consists of particles having sizes less than this diameter (d_{50} is the mass-median diameter)

$d_{84.13}$: 84.13% of the aerosol mass consists of particles having sizes less than this diameter

Table 33 presents comparisons of our calculated values of the GSD with the values calculated by the MCT-2 (NYPA), NAUA-5 (IT), and REMOVAL (JN) code versions. The following comments can be made about the data in this table:

1. Equations 8 and 9 consistently give different estimates of the GSD; and in all cases, the GSD calculated by Eq. 8 is less than that calculated by Eq. 9. which illustrates that the code calculated size distribution is not log-normal. Therefore (as was discovered by J. H. Wilson in analysis of the LA2 posttest data[14]) we recommend that all codes should calculate the GSD using Eq. 7, the generalized formula to calculate the standard deviation.
2. The results in Table 33 show that for times greater than 3,600 s, the MCT-2 (NYPA), NAUA-5 (IT), and REMOVAL (JN) codes did not correctly calculate the GSD as determined using Eq. 7. These codes under-calculated the GSD, which is consistent with the results illustrated in Figs. 58 and 59. It is interesting to note that the NAUA-4 (EPRI) code uses Eq. 7 to calculate the GSD, and that (as shown in Fig. 59) the NAUA-4 (EPRI) version did better than other NAUA versions in calculating it.
3. The NAUA-5 (IT) results in Table 31 for 3,600.1 s suggest that the size distribution at that time was not log-normal. However, that suggestion does not make sense, since the calculation was started at 3,600 s; we do not have an explanation for this result.

Table 33. Comparisons of geometric standard deviations (GSD) calculated by different methods (Eqs. 7-9) with code results

Code	Test time (s)	Equation No 7	8	9	Code calculated
MCT-2 (NYPA)	4,800	2.12	2.30	2.43	1.70
NAUA-5 (IT)	3,600.1	2.57	2.37	2.87	2.66
NAUA-5 (IT)	5,470	2.19	1.98	2.55	1.72
REMOVAL (JN)	4,800	1.99	1.84	2.22	1.58

Once more we believe that differences in wall plateout modeling, and in particular, how steam condensation on the walls was modeled, had the major influence on differences in calculated results. Table 34 summarizes differences in wall plateout modeling assumptions used by the different code analysts. We will also discuss how these parameters influenced the different code results.

AEROSIM-M (UK)

The same modeling assumptions were used for the first and second sets of calculations. For the second calculation, the code predicted that 2.0 g of aerosol was removed by thermophoresis and diffusion, and that 2.7 g was removed by diffusiophoresis. These plateout values are less than in the first vessel results because the airborne concentration used to start the calculation (at 3,600 s) was less than the predicted concentration at 3,600 s in the "first set" calculation.

CONTAIN (ORNL)

The vessel pressure used to start this calculation (at 3,600 s) was greater than atmospheric (recall that the pressure at 3,600 s was less than atmospheric in the first vessel calculation). Because of this, "back-flow" of gas from the surroundings into the vessel did not occur until 19,200 s (compared to 4,800 s for the first set calculation). Again, because of the back-flow, small amounts of water aerosols were calculated to become airborne for times greater than 19,200 s. The amount of water on the aerosols was always less than .1% of the solid aerosol mass.

CONTAIN calculated that water condensation on the vessel walls started somewhere between 14,620 and 19,240 s; it was initiated when wall temperatures became less than the atmosphere saturation temperatures. In the test, however, measured wall temperatures were not below saturation values until 33,000 s. The values of steam condensation rates calculated by CONTAIN are high compared to those we calculated in Table 11. Because of these differences, CONTAIN is probably over-estimating diffusiophoretic plateout for the second set of calculations. Note in comparing the plateout results in Figs. 23 and 52 CONTAIN (ORNL) calculated more plateout, for t>3,600 s, for the second set of results than the other codes.

Table 34. Summary of major code-input assumptions for second set of vessel calculations

Code	Modeling of steam condensation in vessel	Wall temperature gradients
AEROSIM-M (UK)	Same as for first set of of calculations (see Table 28)	2°C/cm for t>3,600 s
CONTAIN (ORNL)	Wall condensation calculated to start sometime between 14620 and 19,240 s. Average condensation rate for 19,240 to 33,000 s was 7.7 g/s, for 33,000 to 76,020 s 2.23 g/s, no condensation after 76,020 s	a
CONTAIN (UK)	Significant water condensation calculated to start slightly before 10,000 s. Average steam removal rates were 5.5 g/s for 10,000 to 20,000 s, 4.5 g/s for 20,000 to 33,000 s, 2.6 g/s for 33,000 to 80,000 s, 0.08 g/s for 80,000 to 150,000 s.	a
MCT-2 (NYPA)	No steam condensation	a
NAUA-4 (NC,EPRI)	No steam condensation	None
NAUA-4 (C,EPRI)	Same as for first set of calculations (see Table 28)	None
NAUA-5 (FN)	No steam condensation	None
NAUA-5 (NC,IT)	Same as for first set of calculations (see Table 28)	None
NAUA-5 (C,IT)	Same as for first set of calculations (see Table 28)	None
QUICK-M (BCL)	Wall calculation assumed to start at 33,000 s. Condensation rates used were 2.5 g/s at 33,000 s, 2.1 g/s at 60,000 s, 0.03 g/s at 100,000 s, 0.66 g/s at 150,000 s	a
REMOVAL (JN)	Same as for first set of calculations (see Table 28)	6.4°C/cm at t = 3,600 s, 1.14°C/cm at 24,000 s, 0.17°C/cm at 150,000 s

[a]Data not provided for this parameter.

CONTAIN (UK)

Small amounts of water condensation onto the vessel bottom head surface were predicted between 3,900 and 10,000 s. The major water condensation, onto the vessel cylinder walls, was predicted to start at about 10,000 s. This condensation occurred because the calculated wall temperature was less than the vessel atmosphere saturation temperature. The calculated wall temperature at 10,000 s was about 82°C; however, the average measured wall temperature at 10,000 s was about 103°C. Because the CONTAIN (UK) calculation predicts water condensation to start earlier than observed in the test, we believe that deposition by diffusiophoresis was overestimated (as in the ORNL calculation).

MCT-2 (NYPA)

The MCT-2 calculation was performed for times up to 60,000 s; at that time 7 g of aerosol was still calculated to be airborne. Because (as in the first calculation) negligible wall plateout was calculated, we estimate that the total calculated settled mass would be 13.4 + 7.0 = 20.4 g. This amount is larger than the settling calculated by the other codes, but it is within 50% of the overall settled mass. Finally, as in the previous calculations, the code does not correctly calculate the AMMD.

NAUA-4 [NC,C (EPRI)].

The EPRI version of NAUA again had an error in the diffusiophoresis model that caused it to over-calculate diffusiophoresis by about a factor of 2.

NAUA-5 [NC,C (IT)]

Once more one calculation was performed ("NC") in which steam condensation on the walls was modeled, while in the other calculation ("C") steam condensation on the walls and on particles was modeled. The code inputs were the same as for the first set of calculations. When condensation on the aerosols was modeled, shortly after 33,000 s the aerosols

grew to large sizes (as illustrated in Fig. 57); this enlargement caused the aerosol settling rate to sharply increase shortly after 33,000 s (Fig. 50). As for the previous results, the AMMD based on "dry" aerosol mass was significantly less than that including the water. For example, at 60,468 s the calculated AMMD was 31.8 μm but the AMMD calculated for the dry aerosol mass was 0.97 μm.

The NAUA-5,C (IT) calculation was the only one performed in which water condensation onto the aerosols was calculated; CONTAIN models water condensation onto aerosols but did not calculate it to occur. It is interesting to note that, at 60,468 s the calculated mass of water on the aerosols was about 100 times the dry aerosol mass.

In our analysis of the GSD calculations (Table 31), we discovered that the NAUA-5 (IT) code does not correctly calculate the AMMD, for the same reasons that the MCT-2 and QUICK-M codes did not calculate it correctly. This situation suggests that the AMMD results for the first-set vessel calculations were also in error.

QUICK-M (BCL)

Deposition by diffusiophoresis was modeled in this calculation; the wall condensation rates used were similar to those in Table 11. QUICK-M calculated that about 1.9 g of aerosol was deposited by diffusiophoresis, and that about 0.3 g was deposited by thermophoresis and diffusion. Note also that, as in the previous calculations, QUICK-M incorrectly calculated the AMMD.

REMOVAL (JN).

The modeling assumptions used were similar to those used for the first set of calculations. The code calculated plateout by thermophoresis of 1.9 g, and diffusiophoretic plateout of 4.8 g. These values are, as expected, less than the values calculated in the first set of calculations. Note that, due to the diffusiophoresis modeling error, diffusiophoresis was again over-calculated.

6. SUMMARY AND CONCLUSIONS

Calculations were performed to model the aerosol behavior that occurred in LACE test LA1. Sections 3 to 5 of this report described comparisons of test data with three sets of aerosol transport calculations: (1) for aerosol behavior in the 0.063-m diam, 28.9-m-long test pipe, (2) aerosol behavior in the CSTF vessel, for times during and after aerosols were input to the vessel, and (3) aerosol behavior in the CSTF vessel, for times after aerosols were input to the vessel. This section presents a summary of the code-comparison results and a discussion of insights gained from the LA1 code-comparison effort.

Six calculations of aerosol behavior in the test pipe were performed. For the calculations, the codes used four different models for turbulent aerosol deposition, which was the major deposition mechanism in the test for the flow conditions produced. One of the calculations - that done with the AUX2.9 code - did not model turbulent deposition, and therefore could not model the test results. Because the RETAIN-2C, a log-normal code, incorrectly calculated the change in aerosol size as the aerosol moved through the pipe, the results from this code are not likely to be valid.

In terms of the other pipe calculations performed, the TRAP-MELT2 (IT) and TRAP-MELT2 (UK) calculations came the closest to predicting the aerosol deposition as a function of distance from the pipe inlet (note, however, that the TRAP-MELT2 (UK) calculation had input errors). In addition to calculating the deposition-vs-length well, they calculated the total deposition within 20% of the measured value. However, because about 98% of the aerosol input to the pipe was actually deposited, these two calculations over-estimated transport out of the pipe by factors of five to ten.

The TRAP-MELT2 (BCL) calculation predicted total aerosol deposition in the pipe within 4% of the measured value, and under-predicted the leaked mass by only a factor of 2. However, the code did an inadequate

job of predicting the aerosol deposition vs distance from the pipe inlet; in particular, it over-predicted deposition in the upstream pipe sections by about a factor of six. This result may be an indication that the Wood deposition model[8] is not as valid as the Friedlander and Johnstone model[6,7] used in the other TRAP-MELT2 calculations. It is more likely, however, that the 30-μm surface roughness value used in the TRAP-MELT2 (BCL) calculation was not appropriate.

The AEROSIM-M (UK) calculation was done by using this containment code in a "Lagrangian" mode; that is, following an aerosol/gas packet moving down the pipe. This calculation was performed assuming that the gas moved through the pipe at a fixed velocity of 93 m/s. However, the actual velocity at the pipe outlet was about twice this value, and the turbulent deposition velocity correlation used was dependent on the 5th power of the flow velocity. A consequence of this is that the code under-predicted deposition in the downstream sections of the test pipe. We feel that if the pipe had been broken into two or more segments, and if the velocity had been allowed to increase in these segments, that the code results would have been significantly improved.

It should be noted again that it is not clear if aerosol resuspension or wall-film flow was an important phenomena in test LA1. If it did occur, it would be expected to move upstream deposits into downstream pipe sections. It should be noted in this regard that the TRAP-MELT2 and AEROSIM-M calculations all over-predicted aerosol deposition in the upstream pipe sections, perhaps indicating that aerosols were transported from these regions.

Twelve "first set" calculations were performed to model CSTF vessel aerosol behavior during and after the aerosol source period. In addition to providing comparisons of code and test results in graphical form, estimates of the errors in the calculated aerosol concentrations, settled, plated, and leaked mass values, and aerosol size parameters were made.

Calculated aerosol concentrations agreed well with the measured values during the aerosol source period, but they tended to over-estimate

the airborne aerosol mass during the source plus depletion periods (0 to 100,000 s). We believe that concentrations were over-predicted largely because: (1) the aerosol source value used in the calculations was 28% higher than the sum of the settled, plated, and leaked mass (Table 6); (2) the measured aerosol concentration results showed that the airborne concentration started to drop after about 1,500 s, an indication that aerosol release from the pipe may have nearly stopped; code calculations assumed a constant aerosol release to the vessel for 0 to 3,600 s, and (3) aerosol deposition in the vessel after 33,000 s was enhanced due to steam condensation effects, which were not modeled in all calculations.

The AEROSIM-M, CONTAIN, and QUICK-M codes were the only ones including models for multi-component aerosol behavior. However, none of these codes did a good job of predicting the measured airborne MnO/CsOH mass ratio as a function of time. The largest deviations occurred for times greater than 33,000 s, when enhanced removal of CsOH aerosol occurred.

For the first set of vessel calculations, most codes over-predicted the total aerosol settling and leakage - largely because of using the prescribed incorrect aerosol source - and under-predicted the total aerosol plateout. Most codes calculated the settled and leaked mass values within a factor of 2. For code calculations where diffusiophoresis was not modeled, plateout was under-estimated by more than a factor of 5. When diffusiophoresis was included, roughly half of the codes calculated the measured plateout within a factor of 2.

Overall errors in calculated AMMD were less than 33%, while overall errors in calculated geometric standard deviation were less than 26%. It is not totally surprising that the AMMD could be calculated well for LA1, since this was a low-concentration aerosol test in which agglomeration was not significant. Although the standard deviation errors were not large, a number of codes did not adequately predict the measured time-dependence of the standard deviation.

Differences in modeling of plateout by diffusiophoresis had a major influence on calculated results. Some codes also used incorrect values

of gas leakage rates for t < 3,600 s; this use directly influenced the calculated leaked-mass values. It was found that the MCT-2 and QUICK-M codes (both based on the aerosol modeling approach used in the QUICK code) did not correctly calculate the AMMD. The results from the NAUA-5, C (IT) calculation were particularly interesting because this calculation attempted to model steam condensation onto the vessel walls and onto particles for times greater than 33,000 s. The calculation predicted large amounts of water condensation onto the aerosols, causing the calculated AMMD values (including water) to increase to values in the range of 20 μm. However, the AMMD of the "dry" (not including steam) portion of the aerosol (which is the size measured with a cascade impactor) was about 1.3 μm. That comparison illustrated that AMMD comparisons must be carefully done for conditions where water condenses onto solid aerosols.

Eleven "second set" aerosol calculations were performed to model aerosol behavior after the aerosol source period (t > 3,600 s). For these calculations, the measured airborne concentration and size at 3,600 s were provided as code input. All codes did an improved job (compared to the first set of calculations) of calculating the total airborne aerosol concentration; however, most still tended to overestimate the concentration at long times. None of the codes predicted the drop in CsOH aerosol concentration that occurred between 3,600 and 3,900 s; because of that, all codes did an inadequate job of predicting the CsOH concentration behavior for t > 3,900 s. We believe that, as in the previous calculations, differences between measured and calculated concentrations at long times were largely due to uncertainties in modeling the influence of steam condensation on aerosol behavior.

Differences were again observed between the measured and calculated values of geometric standard deviations. The MCT-2, REMOVAL, and all NAUA results except those from EPRI showed sharp drops in calculated σ_g shortly after 3,600 s; these drops did not correlate with the measured results. Also, calculations illustrated that these codes did not correctly calculate the standard deviation. We recommend that, since airborne aerosol size distributions are unlikely to be log-normal, that all

discrete codes should use the generalized formula (Eq. 7 in this report) to determine the geometric standard deviation. In addition, experimentalists should also use that formula to determine standard deviations of the measured values. If both of these suggestions are done, then future code comparisons of aerosol size can be made on a consistent basis.

As part of our evaluations of the second set of vessel calculations, we found that the Italian version of NAUA-5 did not correctly calculate the AMMD (which suggests that the same was true for the first set of calculations).

Our evaluations showed that all of the LA1 CONTAIN calculations (first and second set) predicted that water condensation onto the vessel walls would occur earlier than it actually did in the test; therefore, diffusiophoretic deposition was over-calculated.

We believe that some final overall comments on the LA1 posttest code comparisons are in order:

1. Considering the complexity of aerosol transport through the test pipe at the high velocities produced in LA1, the results from this first effort to calculate aerosol deposition in pipes are quite encouraging.
2. Overall, the results from the vessel calculations are also encouraging. In many cases the codes calculated aerosol settling, plateout, and aerosol transport to the scrubber to values within a factor of 2 of those measured.
3. Past code-comparisons for containment aerosol behavior have concentrated on comparisons of the airborne aerosol concentration. We believe and would like to emphasize, however, that comparisons of calculated aerosol settling, plateout, leakage, and size are more important than concentration comparisons. In particular, aerosol concentration comparisons can look "valid" when the individual values of aerosol settling, plateout, and leakage are incorrect.

4. All code developers and code users should determine if their codes are calculating the AMMD and the GSD correctly. As was discussed previously, we believe that all codes should use the general formula, Eq. 7, to calculate the GSD.

5. We believe that a blind code-comparison is not only a test of computer codes but also of the code modelers. The results in this report illustrate that a major source of error in code calculations can be related to code input assumptions used by some code users.

7. ACKNOWLEDGEMENTS

We would like to thank the code analysts who participated in this study for their efforts and cooperation. We would also like to thank the HEDL staff, and in particular Gerry Bloom, for their cooperation in providing us with the experimental data from test LA1.

8. REFERENCES

1. L. D. Muhlestein, "Transmittal of Final Test Plan for LACE Test LA1," letter to LACE program participants, Hanford Engineering Development Laboratory, March 30, 1985.

2. A. L. Wright, "Initial Instructions for LA1 Blind Posttest Aerosol Calculations," letter to LACE program participants, Oak Ridge National Laboratory, February 13, 1986.

3. A. L. Wright, "Initial Instructions for the Second Set of LA1 Blind Posttest Calculations," letter to LACE program participants, Oak Ridge National Laboratory, May 20, 1986.

4. G. R. Bloom, et al., "Containment Bypass Test LA1 - Input Conditions for Blind Posttest Aerosol Behavior Code Calculations," report on IBM-PC floppy disks to LACE participants, Hanford Engineering Development Laboratory, January 24, 1986.

5. G. R. Bloom, personal communications to provide LA1 aerosol results, May-June 1986.

6. Friedlander, S. K. and Johnstone, H. F., "Deposition of Suspended Particles from Turbulent Gas Streams," Ind. Eng. Chem. 49, 1151 (1957).

7. J. A. Gieseke, K. W. Lee, and M. A. Goldenberg, "Measurement of Aerosol Deposition Rates in Turbulent Flows," Battelle-Columbus Laboratories, NUREG/CR-1264 (January 1980).

8. Wood, N. B., "A Simple Method for the Calculation of Turbulent Deposition to Smooth and Rough Surfaces," J. Aerosol Sci. 3, 275-290 (1981).

9. Kuhlman, M. R., Kogan, V., and Schumacher, P. M., TRAP-MELT2 Code: Development and Improvement of Transport Modeling, NUREG/CR-4677 (July 1986).

10. Liu, B. Y. H. and Agarwal, J. K., "Experimental Observation of Aerosol Deposition in Turbulent Flow," J. Aerosol Sci. 5, 145 (1974).

11. Sehmel, G. A., "Particle Deposition from Turbulent Air Flow," J. Geo. Res. 75, 1766 (1970).

12. Wilson, J. H. and P. C. Arwood, Summary of Pretest Aerosol Code Results for LWR Aerosol Containment Experiment (LACE) LA2, LACE TR-004, ORNL/M-331, Oak Ridge National Laboratory (June 1987).

13. R. D. Dennis, ed., "Handbook on Aerosols," Technical Information Center, U.S. Energy Research and Development Administration (1976).

14. J. H. Wilson, personal communication on LA2 posttest code-comparison efforts, March 1987.

LACE TR-022
ORNL/M-365

INTERIM DISTRIBUTION

1-3. P. C. Arwood
4. J. R. Hightower, Jr.
5. E. K. Johnson
6. T. S. Kress
7. R. A. Lorenz
8. A. P. Malinauskas
9. J. R. Merriman
10. F. M. Scheitlin
11. M. G. Stewart
12. M. L. Tobias
13-15. J. H. Wilson
16-18. A. L. Wright
19. R. G. Wymer
20-21. Technical Information Center
22. Office of Assistant Manager, Energy Research and Development, Oak Ridge Operations Office, Oak Ridge, Tennessee.
23. Laboratory Records - RC
24. ORNL Patent Section
25. Central Research Library
26. Document Reference Section